UP-SCALING RELATIVE PERMEABILITY FOR STRATIFIED RESERVOIR WATERFLOODING

by

©Mohammad Shadadeh

A Thesis submitted to the

School of Graduate Studies

in partial fulfillment of the requirements for the degree of

Master of Engineering

Department of Engineering and Applied Science

Memorial University of Newfoundland

May, 2015

St.John's Newfoundland and Labrador

Dedication

TO GOD, THE CREATOR, THE WHOM I OWE MY EXISTENCE, LIFE AND PROSPERITY,

TO MY BELOVED WIFE,

TO MY SUPERVISORS DR. LESLEY JAMES, DR. THORMOD JOHANSEN

&

TO ALL MY FRIENDS WHO HELPED AND ENCOURAGED ME IN THIS WORK.

Abstract

This research presents an improved procedure for generating pseudo relative permeability curves for stratified waterflooding using either constant pressure or constant flux at the reservoir boundaries. Pseudo relative permeability reflects the generation of a relative permeability curve that can be used to represent the entire reservoir thickness, rather than a specific layer during reservoir simulation, thus saving computational time.

In this project, Fractional Flow Theory is applied to the generation of pseudo relative permeability curves for i) constant flow rate condition, and ii) constant pressure boundary condition. Previously pseudo relative permeability curves were generated for the constant flow rate condition only. The method differs from previous methodologies and studies, which are all based on a piston-like displacement for water flooding. Instead, this new model uses fractional flow theory to generate a pseudo relative permeability curve that is physically more realistic. The solution is extended to generate pseudo relative permeability curves for simulating the waterflood of a reservoir under the constant pressure boundaries which is a more realistic assumption in compared to constant flow rate. The generated pseudo relative permeability curve is used in a 2D areal reservoir model in an ECLIPSE simulator to predict the behavior of the full layered 3D reservoir model. It was found that there is good agreement between the results corresponding to this new method and the full layered reservoir model, which is very important.

Acknowledgments

I would like to express my most sincere gratitude and appreciation to my supervisors, **Dr. Lesley James** and **Dr. Thormod Johansen** for their great support, patience, generosity and valuable guidance during this work.

I would like to thank my wife and my family for their encouragement and consideration during this project.

I would like to express my appreciation to my thesis defence examiner and committee members.

I would like to thank the Faculty of Graduate Studies and Research for its financial support in the form of graduate scholarships and teaching assistantship awards.

Finally, I would like to extend my grateful gratitude to my past and present research group members, for their knowledge, friendship, and encouragement during my studies at the University of Memorial.

Nomenclature

Nomenclature

A	Area open to flow $[m^2]$
A	Parameter in the water breakthrough time calculation for constant pressure case $[-]$
a_o, a_w, a_g	End point relative permeabilities $[-]$
B	Permeability variance between zones in Testerman zonation method $[-]$
B	Parameter in the water breakthrough time calculation for constant pressure case $[-]$
b	Dip normal sand thickness $[m]$
b	Scaling number $[-]$
C	Parameter in the water breakthrough time calculation for constant pressure case $[-]$
$\Delta\overline{D}$	Average depth difference between the coarse grid-block and adjacent coarse grid-block $[m]$
DFC	Displacing front conductivity $[m^2]$
E	Parameter in the Lomeland *et al.* correlation $[-]$
FR	Facies rules $[-]$
f_w	Water fractional flow $[-]$

$\bar{f}_w$	Average water fractional flow $[-]$
$f'(S_f)$	Displacing front velocity at displacing front saturation [*m/s*]
G	Dimensionless group defined by Coats et al. [–]
g	Gravity acceleration $[m/s^2]$
H	Depth to the centre of coarse grid-block $[m]$
h_1, h_2	Monometer heights in Darcy apparatus $[m]$
h_i	Thickness of Layer i $[m]$
I_1	Parameter in the water breakthrough time calculation for constant pressure case $[-]$
$\tilde{k}_r$	Pseudo relative permeability $[-]$
$\tilde{k}_{ro}$	Pseudo relative permeability of oil $[-]$
$\tilde{k}_{rw}$	Pseudo relative permeability of water $[-]$
$\tilde{k}_{rg}$	Pseudo relative permeability of gas $[-]$
k_{ro}	Relative permeability of oil $[-]$
k_{rw}	Relative permeability of water $[-]$
k_{rg}	Relative permeability of gas $[-]$
K	Absolute permeability $[m^2]$
K_{xy}	Absolute permeability for flow parallel to the x-y plane $[m^2]$
k_e^x	Effective permeability $[m^2]$
k_h	Horizontal permeability $[m^2]$
$\bar{k}_{ij}$	Permeability data $[m^2]$

$\bar{k}_{h\,.}$	Arithmetic average of the permeability data of the hth zone in one well $[m^2]$
$\bar{k}_{i\,.}$	Mean of the permeability data in the ith zone $[m^2]$
$\bar{k}_{..}$	Overall mean of the data in the well $[m^2]$
L	Length of the reservoir $[m]$
L	Number of zones for Testerman equations [–]
L	Parameters in the Lomeland *et al.* correlation $[-]$
M	Mobility ratio $[-]$
m_i	Number of data in the ith zone $[-]$
$\bar{M}$	Mean of property of interest [–]
n_h, n_i	Number of data in the hth and ith zones $[-]$
n_o, n_w, n_g	Indexes in the relative permeability correlation $[-]$
N	Total number of layers $[-]$
N	Total number of data in Testerman zonation method [–]
NG	Net to gross ratio of V_{bulk} $[-]$
ΔP	Pressure difference for the reservoir $[Pa]$
∇p	Partial derivative of p $[Pa/m]$
P_b	Bubble point pressure $[Pa]$
P_c	Capillary pressure $[Pa]$
$P_{c,ow}$	Capillary pressure between oil and water $[Pa]$
p	Pressure $[Pa]$
$\bar{P}_w$	Average water pressures for each coarse grid-block $[Pa]$

$\bar{P}_o$	Average oil pressures for each coarse grid-block $[Pa]$
Q, q	Flow rate $[m^3/s]$
R	Zonation index [–]
R	Residual function [–]
r	A rule that discriminates facies [–]
Δr	Average of the first-degree differences of r [–]
$\underline{S_b}$	Upper shock saturation [–]
$\underline{S_e}$	Lower shock saturation
$\underline{S_i}$	Initial uniform column saturation [–]
S_w	Water saturation [–]
S_o	Oil saturation [–]
S_g	Gas saturation [–]
$\bar{S}_w$	Average water saturation at the outlet reservoir $[-]$
$\bar{S}_{wi}$	Average water saturation behind water oil displacing for each layer $[-]$
S_{or}	Residual oil saturation $[-]$
S_{gc}	Critical gas saturation $[-]$
S_{wc}	Connate water saturation $[-]$
S_{w,out_i}	Water saturation at the outlet for each layer $[-]$
S_{wt}	Wetting phase saturation [–]
S_{nwt}	Non wetting phase saturation [–]

S_{rwt}	Residual wetting phase saturation $[-]$
S_{rnwt}	Residual non wetting phase saturation $[-]$
S_L	Liquid phase saturation $[-]$
S_R	Right side or initial water saturation $[-]$
S_{wn}	Normalized water saturation [–]
S^*	Leading shock saturation $[-]$
S_f	Displacing front saturation $[-]$
T	Transmissibility $[m^3/(Pa.s)]$
T	Parameters in the Lomeland *et al.* correlation $[-]$
$\bar{T}$	Up-scaled transmissibility $[m^3/(Pa.s)]$
t_{BT}	Breakthrough time $[s]$
U_T	Total flux velocity $[m^3/s]$
$\bar{u}$	Mean superficial velocity of fluids in the reservoir $[m^2/s]$
v_2	Slope of fractional flow curve at S^* $[-]$
V_p	Pore volume $[m^3]$
W	Width of layered cross-section $[m]$
W	Pooled variance within zones $[-]$
w	Weight varying between 0 and 1 [–]
x_s	Saturation position $[m]$
λ	Mobility $[m^2/(Pa.s)]$
$\bar{\lambda}_t$	Pseudo total mobility $[m^2/(Pa.s)]$

ϕ	Porosity $[-]$
$\psi\,(S)$	A parameter to define G dimensionless group $[1/(Pa.s)]$
ψ'	Derivative of $\psi(S)$ respect to normalized saturation $[1/(Pa.s)]$
γ	Fluid density $[psi/ft]$
μ	Viscosity $[Pa.s]$
$\nabla \cdot \vec{F}$	Divergence of vector $\vec{F}$ [–]
ρ	Density $[Kg/m^3]$
σ	Standard deviation $[-]$
$z(v,p)$	z values for given probability level $[-]$

Subscripts

i , j, k	Summation index
n	General layer
o	Oil
r	Relative
w	Water
g	Gas
BT	Breakthrough
c	Coarse layer
f	Fine layer
wt	Wet phase
nwt	Non wet phase

Table of Contents

Dedication ii

Abstract iii

Acknowledgments iv

Nomenclature v

Table of Contents xi

List of Figures xiv

List of Tables xvii

CHAPTER 1 INTRODUCTION 1

1.1 Problem statement 1

1.2 Project overview 4

CHAPTER 2 LITERATURE REVIEW 5

2.1 Permeability 6

2.1.1 Absolute Permeability 6

2.1.2 Relative Permeability 8

2.1.3 Relative Permeability Correlations 10

2.2 Up-scaling 15

2.2.1 Single phase up-scaling 16

2.2.2 Two-phase up-scaling 18

2.3 Pseudo functions 21

2.3.1 Categorizing Pseudo Functions 21

2.3.2 Evolution of pseudo relative permeability curves 24
CHAPTER 3 METHODOLOGY 33
3.1 New method 33
3.1.1 Generating the Fractional Flow Curves. 35
3.1.2 Calculation of breakthrough time and outlet water saturation 36
3.1.3 Average water saturation in the reservoir 39
3.1.4 Generating pseudo relative permeabilities 42
3.2 Alternative methods 45
CHAPTER 4 RESULTS AND DISCUSSIONS 49
4.1 Analysis of up-scaled relative permeability curves 49
4.1.1 Reservoir Description: 49
4.1.2 The Effect of Flow Rate on Up-scaled Relative Permeability for Constant Flow Rate Boundaries Case: 50
4.1.3 The Effect of Pressure Difference on Up-scaled Relative Permeability Curve for Constant Pressure Boundaries Case: 53
4.1.4 The Effect of Reservoir Length on Up-scaled Relative Permeability Curve:. 55
4.1.5 The Effect of Fluids Viscosity Ratio on Up-scaled Relative Permeability..... 59
4.1.6 The Comparison of Up-scaled Relative Permeability Curve 63
4.2 ECLIPSE Set Up for The Constant Flow Rate Case: 67
4.2.1 How to overcome the non-monotonic error in ECLIPSE: 68
4.2.2 General Description of the model: 69
4.3 ECLIPSE Set Up for the Constant Pressure Boundary Case: 77
4.3.1 General Description of the model: 78
4.4 Economic Analysis 89

CHAPTER 5 CONCLUSIONS AND RECOMMENDATIONS 95

5.1 Conclusions 95

5.2 Recommendations 98

REFERENCES 99

APPENDIX A 104

A.1 Dimensionless group G developed by Coates *et al*. (1971) 104

APPENDIX B 107

B.1 MATLAB code for constant pressure boundary condition: 107

B.2 MATLAB code for constant flux boundary condition: 114

B.3 MATLAB code for Hearn's method: 120

B.4 MATLAB code for Dykstra-Parson's method: 124

B.5 ECLIPSE code for multi-layer constant pressure boundary reservoir model: 127

B.6 ECLIPSE code for multi-layer constant flux reservoir model: 141

B.7 ECLIPSE code for 2D constant pressure boundaries reservoir model: 142

B.8 ECLIPSE code for 2D constant flow rate reservoir model: 146

List of Figures

Figure 2.1: Darcy's Experiment (from Johansen, 2008).....6

Figure 2.2: Two Phase Relative Permeability Curves (from Johansen, 2008) 10

Figure 2.3: Random Lumping (a) vs. Zonation or Up-layering (b) (from Li et al., 2000) 20

Figure 2.4: Rock and Pseudo Relative Permeabilities for Stone's example. Fine Grid 50x2 and Coarse Grids 5x1 (after Guzman, 1996) 32

Figure 3.1: Stratified Reservoir Model 34

Figure 3.2: Flow Chart for Generating Pseudo Relative Permeability Curves.....35

Figure 3.3: Determining the Front Water Saturation (after Welge, 1952).....37

Figure 3.4: Determining Average Water Saturation behind the Front for $t < t_{BT}$...41

Figure 3.5: Determining Average Water Saturation behind the Front for $t > t_{BT}$...42

Figure 4.1: Effect of Flow Rate on Up-Scaled Relative Permeability for Constant Flow Rate Case 51

Figure 4.2: Effect of Pressure Difference on Up-Scaled Relative Permeability for Constant Pressure Boundary Case 54

Figure 4.3: Effect of Reservoir Length on Up-Scaled Relative Permeability for Constant Flow Rate Case 57

Figure 4.4: Effect of Reservoir Length on Up-Scaled Relative Permeability for Constant Pressure Boundary Case 58

Figure 4.5: Effect of Viscosity Ratio on Up-Scaled Relative Permeability for Constant Flow Rate Case 60
Figure 4.6: Effect of Viscosity Ratio on Up-Scaled Relative Permeability for Constant Pressure Boundary Case 61
Figure 4.7: Up-scaled Relative Permeability Corresponding to Average Water Saturation in the Entire Reservoir (Constant Pressure Boundary Case versus Constant Flow Rate Case)..... 64
Figure 4.8: Up-scaled relative Permeability Corresponding to Average Water Saturation at the Outlet Reservoir Face (Constant Pressure Boundary Case Versus Constant Flow Rate Case) 65
Figure 4.9: Up-scaled Relative Permeability (Hearn Versus Dykstra-Parson's Method)..... 67
Figure 4.10: Procedure to Find a Polynomial Trend Line to the Up-scaled Relative Permeability 68
Figure 4.11: Initial Pressure Distribution for the Constant Flow Rate Case 71
Figure 4.12: Oil Production Rate Comparison for the Constant Flow Rate Case 72
Figure 4.13: Oil Recovery Comparison for the Constant Flow Rate Case..... 73
Figure 4.14: Total Oil Production Comparison for the Constant Flow Rate Case 74
Figure 4.15: Water Cut Comparison for the Constant Flow Rate Case..... 75
Figure 4.16: Initial Water Saturation Distribution for the Constant Pressure Boundary case 80

Figure 4.17: Final Water Saturation Distribution for the Constant Pressure Boundary Case 81
Figure 4.18: Oil Production Rate Comparison for the Constant Pressure Boundary Case 82
Figure 4.19: Oil Recovery Comparison for the Constant Pressure Boundary Case .. 83
Figure 4.20: Total Oil Production Comparison for the Constant Pressure Boundary Case 84
Figure 4.21: Water Cut Comparison for the Constant Pressure Boundary Case 85
Figure 4.22: Net present value for the constant flow rate case 90
Figure 4.23: Net Present Value for the Constant Pressure Boundary Case 91
Figure 4.24: Net Present Value for the Constant Flow Rate Case over Production Time 92
Figure 4.25: Net Present Value for the Constant Pressure Boundary Case over Production Time 93
Figure A.1: Gravity Segregation in a Closed Vertical Column. (after Coats et al., 1971) 104

List of Tables

Table 2.1: Categorizing pseudo functions 22

Table 2.2: Basic reservoir description for Stone's example 30

Table 4.1: Reservoir Properties..... 50

CHAPTER 1

INTRODUCTION

1.1 Problem statement

Reservoir simulation is a powerful tool to study and predict oil recovery by study displacement processes. The results of these studies are used to make capital management decisions for field development and future reservoir operating strategies.

Three-dimensional multiphase fluid flow simulation of a complex reservoir with high grid-block definition can require much human effort and computer resources. Reducing the number of grid-blocks or making the model coarser is one option to reduce computational time but it can ignore important finer scale reservoir details, resulting in discrepancies between simulation results and actual production history.

Generally speaking, with current computer technology maximum number of grid-blocks (with typical number of time dependent variables such as saturations, pressure and components accumulation) is in order of magnitude of 100,000 in most reservoir flow simulators, where a typical grid-block size is 10 *m* in each dimension. This grid-block

volume potentially exhibits a large degree of heterogeneity and if a rock relative permeability curve is used to simulate such a large grid-block, the important effects of heterogeneity may be neglected, thus significant errors may occur in simulation results (Cao and Aziz, 1999).

Relative permeability curves are the main controllers for phases flow in simulators. They are normally obtained using a small core plug in laboratory. To consider the heterogeneity within a large grid-block, pseudo (up-scaled) relative permeability curves are used to replace the intrinsic relative permeability curves (Cao and Aziz, 1999). Through the use of pseudo relative permeability, the effects of heterogeneity are captured within the coarse grid-blocks. The aim of up-scaling is to reduce the computational time needed for calculation either "by reducing the number of grid-blocks or reducing the number of dimensions of the problem, such as reducing a 3D field case model to a 2D areal model" (Cao and Aziz, 1999). In other words, through up-scaling we hope to retain accurate information while conducting less computations (Cao and Aziz, 1999).

The vertical definition of a reservoir is one of the most important considerations in reservoir simulation. The only rigid way to consider vertical effects is to use a 3D reservoir simulator, but due to the computational constraints previously mentioned for 3D simulation, the use of 2D simulators is a solution. A "2D reservoir simulator implies uniform reservoir properties and fluid saturation throughout the reservoir thickness," (Hearn, 1971) an assumption that surely is not physically correct. Thus, the input data requires tuning to approximate the vertical effects (Hearn, 1971).

Hearn (1971) presented a method to develop a pseudo relative permeability curve for the permeability variation case under a constant flow rate boundary condition assuming piston-like displacement. By modifying Hearn's method using fractional flow theory, this thesis presents an alternative method for developing pseudo relative permeability curves for the two-dimensional simulation of fluid displacement under a constant flow rate boundary condition. The solution is then extended to generate pseudo relative permeability curves under the constant pressure boundaries condition which is a realistic model of producing oil with constant reservoir pressure and constant well flow pressure. For example, unless reservoir pressure is very close to bubble point, the wellbore pressure must be kept close to but above bubble point, P_b. Then, injectors are also conveniently operated at constant wellbore pressure.

Another main advantage of this study over previous studies is that this method does not assume a piston-like displacement: we assume that after water breakthrough, the water saturation at the outlet increases continuously with time as a consequence of using fractional flow theory. This is physically more realistic than previous approaches taken by Hearn (1971) and Dykstra-Parson (1950) where they simply consider $1 - S_{or}$ for water saturation after water breakthrough. The idea of generating a pseudo relative permeability curve to simulate waterflooding in a reservoir with constant pressure boundaries has not been previously studied.

1.2 Project overview

The literature review of up-scaling is presented in chapter 2. This chapter starts with the definition of absolute permeability and relative permeability and then presents an overview on up-scaling methods and finally finishes with pseudo functions used for up-scaling. Chapter 3 outlines the procedure of the two new methods for generating pseudo relative permeabilities for a stratified waterflooded reservoir with i) constant flow rate boundary condition, and ii) constant pressure boundary condition. In chapter 4, the results for the generated pseudo relative permeability curves are shown, compared and discussed. The generated pseudo relative permeability curve is used in a 2D areal reservoir model in an ECLIPSE simulator to predict the behavior of the full layered 3D reservoir model, and reservoir performance is compared to the results of the corresponding 3D reservoir model. Finally chapter 5 presents the conclusions and recommendations.

CHAPTER 2

LITERATURE REVIEW

This chapter presents a literature review for up-scaling in reservoir simulation. This chapter starts from the absolute permeability and leads to the pseudo functions and up-scaled relative permeability which is the aim of this project. In section 2.1, absolute permeability is explained and then relative permeability and its different correlations will be introduced. In section 2.2, up-scaling for single phase and two-phase flow is overviewed with focus on statistical methods. In section 2.3, pseudo functions used for up-scaling are described. This section categorizes pseudo functions and shows the evolution of them.

2.1 Permeability

2.1.1 Absolute Permeability[1]

Permeability is a property of the porous medium that measures the capacity and ability of the formation to transmit fluids. The absolute (or intrinsic) permeability, K (m^2), is a very important rock property because it controls the directional movement and the flow rate of the reservoir fluids in the formation. This parameter was first defined mathematically by Henry Darcy in 1856. In fact, the equation that defines permeability in terms of measurable quantities is called Darcy's Law. Darcy's apparatus is shown in Figure 2.1.

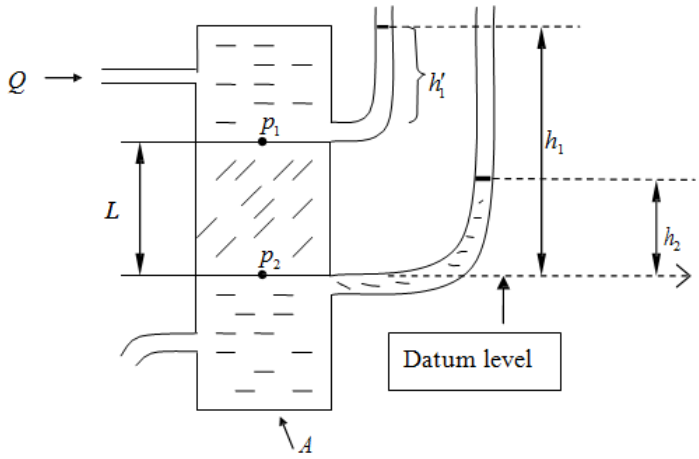

Figure 2.1: Darcy's Experiment (from Johansen, 2008)

[1] Sections 2.1.1 and 2.1.2 are from Dr. Johansen's book, "Principles of Reservoir Engineering," with few adaptation by his courtesy

In Figure 2.1 a homogeneous sand pack with length L (m) and cross section A (m^2) is placed in a cylinder through which a flow rate of water, Q (m^3/s), can be injected. In Figure 2.1, h_1 and h_2 are manometer heights (m) relative to a datum level.

In his experiments, Darcy varied Q, A and L, and also the sand packs. He found that for a given sand pack,

$$Q = kA\frac{h_1 - h_2}{L}, \tag{2.1}$$

where k is constant named hydraulic conductivity, which is a rock and fluid property. However, k varied from sand pack to sand pack. We can also express Darcy's Law in terms of the pressures p_1 and p_2. Let the water density be ρ (kg/m^3) and let g be the acceleration of gravity (9.81 m/s^2). Then $p_1 = \rho g h_1'$ and $p_2 = \rho g h_2$. Since $h_1 = h_1' + L$, resulting in

$$Q = k\frac{A}{\rho g}\left(\frac{p_1 - p_2}{L} + \rho g\right). \tag{2.2}$$

Subsequent experimentalists extended Darcy's experiments to include different fluids and flow directions. They found that

$$Q = \frac{KA}{\mu}\left(\frac{p_1 - p_2}{L} + \rho g\right), \tag{2.3}$$

where μ is the fluid viscosity *(Pa.s)*, and ρ is the fluid density (kg/m^3). The constant *K* is called the permeability of the sand pack. It is a property of the sand pack (or rock) and is a function of the space coordinates.

2.1.2 Relative Permeability

The absolute permeability, *K*, is a rock property and it relates to flow of a single fluid phase through the porous media. It is not dependent on the fluid properties. However, in reality a reservoir may contain several fluids simultaneously and Darcy's law will not describe the simultaneous flow of these fluids through the porous media. Instead, the concept of effective permeabilities applies, which states that Darcy's law is valid for each individual phase using a phase-specific effective permeability (k_o, k_g , k_w):

$$q_o = \frac{k_o A}{\mu_o}\left(\frac{p_1 - p_2}{L} + \rho g\right), \tag{2.4}$$

$$q_w = \frac{k_w A}{\mu_w}\left(\frac{p_1 - p_2}{L} + \rho g\right), \text{ and} \tag{2.5}$$

$$q_g = \frac{k_g A}{\mu_g}\left(\frac{p_1 - p_2}{L} + \rho g\right). \tag{2.6}$$

In these equations, the indices o, g, w refer to oil, gas and water, respectively. The saturations, i.e., S_o, S_g and S_w, must be specified to completely define the conditions at which a given effective permeability exists.

The concept of relative permeability is the most common format for the description of multi-phase flow in porous media:

$$k_{ro} = \frac{k_o}{K}, \tag{2.7}$$

$$k_{rw} = \frac{k_w}{K}, \tag{2.8}$$

$$k_{rg} = \frac{k_g}{K}. \tag{2.9}$$

The phase permeabilities are functions of their respective saturations; hence the relative permeabilities are also functions of saturations. Since phase permeabilities may range from zero to k, therefore $0 \leq k_r \leq 1$. Figure 2.2 shows typical relative permeability curves in an oil/water system, where water is the wetting phase.

On Figure 2.2, S_{wc} is the connate water saturation and S_{wro} is the water saturation at residual oil saturation. Observe that $k_{ro} + k_{rw} \leq 1$, which is also an experimental result. The experimental results mentioned above reflect the fact that relative permeabilities are not pure rock properties. They are fluid/rock interaction parameters and they therefore rely on the fluid saturations. Usually, gas/oil relative permeability curves are established in the presence of connate water, since in water wet systems, connate water will always be present. It is therefore convenient to express them as functions of the liquid saturation $S_L = S_{wc} + S_o$. The oil becomes immobile for $S_L = S_{wc} + S_{or}$.

If core samples are not available for Special Core Analyses (SCAL), empirical relationships, capillary models, statistical models, and hydraulic radius theories can be used. However, the alternative methods may not be precise as SCAL.

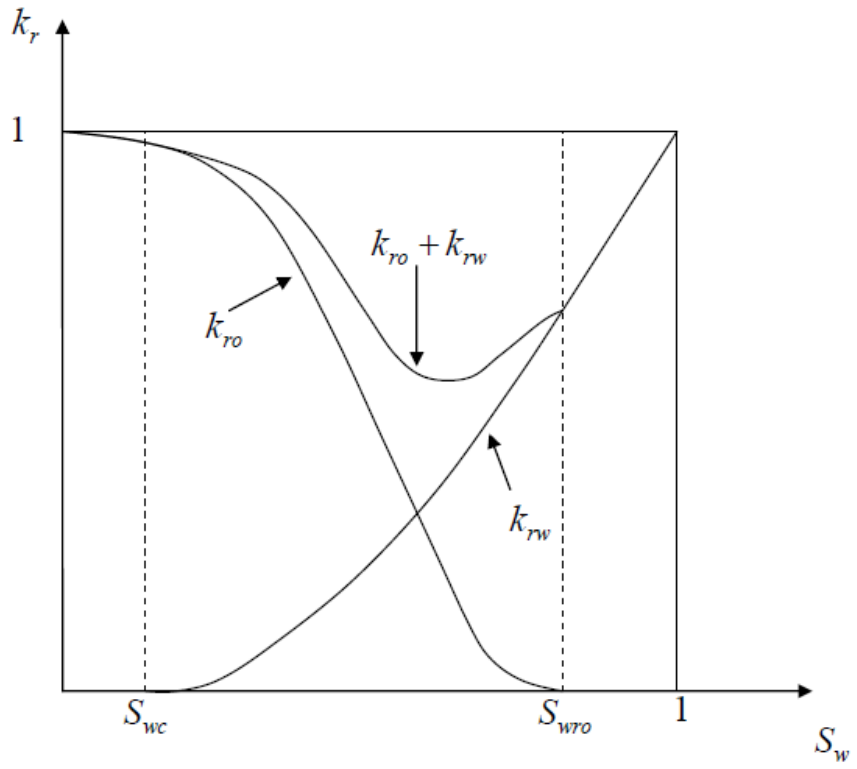

Figure 2.2: Two Phase Relative Permeability Curves (from Johansen, 2008)

2.1.3 Relative Permeability Correlations

Many approaches exist in open literature to calculate relative permeability. An appropriate correlation could be used in chapter 3 to calculate the relative permeability of a reservoir layer in a multilayer reservoir model. Different parameters have been applied to calculate the relative permeability in the correlations including (Tarek, 2000):

- Residual and initial saturations, and
- Capillary pressure data

One method for calculating relative permeability was proposed by Pirson (1958). His method was achieved from petro physical consideration for the wetting and non-wetting phase relative permeabilities for clean, water wet and coarse grain sandstones. His method is capable of calculating the wetting and non-wetting phase relative permeability for both imbibition and drainage processes. He proposed the following set of equations:

For the wetting phase

$$k_{rwt} = \sqrt{S_w{}^*}S_w{}^3. \tag{2.10}$$

The above equation is the same for calculating relative permeability of wetting phase for both imbibition and drainage processes.

For the non-wetting phase

- **Imbibition**

$$k_{rnwt} = \left[1 - \left(\frac{S_w - S_{wc}}{1 - S_{wc} - S_{nw}}\right)\right]^2, \tag{2.11}$$

- **Drainage**

$$k_{rnwt} = (1 - S_w{}^*)\left[1 - (S_w{}^*)^{0.25}\sqrt{S_w}\right]^{0.5}, \tag{2.12}$$

where $S_w{}^*$ is effective water saturation and is calculated as:

$$S_w{}^* = \frac{S_w - S_{wc}}{1 - S_{wc}}. \tag{2.13}$$

Another method was presented by Brook and Corey (1964, 1966) that is able to predict drainage relative permeability for a variety of pore size distribution:

$$S_w{}^* = \left(\frac{P_b}{P_c}\right)^{\lambda} \; for\; P_c \geq P_b, \tag{2.14}$$

$$k_{rwt} = (S_w{}^*)^{\frac{2+3\lambda}{\lambda}}, \tag{2.15}$$

$$k_{rnwt} = (1 - S_w{}^*)^2(1 - S_w{}^*)^{\frac{2+\lambda}{\lambda}}, \tag{2.16}$$

where λ and P_b are constants characteristic of the porous media; λ is a measure of pore size distribution of the media, and P_b is threshold primary drainage capillary pressure, k_{rwt} and k_{rnwt} are the wetting and non-wetting phase relative permeabilities , respectively.

Relative permeability can also be calculated from capillary pressure data. Capillary pressure (p_c), as illustrated by Rose and Bruce (1949) is a reservoir formation characteristic accounting for the rock texture, surface area and cementation. There are correlations relating capillary pressure to relative permeability. Useful in understanding such process is the series of equations published in 1958 by Wyllie and Gander who used them in measuring the relative permeability of water-oil drainage using capillary pressure data:

$$k_{rw} = \left(\frac{S_w - S_{wc}}{1 - S_{wc}}\right)^2 \frac{\int_{S_{wc}}^{S_w} dS_w / p_c^2}{\int_{S_{wc}}^{1} dS_w / p_c^2}, \tag{2.17}$$

$$k_{ro} = \left(\frac{1-S_w}{1-S_{wc}}\right)^2 \frac{\int_{S_{wc}}^{1} dS_w / p_c^2}{\int_{S_{wc}}^{1} dS_w / p_c^2}. \tag{2.18}$$

Wyllie and Gardner (1958) expressed separate equations for calculating the oil and gas relative permeabilities in the existence of connate water saturation by considering it as a part of rock matrix:

$$k_{ro} = \left(\frac{S_o - S_{or}}{1-S_{or}}\right)^2 \frac{\int_{0}^{S_o} dS_o / p_c^2}{\int_{0}^{1} dS_o / p_c^2}, \tag{2.19}$$

$$k_{rg} = \left(1 - \frac{S_o - S_{or}}{S_g - S_{gc}}\right)^2 \frac{\int_{S_o}^{1} dS_o / p_c^2}{\int_{0}^{1} dS_o / p_c^2}, \tag{2.20}$$

where

S_{gc} = critical gas saturation,

S_{wc} = connate water saturation, and

S_{or} = residual oil saturation.

Another method for calculating relative permeabilities is analytical equations, where usually used in numerical simulators. Tarek (2000) presented the most frequently used analytical equations for calculating relative permeability as below:

Oil-Water Systems:

$$k_{rwi} = a_w \left(\frac{S_w - S_{wc}}{1 - S_{wc} - S_{or}} \right)^{n_w}, \quad (2.21)$$

$$k_{roi} = a_o \left(\frac{1 - S_w - S_{or}}{1 - S_{wc} - S_{or}} \right)^{n_o}, \quad (2.22)$$

where

$a_w =$ water relative permeability at the residual oil saturation,

$a_o =$ oil relative permeability at connate-water saturation,

n_w, n_o = exponents on relative permeability curves,

S_{wc} = connate water saturation, and

S_{or} = residual oil saturation.

There are many other correlations to calculate relative permeabilities that can be found in the literature (Tarek, 2000, Honarpour *et al.,* 1982, 1988). However, there is a new type of relative permeability correlation with three degrees of freedom, called LET-type. The LET-correlation (Lomeland *et al.*, 2005) adds more parameters to better capture the shape of measured relative permeability curves determined by experiments. The authors used three empirical parameters *L*, *E* and *T,* where they are tuned based on experimental data. The correlation for oil-water system as follow:

$$k_{rw} = \frac{k_{rw}^{o} {S_{wn}}^{L_w}}{{S_{wn}}^{L_w} + E_w (1 - S_{wn})^{T_w}}, \quad (2.21)$$

$$k_{ro} = \frac{(1 - S_{wn})^{L_o}}{(1 - S_{wn})^{L_o} + E_o(S_{wn})^{T_o}}. \quad (2.22)$$

where,

$$S_{wn}(S_w) = \frac{S_w - S_{wc}}{1 - S_{wc} - S_{or}}. \quad (2.23)$$

For gas-water or gas-oil system there are *LET* correlations similar to the oil-water relative permeabilities correlations shown in equations 2.23-2.25.

Lomeland *et al.* (2012) extended their correlation to *LETx* version. In the new version they extend the water relative permeability to unity at unity water saturation, while the oil relative permeability uses the standard normalization of saturation. The authors reported that this new version provides fast and easy to handle up-scaling and history matching.

2.2 Up-scaling

Up-scaling, or homogenization, is a process that replaces regions of a heterogeneous properties consisting of fine grid-blocks with an equivalent homogenous region made up of a single coarse grid-block with a representative property value. Up-scaling is performed for all coarse grid-blocks and for all of grid-block properties in the reservoir simulation model. The aim of up-scaling is to achieve the balance between the number of grid-blocks needed for accurate reservoir simulation and computational time.

2.2.1 Single phase up-scaling

As Christie (1996) mentioned, the most straightforward type of up-scaling is single-phase up-scaling. In single-phase up-scaling the only parameter that is scaled is absolute permeability. The most common method of this kind is the pressure solver method. In this method, a single phase flow system is set up and then the equivalent permeability providing the same flow rate as the fine grid system is calculated. The results will depend on boundary conditions. In this method, a vertical no flow boundary condition is most commonly used. Christie (1996) provided the following procedure for this method, where first the matrix is set up as:

$$\nabla \cdot [k(\vec{x})\nabla p] = 0. \tag{2.24}$$

Boundaries are assumed no-flow at the side with $p = 1$ and $p = 0$ at the inlet and outlet respectively. The effective (representative) permeability is then given by

$$k_e^x = -\frac{\Delta x \mu q}{A \Delta \mathrm{p}}. \tag{2.25}$$

The representative directional permeability for the remaining directions could be calculated by similar method. This approach is straightforward, and as reported by some authors (Christie, 1996) it provide results in agreement with history matching.

Another method of single phase up-scaling is the stream-line method. This method is based on the use of stream-tubes generated from a single-phase fine grid simulation, which basically provides the direction of fluid travel in the reservoir. Hewett and Yamada (1997) used stream-lines to calculate pseudo functions along stream-lines. Stream-lines can

indicate the density of flow, thus detect the regions in the model that need to have finer resolution.

Another vertical up-scaling method is zonation, which is performed by many authors (Testerman, 1962; Li *et al.,* 1999; Li and Beckner 2000). This method is based on grouping the layers together in order to decrease the number of grid-blocks in the vertical direction. Testerman (1962) proposed a statistical method to recognize and define inherently occurring zones within a reservoir and to connect these zones form well to well. This method includes two major steps. In the first step, the zones are detected based on permeability data from the wells. These zones are selected so that variation is minimized within the zones and maximized between the zones. For this aim the following equations are recommended:

$$B = \frac{1}{L-1}\left[\sum_{i=1}^{L} m_i \left(\bar{k}_{i.} - \bar{k}_{..}\right)^2\right], \tag{2.26}$$

$$W = \frac{1}{N-L}\left[\sum_{i=1}^{L}\sum_{j=1}^{m_i} \left(\bar{k}_{ij} - \bar{k}_{i.}\right)^2\right], \tag{2.27}$$

$$R = \frac{B-W}{W}, \tag{2.28}$$

where $B =$ the permeability variance between the zones, $L =$ the number of zones, $i =$ the summation index or the number of zone, $j =$ the summation index for the number of data within the zone, $m_i =$ the number of data in the ith zone, $\bar{k}_{i.} =$ the mean of the permeability data in the ith zone, $\bar{k}_{..} =$ the overall mean of the data in the well, $W =$ the

pooled variance within zones, $N =$ the total number of data, the $\bar{k}_{ij}$ =the permeability data, and $R =$ the zonation index.

After selecting the zones, the author proposes the next step, which is the correlation across the reservoir. In the second part, the zones from well to well throughout the reservoir are correlated, based on comparison of the difference of the means, to aid the engineer in determining continuity of the strata. Zones are correlated if the difference of the means is less than or equal to one expected from the individual data variation or if

$$\left(\bar{k}_{h\,.} - \bar{k}_{i\,.}\right) \geq \sqrt{\frac{1}{2}\left(\frac{1}{n_h} + \frac{1}{n_i}\right)}\sigma z(v,p)\,. \tag{2.29}$$

Where $\bar{k}_{h\,.} =$ the arithmetic average of the permeability data of the hth zone in one well and $\bar{k}_{i\,.} =$ the arithmetic average of the permeability data in in ith zone in an adjacent well, n_h and $n_i =$ the number of data in the hth and ith zones, $\sigma =$ the standard deviation of all the permeability data from the reservoir and $z\ (v,p) =$ z values for given probability level.

2.2.2 Two-phase up-scaling

Up-scaling of absolute permeability solely is not sufficient to completely characterize a two-phase displacement project in a heterogeneous medium. For the clarity, Christie (1996) provided an example that, in presence of a high permeability streak in the reservoir model, water break through occurs early; however, using an effective (representative) absolute permeability in conjunction with intrinsic relative permeability curve does not capture this effect. Thus, two-phase up-scaling accounts for the dispersion effect of

permeability variation on the two-phase flow. Li *et al.* (1999) and Li and Beckner (2000) have developed Testerman's work for two-phases. They analysed the residuals as an indicator of the precision of up-scaling and instead of applying it only for permeability they applied it independently on two up-scaling properties, including displacing front conductivity (DFC) and facies rules (FR). They recommended the following equations:

$$R = \sum_{k=1}^{n_z} \frac{\left(\overline{M}_k^c - \overline{M}_k^f\right)^2}{n_z} + w \sum_{k=1}^{n_z} \frac{\left(\sigma_k^c - \sigma_k^f\right)^2}{n_z}, \tag{2.30}$$

where R is the residual function, $\overline{M}$ and σ are the mean and standard deviation respectively for the up-layering property of interest, c and f are denoted for coarse and fine layer respectively and w is the weight varying between 0 and 1. In this method, up-layering properties are defined as

$$DFC = \frac{k_h}{\varphi} f'\left(S_f\right), \tag{2.31}$$

$$FR = a\frac{k_h}{\varphi} + r, \tag{2.32}$$

where k_h is horizontal permeability, φ is porosity, $f'(S_f)$ is displacing front velocity at S_f (displacing front saturation) and r is a rule that discriminates facies. Parameter a is defined as

$$a = \frac{b}{\left(\frac{k_h}{\varphi}\right)_{max}} \Delta r, \tag{2.33}$$

where b = a scaling number between 0 and 1; Δr = the average of the first-degree differences of r and max denotes maximum value among up-scaled layers.

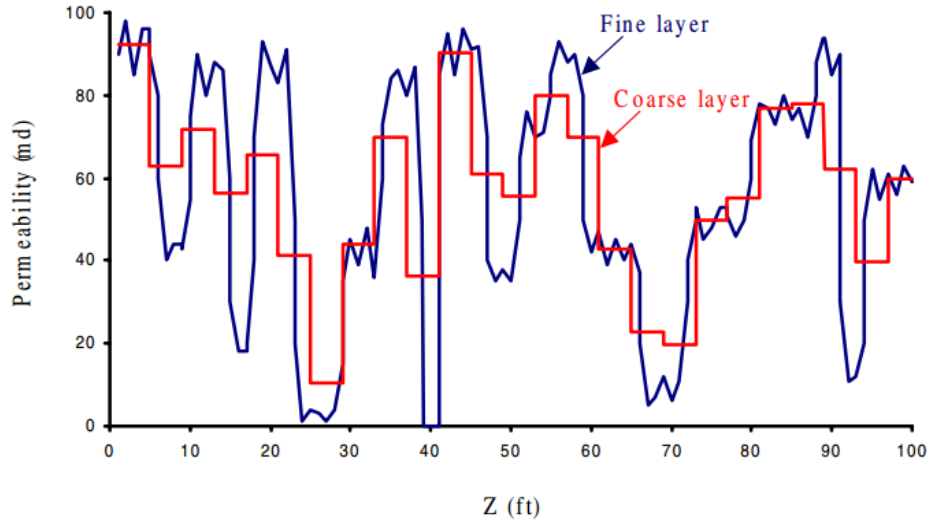

(a)

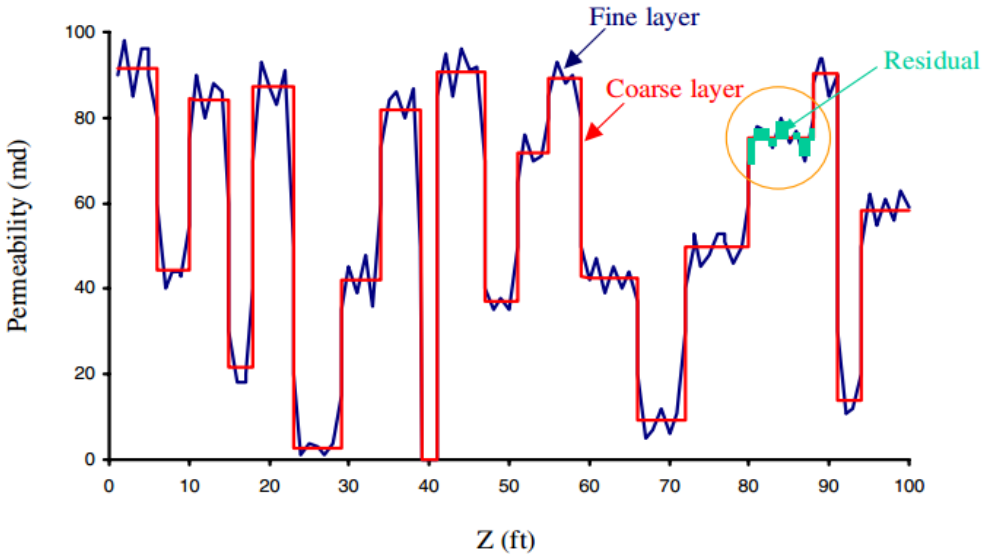

(b)

Figure 2.3: Random Lumping (a) vs. Zonation or Up-layering (b) (from Li et al., 2000)

Figure 2.3 schematically shows the random lumping versus the zonation method. This figure illustrates that model generated by random lumping differs significantly from the original geologic model; because high permeability zones and low permeability barriers have been homogenized during up-layering. However, the zonation method preserves reservoir heterogeneity and geologic details via optimal layer grouping.

2.3 Pseudo functions

A more advanced method of up-scaling is using pseudo functions. By substituting the permeability distribution with a representative value and using rock relative permeability curves for reservoir simulation, the results are different from fine-grid simulation results, thus the idea of pseudo functions was introduced. In order to overcome the different results, modifications are made to relative permeability curves. Depending on the assumptions used for the simulation and the different estimation methods there are different relative permeabilities called pseudo functions. These curves are different than the intrinsic rock relative permeability curves and sometimes have strange shapes; however, using them in coarse-grid (up-scaled) simulation promises results that are in agreement with results of fine-grid simulation (down-scaled cases). Table 2.1 shows the categories for different pseudo functions and their evolution.

2.3.1 Categorizing Pseudo Functions

There are two types of pseudo functions: vertical equilibrium pseudo functions and the more widely-used dynamic pseudo functions. Vertical equilibrium means complete communication between the layers, so the interchange between them is immediate. The

vertical equilibrium pseudo functions are based on vertical equilibrium assumption. They were developed by the Coats et al. (1967, 1971) pseudo function approach and the Hearn (1971) approach for generating pseudo relative permeability for stratified water flooding. Dynamic pseudo functions need fine-grid simulation results (pressure and saturation distributions) at different times. This is also why they are called dynamic.

Table 2.1: Categorizing pseudo functions

Pseudo functions category		**Evolution**
Vertical equilibrium		Coats *et al.* (1967) Coats *et al.* (1971) Hearn 1971)
Dynamic pseudo functions	Based on Darcy law for individual phases	Jacks *et al.* (1973) Kyte and Berry (1975) Flux weighted potential method (Intera Information Technology, 1994) Pore volume weighted method (Intera Information Technology, 1994)

	Based on average total mobility	Stone (1991), Hewett and Behrens (1991), Beier (1992)
	Based on stream-tubes provided from single-phase fine grid simulation	Hewett and Yamada (1997)

There are several methods for generating dynamic pseudo functions. According to the literature (Cao and Aziz, 1999), there are three kinds of dynamic pseudo functions. The first kinds are based on using Darcy law to find pseudo functions for individual phases. They differ in the way to find average quantities from fine-grid simulation results. As Cao and Aziz (1999) mentioned, they include Jacks *et al.* (1973), Kyte and Berry (1975), flux weighted potential method (Intera Information Technology, 1994) and pore volume weighted method (Intera Information Technology, 1994).

The second kinds of dynamic pseudo functions are based on an average total mobility. In these types it tried to match coarse and fine grid pressure or potential gradients. These methods include Stone (1991), Hewett and Behrens (1991) and Beier (1992), see Cao and Aziz (1999).

The last kinds of dynamic pseudo functions are based on stream-tubes provided from a single-phase fine grid simulation. In these methods, they build pseudo curves along stream-tubes. Hewett and Yamada's (1997) Streamline Method is one well-known method of

these kinds. However, currently this method is limited to two-dimensional problems (Cao and Aziz, 1999).

2.3.2 Evolution of pseudo relative permeability curves

Coats *et al.* (1967) presented the first pseudo relative permeability curves based on vertical equilibrium assumption. The authors suggest the following equations to calculate the pseudo relative permeability:

$$\tilde{k}_{rw} = \int_{-b/2}^{b/2} K_{xy}(z)\, k_{rw}(z)dz \Big/ \int_{-b/2}^{b/2} K_{xy}(z)dz\,, \tag{2.34}$$

$$\tilde{k}_{ro} = \int_{-b/2}^{b/2} K_{xy}(z)\, k_{ro}(z)dz \Big/ \int_{-b/2}^{b/2} K_{xy}(z)dz, \tag{2.35}$$

$$\bar{S}_w = \int_{-b/2}^{b/2} \varphi(z)\, S_w(z)dz \int_{-b/2}^{b/2} \varphi(z)dz, \tag{2.36}$$

where $b =$ dip normal sand thickness, $K_{xy}(z) =$ absolute permeability for flow parallel to the *x*-*y* plane.

Coats *et al.* (1971) presented a new dimensionless group, G, which can be used to check the vertical equilibrium assumption. As the authors claimed, the value of dimensionless group G is directly proportional to the degree of validity of the vertical equilibrium assumption.

Coats *et al.* (1971) recommended further work to attach a meaningful critical value to the dimensionless group G. Two-dimensional cross sectional calculations must be compared

with 1-D areal calculations for a wide range of reservoir and fluid properties yielding a range of values for G and then using then find the critical values for G that VE assumption is valid.

Hearn (1971) proposed a method for developing pseudo relative permeability curves for two-dimensional simulation of a stratified waterflood for a three-dimensional reservoir where the vertical flow is controlled by viscous forces. In this method, the layers are arranged based on breakthrough of the water to calculate the pseudo relative permeability curve. This model assumes piston-like displacement. In other words, to calculate the average water saturation at the outlet, any layers in which water breakthrough has occurred assume to be at residual oil saturation and the layers that water breakthrough has not occurred are at the connate water saturation. Hearn used the following equations to calculate the pseudo relative permeabilities:

$$\bar{S}_w = \frac{\sum_{i=1}^{n} h_i \varphi_i \left(1 - S_{ro_i}\right) + \sum_{i=n+1}^{N} S_{wc_i} h_i}{\sum_{i=1}^{N} h_i \, \varphi_i}, \tag{2.39}$$

$$\tilde{k}_{rw} = \frac{k_{rw}(S_{ro}) \sum_{i=1}^{n} K_i h_i}{\sum_{i=1}^{N} K_i h_i}, \tag{2.40}$$

$$\tilde{k}_{ro} = \frac{k_{ro}(S_{wc}) \sum_{i=n+1}^{N} K_i h_i}{\sum_{i=1}^{N} K_i h_i}, \tag{2.41}$$

where $n =$ the number of layers that water breakthrough have occurred, $N =$ total number of layers, $k_{rw}(S_{ro}) =$ relative permeability of water at residual oil saturation, $k_{ro}(S_{wc}) =$

relative permeability of oil at connate water saturation, $\tilde{k}_{rw}$ = pseudo relative permeability of water, $\tilde{k}_{ro}$ = pseudo relative permeability of oil and $\bar{S}_w$ = average water saturation.

Jacks *et al.* (1973) proposed a method to generate pseudo relative permeability curves based on the assumption that the reservoir model can be simulated by a two-dimension model. They developed a technique to use the vertical cross section to calculate the vertical saturation profile and then up-scaling in the vertical direction. In this method, the pseudo relative permeability is directly calculated by the transmissibility ($T = Kh/\mu$) weighted relative permeability for each column of blocks. It uses the following equations:

$$\bar{S}_w = \frac{\sum_i \left(V_p S_w\right)_i}{\sum_i V_{pi}}, \tag{2.42}$$

$$\tilde{k}_{rw} = \frac{\sum_i (T k_{rw})_i}{\bar{T}}, \tag{2.43}$$

$$\tilde{k}_{ro} = \frac{\sum_i (T k_{ro})_i}{\bar{T}}, \tag{2.44}$$

and the up-scaled transmissibility is calculated as:

$$\bar{T} = \sum_i T_i\,, \tag{2.45}$$

where V_p = pore volume, T = transmissibility, i = index for layer, $\tilde{k}_{rw}$ = pseudo relative permeability of water, $\tilde{k}_{ro}$ = pseudo relative permeability of oil and $\bar{S}_w$ = average water saturation.

This model assumes equal potential for all of the vertically piled grid-blocks. This method is identical to the equation for vertical equilibrium, if the vertical equilibrium assumption is satisfied. This method is only partially dynamic, because the pseudo relative permeability is only dependent on the saturation distribution, and totally independent of phase pressure distribution.

Kyte and Berry (1975) proposed a development over the Jacks *et al.* (1973) work on pseudo relative permeability curves. They tried to overcome the unrealistic assumption of equal potential for all of the vertically piled grid-blocks. In this method, average pressures for each coarse grid-block are calculated from the fine grid-block pressures; thereafter potential for each coarse grid-block could be calculated. He has presented the following equations:

$$\bar{P}_w = \frac{\sum_j ((k_{rw} Kh(P_w + \rho_w g H))_{i,median})_j}{\sum_j ((k_{rw} Kh)_{i,median})_j}, \tag{2.46}$$

$$\bar{P}_o = \frac{\sum_j ((k_{ro} Kh(P_o + \rho_o g H))_{i,median})_j}{\sum_j ((k_{ro} Kh)_{i,median})_j}, \tag{2.47}$$

The pseudo relative permeabilities are then calculated from Darcy's law using calculated potential differences.

$$\tilde{k}_{rw} = \frac{-\bar{\mu}_w \sum_j (q_w)_j}{\bar{T}\,(\Delta \bar{P}_w - \bar{\rho}_w g \Delta \bar{D})}, \tag{2.48}$$

$$\tilde{k}_{ro} = \frac{-\bar{\mu}_o \sum_j (q_o)_j}{\bar{T}\,(\Delta \bar{P}_o - \bar{\rho}_o g \Delta \bar{D})}, \tag{2.49}$$

The pseudo capillary pressure is directly calculated as the difference between the up-scaled phase pressures using

$$P_{c,ow} = \bar{P}_o - \bar{P}_w. \tag{2.50}$$

where $K =$ absolute permeability, $h =$ thickness of grid-block, $H =$ depth to the centre of coarse grid-block, $i, median =$ median horizontal grid-block within coarse grid-block, $j =$ grid-block index in vertical direction, $\rho =$ density, $g =$ gravity acceleration,$\Delta\overline{D} =$ average depth difference between the coarse grid-block and adjacent coarse grid-block, $q =$ flow rate and $P_{c,ow} =$ capillary pressure within coarse grid-block.

Stone (1991) initiated the use of total mobility to avoiding the problems associated with finding coarse grid average potential differences. In this paper, author overview the previous work related to pseudo relative permeability. He recommended the use of fractional flow models over the use of pressure potentials in the calculations. He stated that earlier methods are accurate only for low flow rate and good vertical communication; however, the fractional flow method is accurate for all flow rates and all coarse grid idealized model even non-communicating layers.

In his method the fractional flows of each phase are matched at the coarse and fine grid boundaries.

$$\bar{f_w} = \frac{\sum_i (q_t f_w)_i}{\sum_i (q_t)_i}. \tag{2.51}$$

Stone also defined a pseudo total mobility obtained as a transmissibility weighted average as follows:

$$\bar{\lambda}_t = \frac{\sum_i (T\lambda_t)_i}{\sum_k (T)_k}. \tag{2.52}$$

Pseudo relative permeabilities, assuming a coarse grid viscosity average, may be taken as follows:

$$\tilde{k}_{rw} = \mu_w \bar{f}_w \bar{\lambda}_t, \tag{2.53}$$

$$\tilde{k}_{ro} = \mu_o (1 - \bar{f}_w) \bar{\lambda}_t. \tag{2.54}$$

Because the upstream grid-block fluid viscosity is taken for the above calculations, the resulting pseudo functions are associated with the upstream grid-block.

The author states that all previously published methods are accurate only for low viscosity-gravity ratios, which correspond to a combination of a low production rate and good vertical communication between layers in the reservoir. However, his method is applicable for any production rate even when used for non-communicating layers from single fine grid model into a single coarse grid layer.

Guzman *et al.* (1996) used Stone's example in their paper to compare his method with Kyte and Berry and flux weighted potential method. The reservoir properties for this example are shown in Table 2.2 and the generated pseudo relative permeabilities by Guzman *et al.* are shown in Figure 2.4.

Table 2.2: Basic reservoir description for Stone example

		Layer 1	Layer 2
Porosity	%	15.0	10.0
Permeability	Md	100.0	200.0
Length	Ft	2000.0	2000.0
Height	Ft	10.0	10.0
Width	Ft	1000.0	1000.0
$\boldsymbol{p_c}$	psi	0.0	0.0
$\boldsymbol{S_{oi}}$	%	75.0	80.0
$\boldsymbol{S_{wc}}$	%	25.0	20.0
$\boldsymbol{S_{orw}}$	%	25.0	35.0
Outlet Pressure	psi	2000.0	2000.0
Injection Rate	Res bbl/day	0.07329	0.14658
Tilt of Layers	Ft/ft	0.1	0.1

Relative permeability to Oil $\left(\frac{S_{w2}-S_{wc}}{1-S_{wc2}}\right)^4$ $\left(\frac{S_{w1}-S_{wc}}{1-S_{wc1}}\right)^3$

Relative permeability to Water $\left(\frac{1-S_{w1}-S_{orw1}}{1-S_{wc1}-S_{orw1}}\right)^{1.5}$ $\left(\frac{1-S_{w2}-S_{orw2}}{1-S_{wc2}-S_{orw2}}\right)^{1.7}$

Fluid properties:

$\rho_w = 62.4\ (lb/ft^3)$; $\rho_o = 43.68\ (lb/ft^3)$; $\mu_w = 1\ cp$; $\mu_o = 100\ cp$

Figure 2.4 show that, for this example Kyte and Berry and flux weighted potential method have flow reversal problem (flow reversal means, by increasing the wetting phase saturation the relative permeability of wetting phase decreases and relative permeability of

wetting phase decreases which in opposite natural trend); however, Stone's method is relatively monotonic.

Many other methods have been published up to date. For example, the pore volume weighted method (Intera Information Technology, 1994) is similar to Kyte and Berry (1975) except in the way to find average pressure. The first one uses a pore volume weighted method to calculate up-scaled pressure, while the last one uses the product of effective permeability and thickness.

Cao and Aziz (1999) published a critical evaluation of pseudo functions. They tried to determine the range of validity of pseudo functions for up-scaling of multiphase flow with gravity and capillary pressure, thus they evaluated the performance of different kinds of pseudo functions under condition of different gravity numbers, capillary numbers and up-scaling levels. They expressed that, evaluated pseudo functions for strong gravity numbers do not work very well, and for intermediate gravity numbers it is not possible to use a single grid-block in the vertical direction. They also found that only the Jacks *et al.* (1973) method works well for the highly heterogeneous case and all other methods fail due to flow reversal.

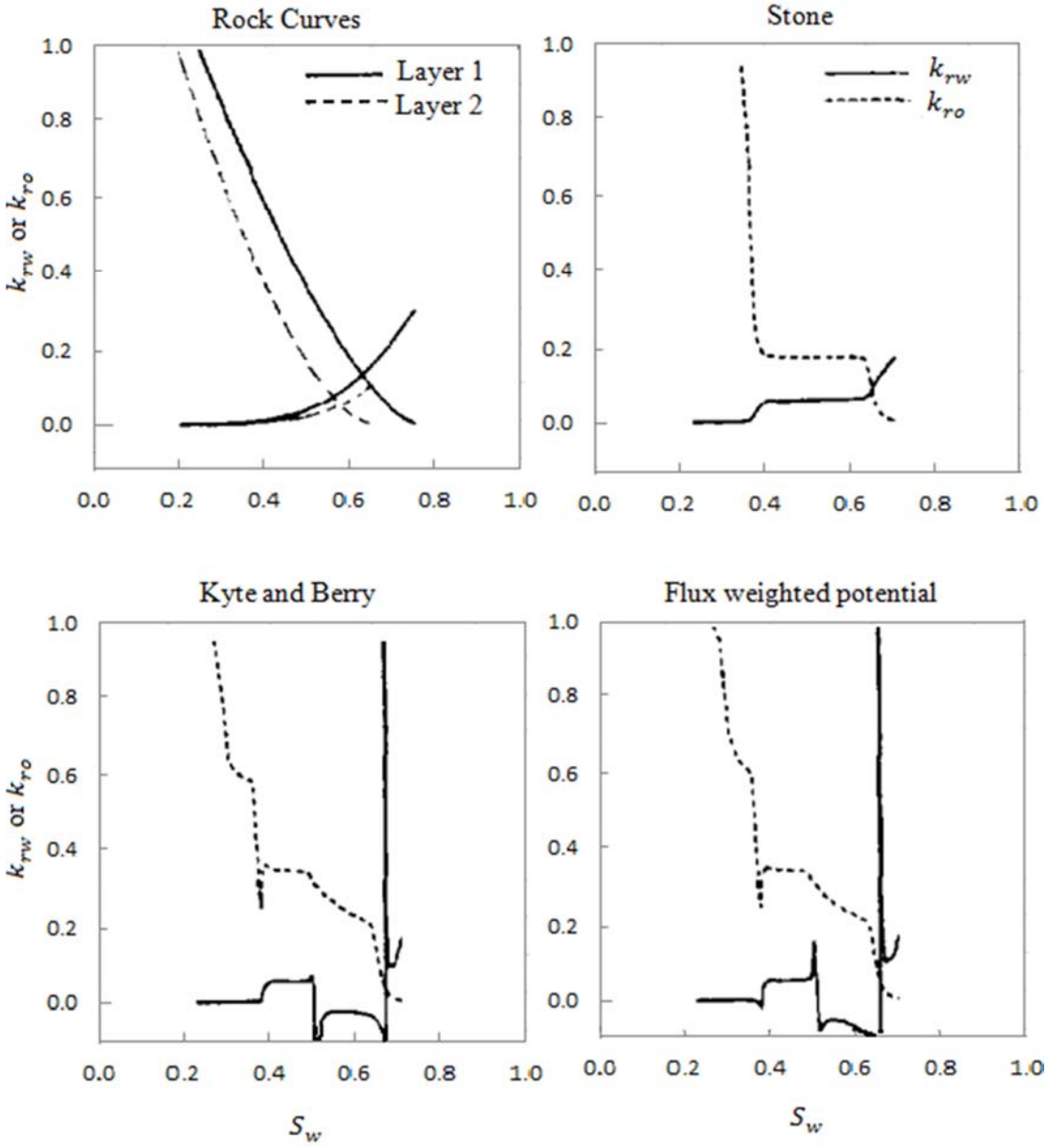

Figure 2.4: Rock and Pseudo Relative Permeabilities for Stone's example. Fine Grid 50x2 and Coarse Grids 5x1 (after Guzman, 1996)

CHAPTER 3

METHODOLOGY

This chapter presents the procedure of the two new methods for generating pseudo relative permeabilities for stratified waterflooding reservoir with i) constant pressure boundary condition and ii) constant flow rate boundary condition.

3.1 New method

The corresponding reservoir is divided into layers based on absolute permeabilities (from core data), with each layer characterized by thickness (h), porosity (ϕ), connate water saturation (S_{wc}), residual oil saturation (S_{or}), and relative permeability curve. These characteristics may be completely different or even the same.

Assumptions of this reservoir model include:

- The reservoir contains several layers with distinct properties as shown in Figure 3.1
- Incompressible fluids
- Gravity and capillary forces are negligible compared to viscous effects

- Each layer assumes a unique water-oil displacement front (1D layer)
- The outlet saturation varies after breakthrough (it is not a piston-like displacement)
- No lateral variation in reservoir properties within a given layer

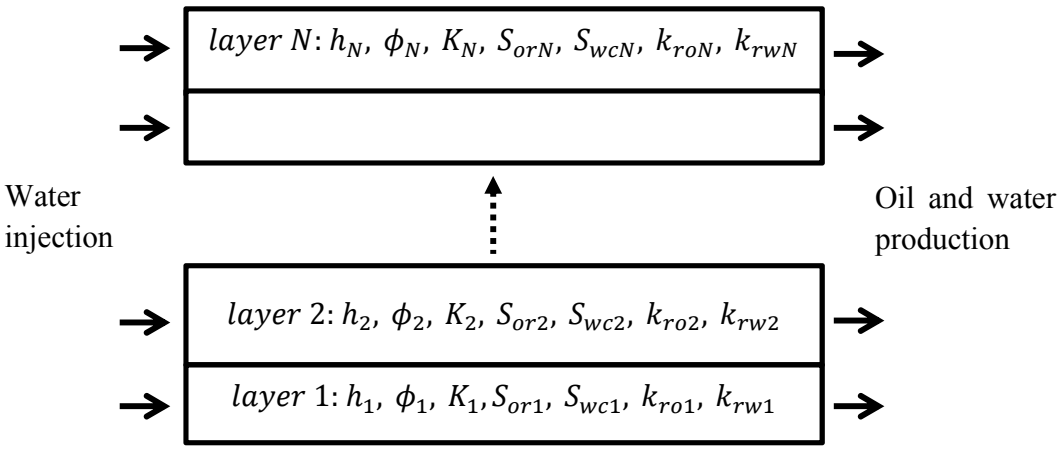

Figure 3.1: Stratified Reservoir Model

A flowchart depicting the proposed methodology is presented in Figure 3.2. It should be noted that the work flow is the same for the constant pressure case and the constant flow rate case with the exception of the calculation of breakthrough time (step 3).

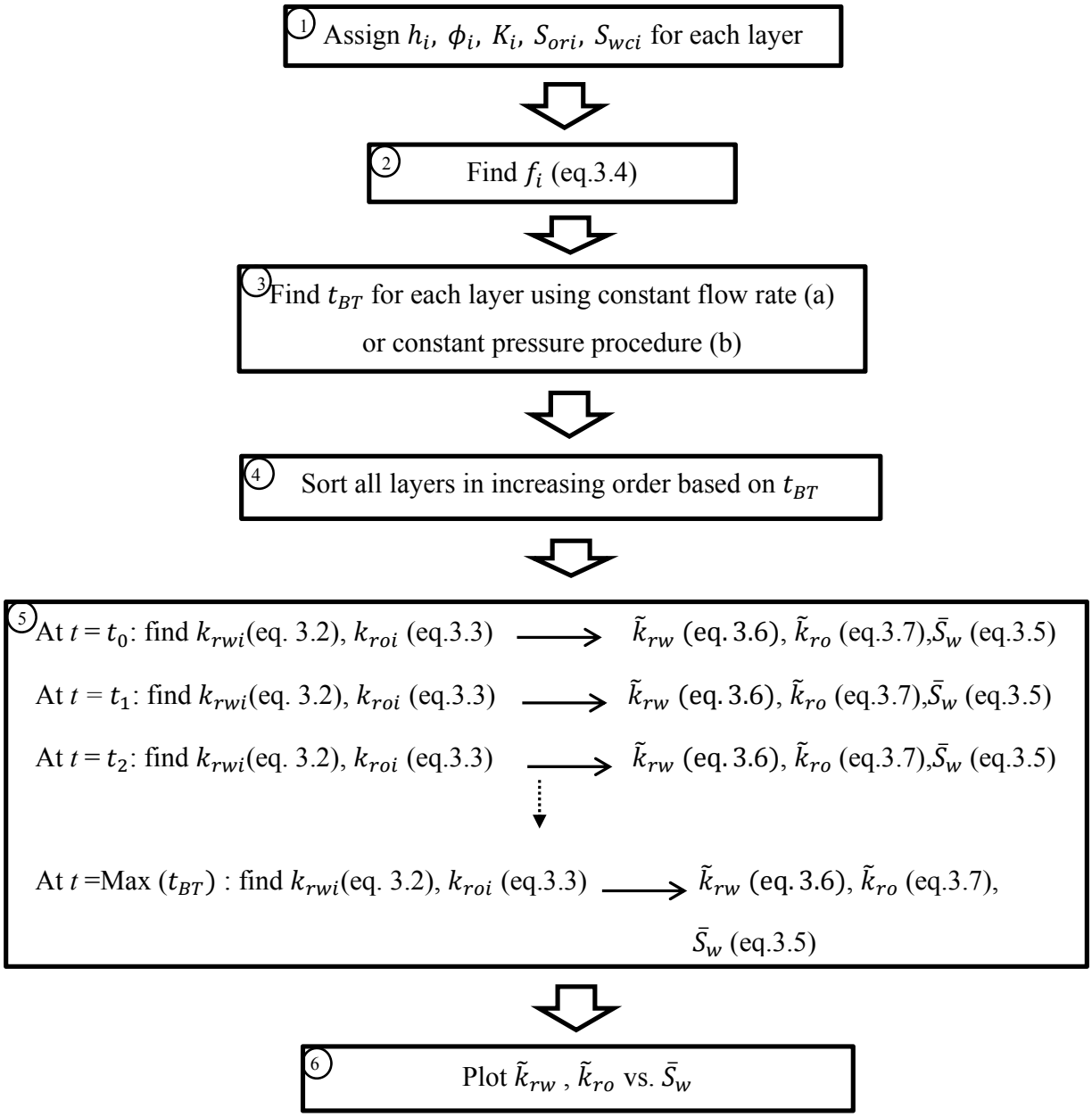

Figure 3.2: Flow Chart for Generating Pseudo Relative Permeability Curves

3.1.1 Generating the Fractional Flow Curves.

The fractional flow curve for each layer is given by

$$f_{wi} = \frac{\lambda_{wi}}{\lambda_{wi} + \lambda_{oi}} = \frac{\frac{k_{rwi}}{\mu_{wi}}}{\frac{k_{rwi}}{\mu_{wi}} + \frac{k_{roi}}{\mu_{oi}}}, \tag{3.1}$$

where k_{rwi} and k_{roi} can be calculated by the analytical model i.e.

$$k_{rwi} = a_w \left(\frac{S_{wi} - S_{wci}}{1 - S_{wci} - S_{ori}} \right)^{n_w}, \tag{3.2}$$

$$k_{roi} = a_o \left(\frac{1 - S_{wi} - S_{ori}}{1 - S_{wci} - S_{ori}} \right)^{n_o}. \tag{3.3}$$

In this investigation, we use $a_w = 0.3$, $a_o = 0.8$ and $n_w = n_o = 2$.

By substituting eq. (3.2) and eq. (3.3) in to eq. (3.1) we get:

$$f_{wi} = \frac{1}{1 + 2.67 \frac{\mu_{wi}}{\mu_{oi}} \left(\frac{1 - S_{wi} - S_{ori}}{S_{wi} - S_{wci}} \right)^2}. \tag{3.4}$$

3.1.2 Calculation of breakthrough time and outlet water saturation

I For the constant flow rate case

The fractional flow theory (Buckley Leverett, 1941) is used to calculate the breakthrough time and water saturation at the outlet after water breakthrough.

A saturation position in this case can be calculated using

$$x_{si} = \frac{q_T}{A\,\phi} f'_{si} t. \tag{3.5}$$

Consequently, by choosing $x_{si} = L$ as the breakthrough time (t_{BT}) is calculated using

$$t_{BT} = \frac{LA\phi}{q_T f'(S^*)}, \tag{3.6}$$

where A is the flow area, ϕ is porosity, q_T is total flow rate and $f'(S^*)$ is the slope of fractional flow at the specific saturation.

For $t < t_{BT}$, the outlet saturation will be S_{wc}. However, for $t > t_{BT}$, we can calculate x_s for some point in the interval (S_w^*, $1 - S_{or}$), then compare all calculated $x_s$with L. The saturation corresponding to $x_s = L$ is considered as the outlet saturation ($S_{w,outlet}$). The leading shock saturation (S_w^*) is calculated based on the Buckley-Leverett method. This method is shown schematically in Figure 3.3.

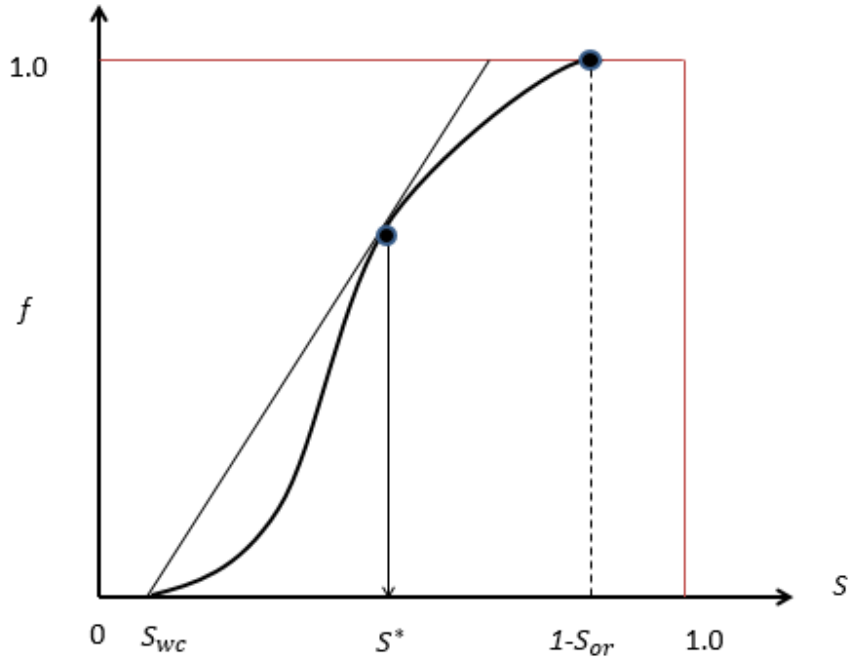

Figure 3.3: Determining the Front Water Saturation (after Welge, 1952)

II The constant pressure boundary case

Unlike the case using the constant flow rate boundary condition, in the constant pressure case the total Darcy velocity ($u_T = q_T/A$) varies over time and consequently the calculation of breakthrough time and saturation positions is different. Since the outlet saturations and breakthrough time are different, the relative permeability of each layer and hence the pseudo relative permeability curve is different.

A new constant boundary pressure extension to the classic Buckley-Leverett fractional flow theory (Johansen and James, 2015) is used to calculate the breakthrough time for each layer and saturation at the outlet after water breakthrough.

A saturation position for the constant pressure boundary case is calculated using

$$x_{si} = \frac{f'_{si}}{\phi} \int_0^t u_T(t)\, dt, \tag{3.7}$$

where $u_T(t)$ is the total flux velocity at time t and is given by

$$u_T(t) = \frac{\Delta p}{\sqrt{B^2 + 4ACt}}. \tag{3.8}$$

The breakthrough time is calculated using

$$t_{BT} = \frac{AL^2 + 2BL}{C}; \tag{3.9}$$

where,

$$A = \frac{1}{v_2} I_1 - \frac{1}{\lambda_T(S_R)}, \tag{3.10}$$

$$B = \frac{L}{\lambda_T(S_R)}, \tag{3.11}$$

$$C = \frac{2\Delta p}{\phi} v_2, \tag{3.12}$$

$$v_2 = \frac{f(S^*) - f(S^R)}{S^* - S^R}, \tag{3.13}$$

$$I_1 = \int_{1-S_{or}}^{S^*} \frac{f''(S)}{\lambda_T(S)} dS, \tag{3.14}$$

$$\lambda_T = K\left(\frac{k_{ro}}{\mu_o} + \frac{k_{rw}}{\mu_w}\right). \tag{3.15}$$

In these equations, S^R is initial water saturation, which normally equals to connate water saturation, S^* is front water saturation, K is absolute permeability and L is reservoir length.

After calculation of saturation position for some points in the interval (S_w^*, $1 - S_{or}$), the same approach as was used for the constant pressure flow rate case is used to detect the outlet saturation ($S_{w,outlet}$).

The layers are then sorted in order of descending breakthrough time to have a simpler data structure, however this step is not essential. Thereafter, average water saturation is calculated for each time step using the following procedure:

3.1.3 Average water saturation in the reservoir

Two different scenarios for calculating average water saturation are used. The first scenario uses average water saturation at the outlet face of reservoir and corresponding this to the

up-scaled relative permeabilities. The second scenario is to corresponding pseudo relative permeabilities to average water saturation in the entire reservoir.

I. At the outlet face

Average water saturation in the outlet reservoir is calculated for each time step using

$$\bar{S}_w = \frac{\sum_{i=1}^{n} S_{w,out_i} \phi_i h_i NG_i + \sum_{i=n+1}^{N} S_{wc_i} \phi_i h_i NG_i}{\sum_{i=1}^{N} \phi_i h_i \, NG_i}, \tag{3.16}$$

where S_{w,out_i} is the water saturation at the outlet face of each layer, which is a function of time; *n* is the number of layers in which water breakthrough has occurred; *NG* is net to gross ratio for V_{bulk} which is equal to V_{sand}/V_{bulk} to consider the existence of shale layers in the reservoir; and *N* is the total number of layers.

II. In the entire reservoir

Average water saturation in the entire reservoir is calculated for each time step using

$$\bar{S}_w = \frac{\sum_{i=1}^{n} \bar{S}_{wi} \, Lh_i \phi_i NG_i + \sum_{i=n+1}^{N} (\bar{S}_{wi} x_i h_i \phi_i NG_i + S_{wci}(L - x_i) \phi_i NG_i)}{\sum_{i=1}^{N} Lh_i \, \phi_i NG_i}, \tag{3.17}$$

where $\bar{S}_{wi}$ is average water saturation behind the leading water-oil displacing front at each layer and each time step; x_i is the water-oil displacing front location for each layer and each time step.

Now we need to calculate the average water saturation behind the leading water-oil displacing front ($\bar{S}_{wi}$). The calculation procedures for before breakthrough and after breakthrough of water are different.

A. Average water saturation in the entire reservoir before breakthrough of water

For this case, as shown in Figure 3.4, a tangent is drawn to fractional flow curve at the point S^*. The saturation corresponding to the intercept of this line and the line $f = 1$ is the average saturation behind the front. This method first developed by Welge (1952).

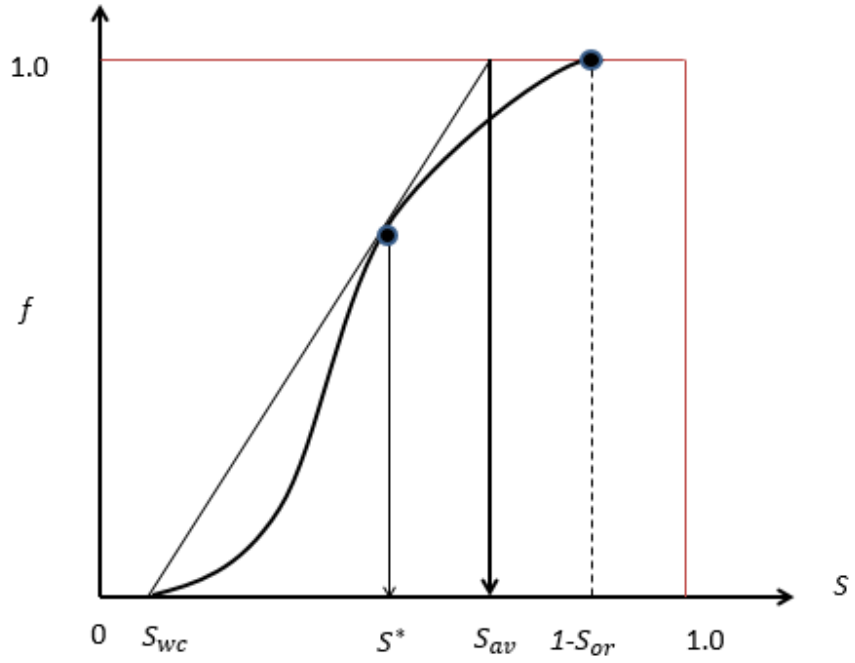

Figure 3.4: Determining Average Water Saturation behind the Front for $t < t_{BT}$

B. Average water saturation in the entire reservoir after breakthrough of water

For this case, as shown in Figure 3.5, first S_{w,out_i} is calculated by the method in section 3.1.2 then a tangent is drawn to fractional flow curve at point S_{w,out_i} instead of point S^* and the saturation corresponding to the intercept of this line and the line $f = 1$ is the average saturation behind the front.

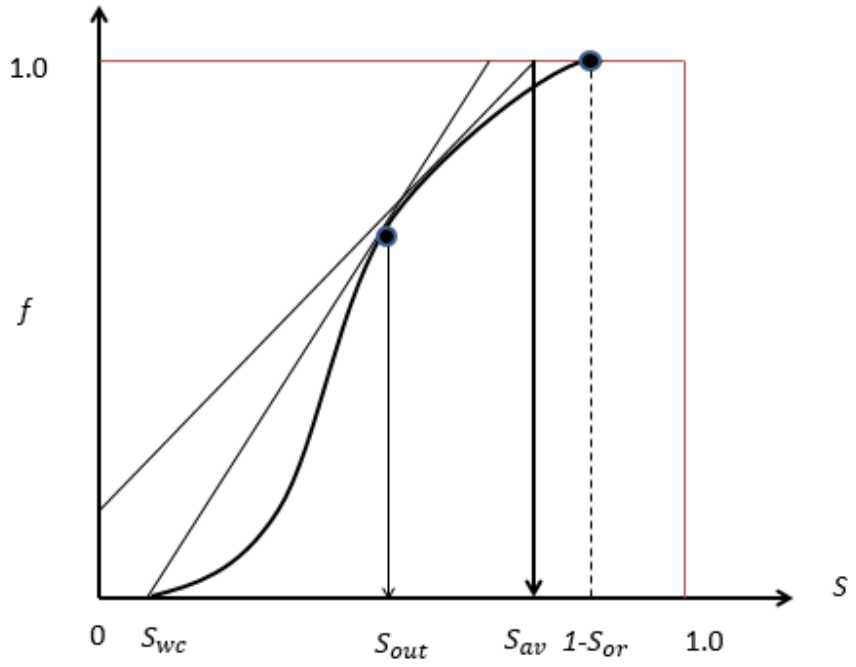

Figure 3.5: Determining Average Water Saturation behind the Front for $t > t_{BT}$

3.1.4 Generating pseudo relative permeabilities

The pseudo relative permeability curves are generated by calculating the average water saturation at the reservoir outlet before breakthrough of the first layer up to breakthrough of the last layer by using a definite time step for updating the average water saturation.

It should be mentioned that reservoir simulators assume constant pressure and constant flow rate for a time step. In reality we cannot have constant pressure boundary and constant flow rate simultaneously over time unless for mobility ratio equal to one ($M = 1$). At mobility ratio equal to one, both phases have the same mobility, so they are equivalent to single phase flow and for single phase flow constant flow rate and constant pressure boundary can be achieved at the same time. Regarding this fact, our new method is more

accurate only if mobility ratio is equal to one ($M = 1$). However, for mobility ratios other than one, time steps should be chosen small enough to avoid excessive error.

For each updated average water saturation ($\bar{S}_w$), the pseudo relative permeability to water and to oil, $\tilde{k}_{rw}$ and $\tilde{k}_{ro}$ respectively, are calculated using

$$\tilde{k}_{rw} = \frac{\sum_{i=1}^{N} k_{rwi} K_i h_i NG_i}{\sum_{i=1}^{N} K_i h_i NG_i}, \tag{3.18}$$

and

$$\tilde{k}_{ro} = \frac{\sum_{i=1}^{N} k_{roi} K_i h_i NG_i}{\sum_{i=1}^{N} K_i h_i NG_i}. \tag{3.19}$$

where k_{rwi} and k_{roi} are the relative permeability to water and the relative permeability to oil respectively at the outlet for each layer and each time-step.

It should be mentioned that relative permeability for each layer is normally obtained from a small core plug and then formulated by analytical correlations. The lateral up-scaling for relative permeability should also be considered, which is not in the scope of this thesis. We consider that we have the proper relative permeability for each layer and then we do vertical up-scaling for relative permeability.

The same method can be applied to generate up-scaled relative permeability of oil and gas. If the up-scaling relative permeability for oil and gas is done, the model would also be capable to handle three-phase systems.

The gas phase fractional flow curves similar to the water flood case are generated by:

$$f_{gi} = \frac{\lambda_{gi}}{\lambda_{gi} + \lambda_{oi}} = \frac{\frac{k_{rgi}}{\mu_{gi}}}{\frac{k_{rgi}}{\mu_{gi}} + \frac{k_{roi}}{\mu_{oi}}}. \quad (3.20)$$

The relative permeability correlation for gas and oil differs from water and oil. The following equation with proper indices can be used to calculate relative permeability of oil and gas:

$$k_{rgi} = a_g \left(\frac{S_g - S_{gc}}{1 - S_{lc} - S_{gc}} \right)^{n_g} \quad (3.21)$$

$$k_{roi} = a_o \left(\frac{1 - S_g - S_{lc}}{1 - S_{gc} - S_{lc}} \right)^{n_o} \quad (3.22)$$

$$S_{lc} = S_{wc} + S_{org} \quad (3.23)$$

where,

a_g = gas relative permeability at the residual liquid saturation,

a_o = oil relative permeability at residual gas saturation,

n_g, n_o = exponents on relative permeability curves,

S_{lc} = total critical liquid saturation,

S_{wc} = connate water saturation, and

S_{org} = residual oil saturation in the gas-oil system

S_{gc} = critical gas saturation

The rest of the procedure for generating up-scaled relative permeability of oil and gas is the same as water flooding case. The only difference is that we do our calculations based on gas phase fractional flow curve.

3.2 Alternative methods

Hearn's method is used as an alternative to generate a pseudo relative permeability curve for the constant flow rate case. Hearn's method is unable to handle the constant pressure boundary condition, because it is restricted to constant flow rate condition for finding the order of layering.

In Hearn's method, layers are sorted based on decreasing water breakthrough time. To determine the ordering, the layers are first arranged by decreasing the following expression:

$$\frac{K_i}{\varphi_i(1 - S_{wci} - S_{roi})}. \tag{3.20}$$

This equation is a good approximation to find the ordering of the water breakthrough of the layers, however it is not precise. The idea for this equation comes from physical facts that higher permeability result in faster moving of the particles inside porous media, thus smaller breakthrough time. Also, higher porosity and higher ΔS, mobile saturation, means higher available space to be filled with flooding water, thus result in lower breakthrough time.

In the next step, the following expression is calculated:

$$\Delta f_n = \frac{\frac{k_{rw}(S_{ro})}{\mu_w}\sum_1^n K_i h_i}{\frac{k_{rw}(S_{ro})}{\mu_w}\sum_1^n K_i h_i + \frac{k_{ro}(S_{wc})}{\mu_w}\sum_{n+1}^N K_i h_i} - \frac{\frac{k_{rw}(S_{ro})}{\mu_w}\sum_1^{n-1} K_i h_i}{\frac{k_{rw}(S_{ro})}{\mu_w}\sum_1^{n-1} K_i h_i + \frac{k_{ro}(S_{wc})}{\mu_o}\sum_{n+1}^N K_i h_i}. \quad (3.21)$$

Equation 3.21 represents the water flow rate in layer *n* over total flow rate, Q_{wn}/Q_t. Now using the above expression, velocity for each layer is calculated:

$$v_n = \frac{Q_{wn}}{Area\ open\ to\ flow\ in\ layer\ n}, n = 1, 2, \dots, N. \quad (3.22)$$

where

$$Area\ open\ to\ flow\ in\ layer\ n = Wh_n\varphi_n(1 - S_{wcn} - S_{ron}). \quad (3.22)$$

$$Q_{wn} = Q_t\Delta f_n \quad (3.23)$$

By substitute equation 3.22 and 3.23 into equation 3.21 we get

$$v_n = \frac{Q_t\Delta f_n}{Wh_n\varphi_n(1 - S_{wcn} - S_{ron})}, n = 1, 2, \dots, N. \quad (3.24)$$

If the velocities are in decreasing order, the ordering is correct. Otherwise, the layers would be rearranged based on decreasing order of velocity and the calculation would be repeated. This is an iterative procedure because Δf_n depends on the chosen ordering and v_n also

depends on Δf_n. Thus using calculated velocities, the ordering of the layers is modified and new iteration will start. The process is continued until a unique ordering is achieved.

After determining the ordering, the pseudo relative permeabilities are calculated using

$$\tilde{k}_{rw} = \frac{k_{rw}(S_{ro}) \sum_{i=1}^{n} K_i h_i}{\sum_{i=1}^{N} K_i h_i}, \tag{3.25}$$

$$\tilde{k}_{ro} = \frac{k_{ro}(S_{wc}) \sum_{i=n+1}^{N} K_i h_i}{\sum_{i=1}^{N} K_i h_i}, \tag{3.26}$$

$$\bar{S}_w = \frac{\sum_{i=1}^{n} h_i \varphi_i \left(1 - S_{ro_i}\right) + \sum_{i=n+1}^{N} S_{wc_i} h_i}{\sum_{i=1}^{N} h_i \, \varphi_i}. \tag{3.27}$$

Where $Q_t =$ total injection rate, $K =$ absolute permeability, $\mu_w =$ viscosity of water, $\mu_o =$ viscosity of oil, $i =$ summation index, $n =$ the number of layers that water breakthrough have occurred, $N =$ total number of layers, $k_{rw}(S_{ro}) =$ relative permeability of water at residual oil saturation, $k_{ro}(S_{wc}) =$ relative permeability of oil at connate water saturation, $\tilde{k}_{rw} =$ pseudo relative permeability of water, $\tilde{k}_{ro} =$ pseudo relative permeability of oil and $\bar{S}_w =$ average water saturation.

Equations 3.25 and 3.26 is an average weighted by product of absolute permeability and thickness, simply resulted from Darcy law. For derive of these equations it assumed that for the layers that breakthrough has occurred the outlet water saturation is $\left(1 - S_{ro_i}\right)$ and for those that breakthrough of water has not occurred the water saturation is S_{wc_i},

consequently for the layer that breakthrough has occurred $k_{rw} = k_{rw}(S_{ro})$ and $k_{ro} = 0$. Also for the layers that breakthrough has not occurred $k_{rw} = 0$ and $k_{ro} = k_{ro}(S_{wc})$.

Equation 3.27 also is an average weighted by product of porosity and thickness.

The Dykstra-Parson's method is used as an alternative for the constant pressure boundary case. In this method, the Dykstra-Parson (1952) approach for ordering layers, based on water breakthrough, is used. Based on Dykstra-Parson finding, breakthrough occurs first in a layer with a higher value of

$$\frac{K_i \lambda'_{wi}}{\phi_i \Delta S_i} \frac{1}{(1 + M_i)}, \tag{3.28}$$

where λ'_{wi} is endpoint water motility, M_i is endpoint mobility ratio and ΔS_i is mobile saturation that are calculated using

$$\lambda'_{wi} = (\frac{k'_{rw}}{\mu_w})_i, \tag{3.29}$$

$$M_i = (\frac{k_{rw}}{\mu_w} \frac{\mu_o}{k_{ro}})_i, \tag{3.30}$$

and

$$\Delta S_i = (1 - S_{wc} - S_{or})_i \,. \tag{3.31}$$

After determining the ordering of layers using Dykstra-Parson, a pseudo relative permeability curve is generated using the rest of Hearn's approach.

CHAPTER 4

RESULTS AND DISCUSSIONS

4.1 Analysis of up-scaled relative permeability curves

4.1.1 Reservoir Description:

The following hypothetical reservoir (Table 4.1) is used to analyze the up-scaled relative permeability curves. The data corresponding to this reservoir is used in the MATLAB program to generate the up-scaled relative permeabilities (all related MATLAB code is in Appendix B). The input parameters of interest are changed in MATLAB, while all other reservoir properties are kept unchanged in order to investigate their effects on the up-scaled relative permeability. This analysis provides a view to understand sensibility of the up-scaled relative permeability curves to the changing parameters. This procedure is repeated both for constant pressure boundaries and constant flow rate boundaries condition.

Table 4.1: Reservoir Properties

Layer #	K(*mD*)	φ (%)	h (*m*)	S_{wc}	S_{or}
1	8.3	6	2	0.20	0.20
2	10.1	9	2	0.22	0.25
3	8.6	8	2	0.21	0.26
4	7.3	7	2	0.18	0.23
5	8.2	8	2	0.19	0.24
6	11.1	12	2	0.20	0.28
7	11.7	10	2	0.17	0.21
8	13.2	11	2	0.23	0.23
9	11.4	9	2	0.20	0.26
10	7.1	8	2	0.18	0.22
11	10.6	7	2	0.16	0.27
12	11.2	10	2	0.18	0.26
13	8.4	9	2	0.20	0.24
14	8.9	10	2	0.24	0.25
15	12.3	18	2	0.21	0.26
16	17.5	15	2	0.19	0.29
17	17.4	14	2	0.17	0.25
18	13.9	11	2	0.23	0.24
19	12.6	16	2	0.20	0.28
20	5.9	8	2	0.18	0.28
μ_o= 2.8 cp		$\mu_w = 0.8$ cp		$L = 500\ m$	

4.1.2 The Effect of Flow Rate on Up-scaled Relative Permeability for Constant Flow Rate Boundaries Case:

In this section, the flow rate of the reservoir model is changed, while all other reservoir properties are kept constant. This study is done using two different flow rates, $Q_w = 1000\ bbl/day$ and $Q_w = 2000\ bbl/day$, and then the shape of up-scaled relative permeability curves is compared.

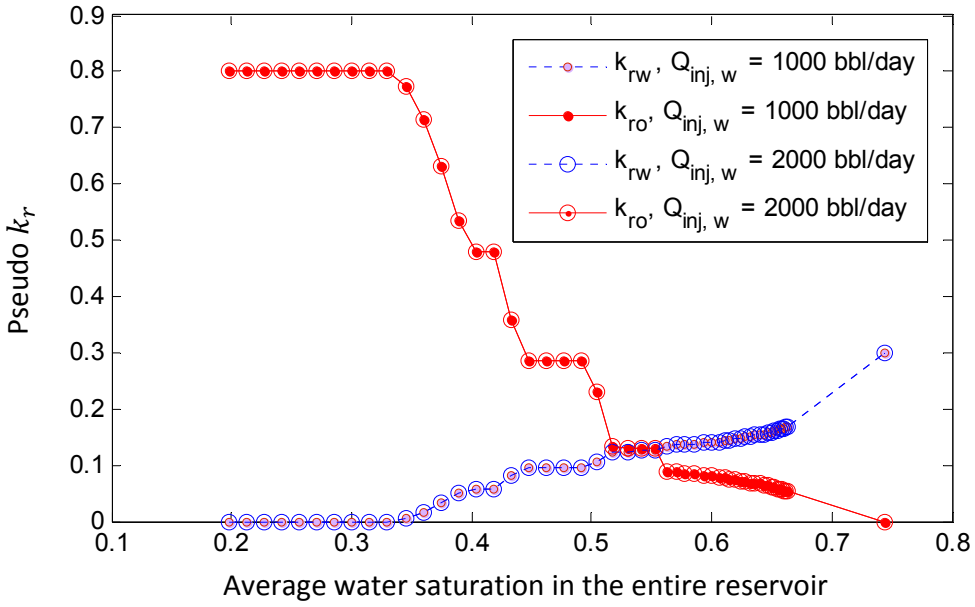

(a)

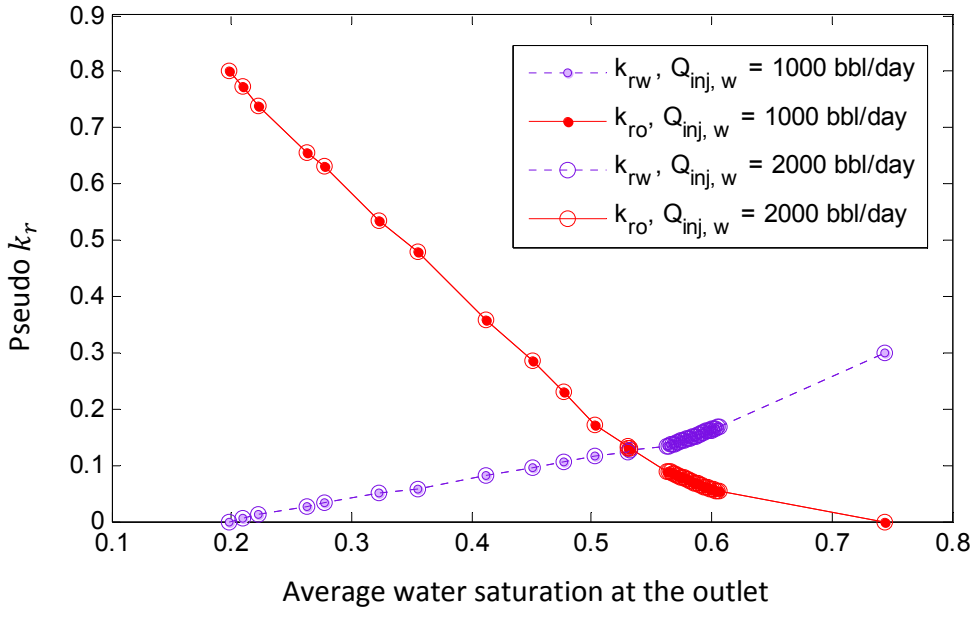

(b)

Figure 4.1: Effect of Flow Rate on Up-Scaled Relative Permeability for Constant Flow Rate Case

Figure 4.1.a is for the up-scaled relative permeability for the average water saturation through the entire reservoir model, and Figure 4.1.b is for up-scaled relative permeability for the average water saturation at the outlet reservoir model. The difference between Figures 4.1.a and 4.1.b is the way to find average water saturation.

If the up-scaled relative permeability is related to the average water saturation in the entire reservoir, as injected water increases the average water saturation in the entire reservoir increases; however, up-scaled relative permeability only changes significantly after breakthrough of water in a new layer. This causes the jumps observed in Figure 4.1.a and all the following up-scaled relative permeabilities corresponding to average water saturation in the entire reservoir. If the up-scaled relative permeability is related to the average water saturation at the outlet reservoir face, both the up-scaled relative permeability and average water saturation change significantly after water breakthrough in a new layer. Therefore, Figure 4.1.b and all the following up-scaled relative permeabilities corresponding to the average water saturation at the outlet reservoir face are monotonic.

Because the total flow rate affects the breakthrough time in each layer and the up-scaled relative permeability is a function of breakthrough time, we would like to investigate the effects of flow rate on up-scaled relative permeability to see how safe it is to use a generated up-scaled relative permeability for another production operating condition.

Figure 4.1.a and Figure 4.1.b show that the amount of flow rate does not have any effect on the shape of up-scaled relative permeability as long as the flow rate is kept constant. In other words, once an up-scaled relative permeability curve is generated for a reservoir

model with constant flow rate boundaries, it will be valid for all other operating flow rates of that model as long as they are kept fixed.

4.1.3 The Effect of Pressure Difference on Up-scaled Relative Permeability Curve for Constant Pressure Boundaries Case:

In this section, sensitivity to the pressure difference of the reservoir model is investigated. All other reservoir properties are kept constant. This study is done for two different pressure differences, $\Delta p = 10^6\ Pa$ and $\Delta p = 10^9\ Pa$, and then the shape of the up-scaled relative permeability curves are compared.

Because the pressure difference affects the breakthrough time in each layer and up-scaled relative permeability is affected by breakthrough time combination of all layers, we would like to investigate the effects of pressure difference on up-scaled relative permeability to see how safe it is to use a generated up-scaled relative permeability for another situation, which operating pressure is changed.

Figure 4.2.a is for up-scaled relative permeability for the average water saturation through the entire reservoir model, and Figure 4.2.b is for up-scaled relative permeability for the average water saturation at the outlet reservoir model.

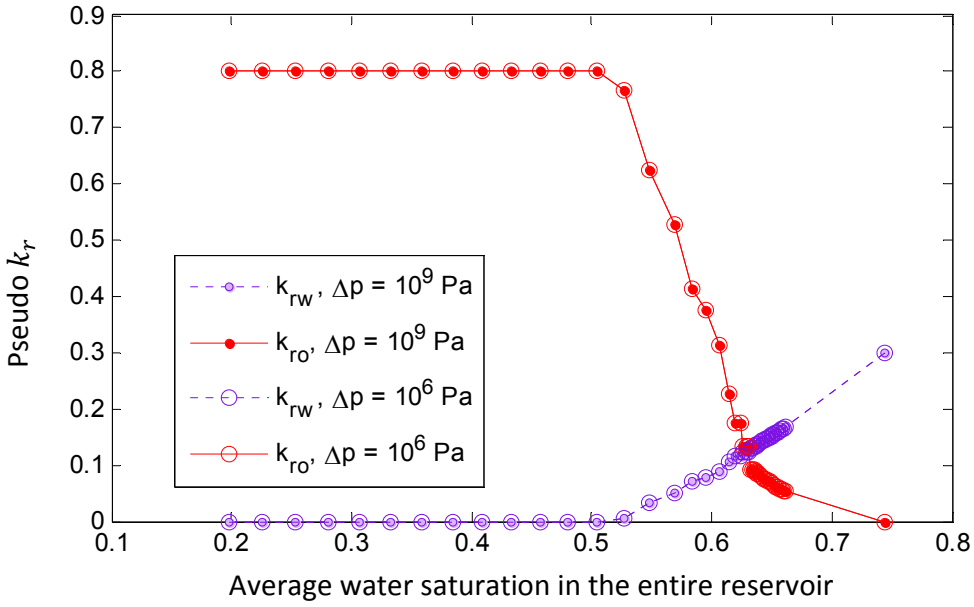

(a)

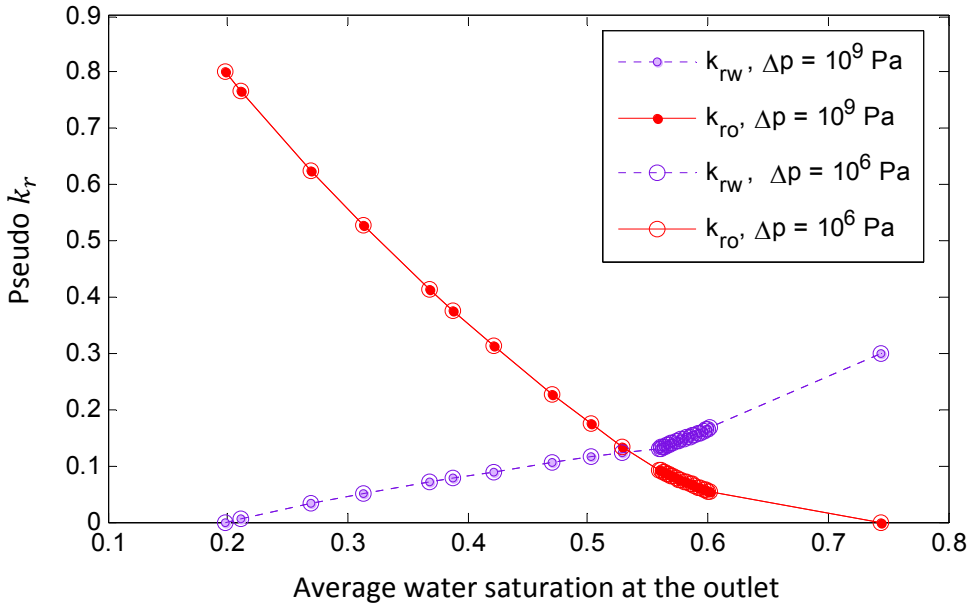

(b)

Figure 4.2: Effect of Pressure Difference on Up-Scaled Relative Permeability for Constant Pressure Boundary Case

By investigating Figure 4.2.a and 4.2.b, it can be determined that the magnitude of pressure difference does not have any effect on the shape of up-scaled relative permeability as long as it is kept constant. In other words, once an up-scaled relative permeability curve is generated for a constant pressure boundaries reservoir model, it is valid for all other operating pressures of that model as long as they are kept fixed.

4.1.4 The Effect of Reservoir Length on Up-scaled Relative Permeability Curve:

In this section, the effect of the reservoir length on the up-scaled relative permeability curves is studied. This study is done for two different reservoir lengths, $L = 1000\ m$ and $L = 500\ m$, and then the shape of up-scaled relative permeability is compared. In these two cases, all other reservoir properties are the same.

Because the reservoir length affects the breakthrough time in each layer and up-scaled relative permeability is affected by breakthrough time combination of all layers, we would like to investigate the effects of reservoir length on up-scaled relative permeability to see how safe it is to use a generated up-scaled relative permeability for another situation which injection well or production well is moved to another location.

Figure 4.3.a shows the up-scaled relative permeability for the average water saturation through the entire reservoir model and constant flow rate case. Figure 4.3.b shows the up-scaled relative permeability versus average water saturation at the outlet reservoir model. Both Figures 4.3.a and 4.3.b are for constant flow rate. Figure 4.4.a shows the up-scaled relative permeability versus average water saturation through entire reservoir model Figure

4.4.b shows the up-scaled relative permeability versus average water saturation at the outlet, both for the constant pressure boundary condition.

By investigating Figure 4.3.a, Figure 4.3.b, Figure 4.4.a and Figure 4.4.b, it can be determined that the reservoir length has no effect on the shape of up-scaled relative permeability, neither for constant flow rate case nor for the constant pressure boundary case, as long as all other reservoir properties are kept unchanged. In other words, once a pseudo relative permeability curve is generated for a reservoir, it can be used in the case that injection well or production well moved to another location, or for any reason the distance between injection well and production well is updated.

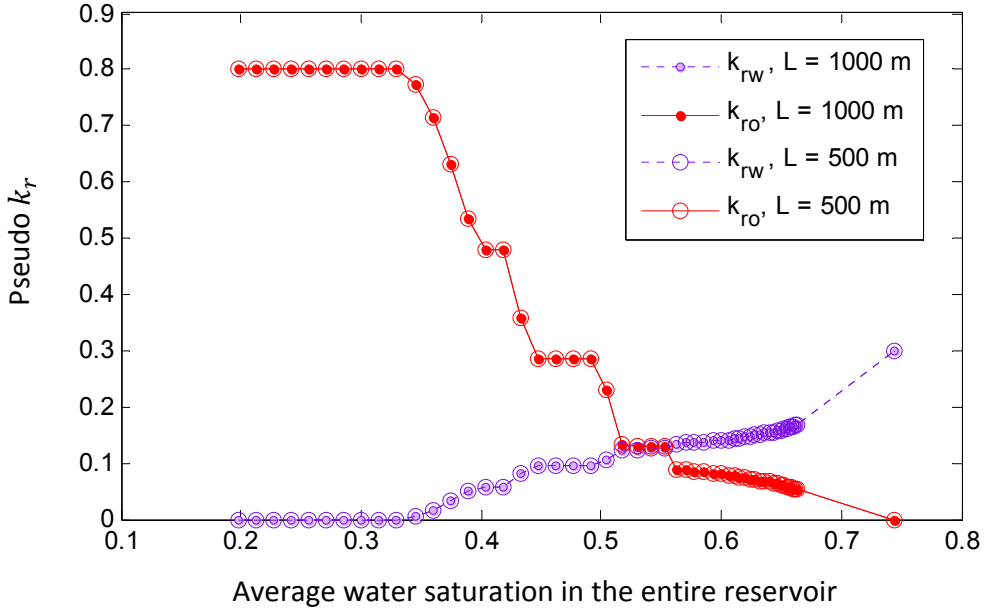

(a)

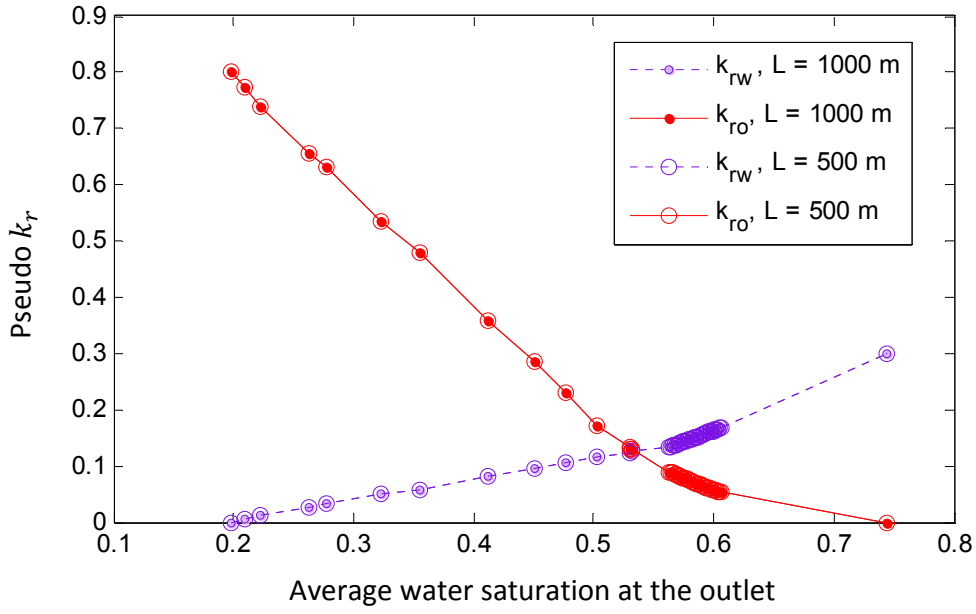

(b)

Figure 4.3: Effect of Reservoir Length on Up-Scaled Relative Permeability for Constant Flow Rate Case

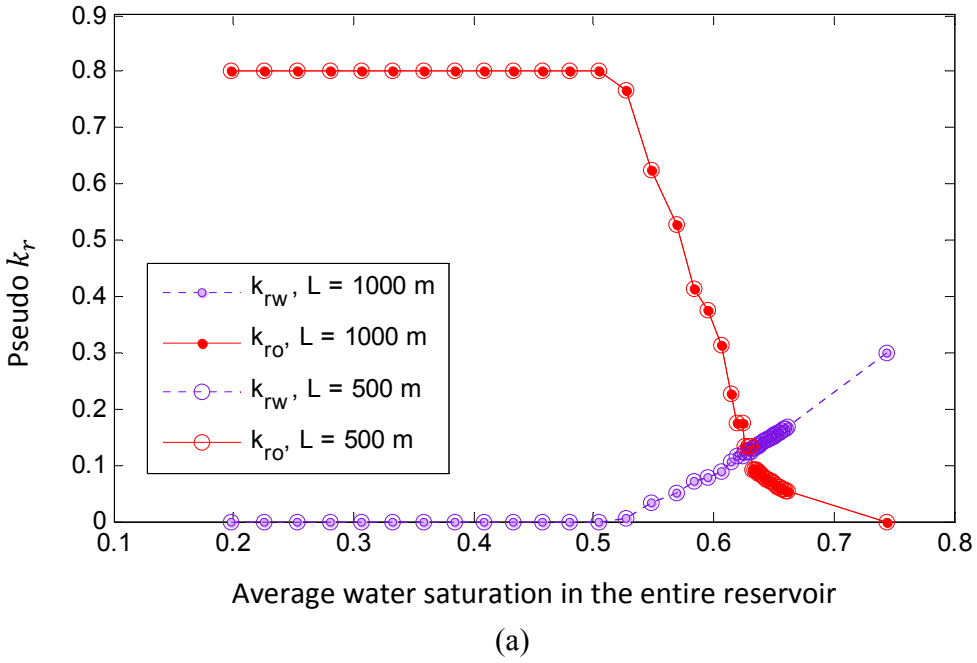

(a)

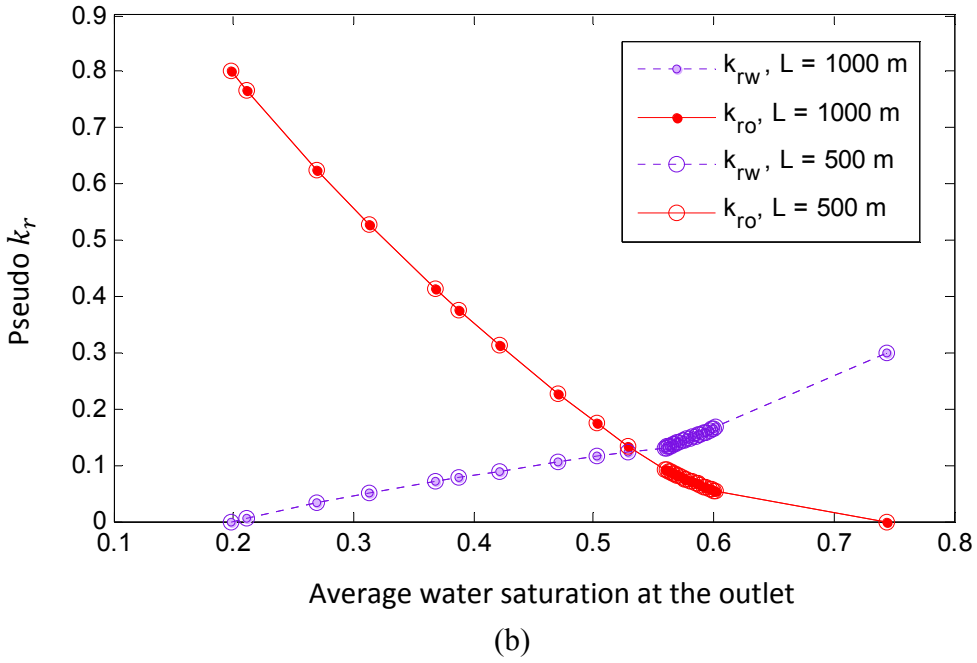

(b)

Figure 4.4: Effect of Reservoir Length on Up-Scaled Relative Permeability for Constant Pressure Boundary Case

4.1.5 The Effect of Fluids Viscosity Ratio on Up-scaled Relative Permeability

In this section, the effect of reservoir viscosity ratio on the shape of up-scaled relative permeability curves is studied. This study is done for two different reservoir viscosity ratios of $\mu_w / \mu_o = 0.25$ and $\mu_w / \mu_o = 4$ for water flood, then the shape of up-scaled relative permeability is compared. In these two cases all other reservoir properties remain the same.

Figure 4.5.a shows that by increasing the viscosity ratio of water to oil for the up-scaled relative permeability corresponding to average water saturation in the entire reservoir for the **constant flow rate case**, the water breakthrough occurs at a higher average water saturation in the entire reservoir. The up-scaled relative permeability of oil also increases for water saturations up to 0.57 and then decreases dramatically. However, the up-scaled relative permeability of water decreases until an average water saturation of 0.43 is reached and then increases significantly.

By investigating Figure 4.5.b, it can be determined that by increasing the viscosity ratio of water to oil for the up-scaled relative permeability corresponding to average water saturation at the outlet reservoir for the **constant flow rate case**, both the up-scaled relative permeability of water and oil increases significantly.

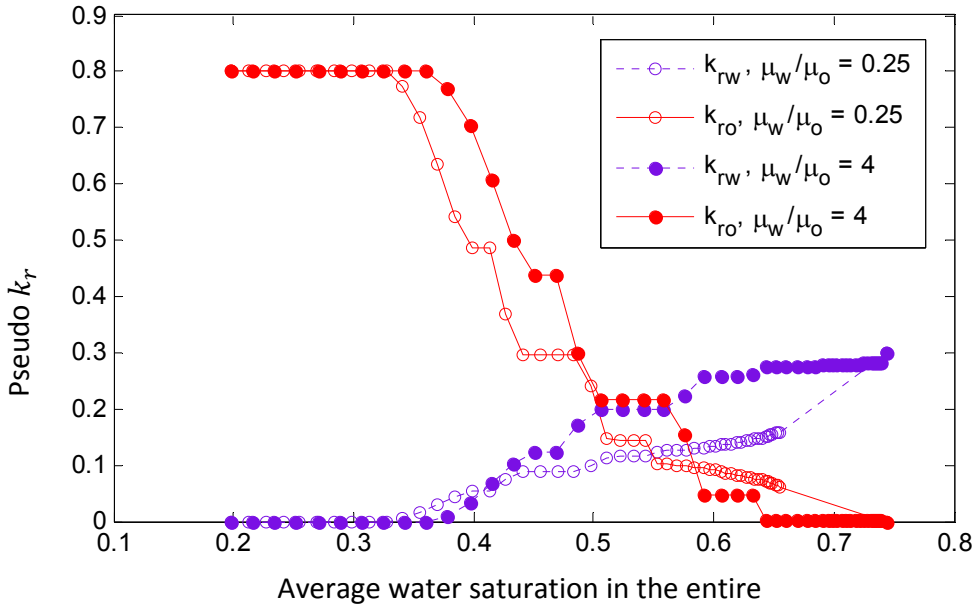

(a)

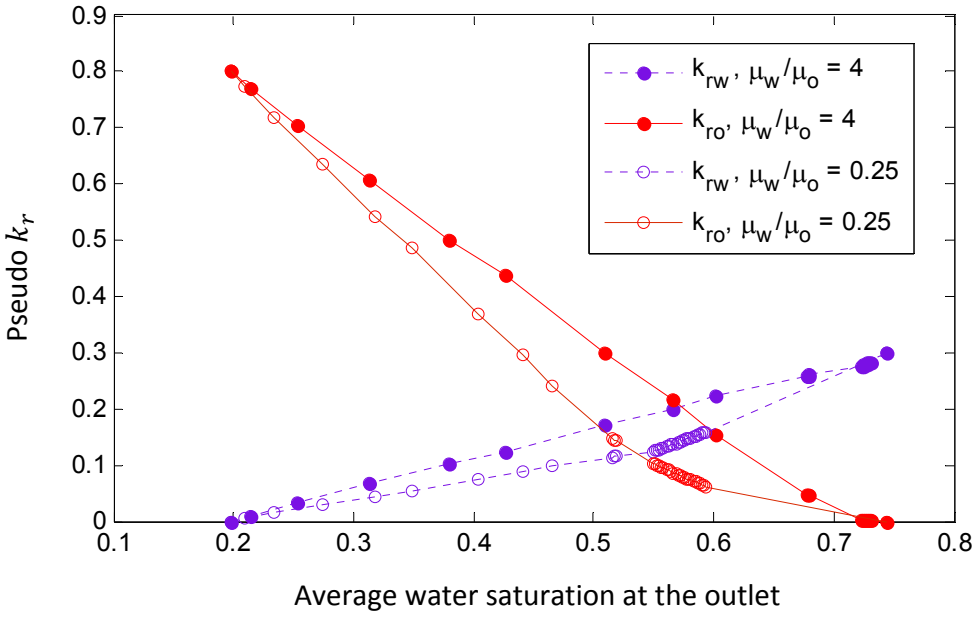

(b)

Figure 4.5: Effect of Viscosity Ratio on Up-Scaled Relative Permeability for Constant Flow Rate Case

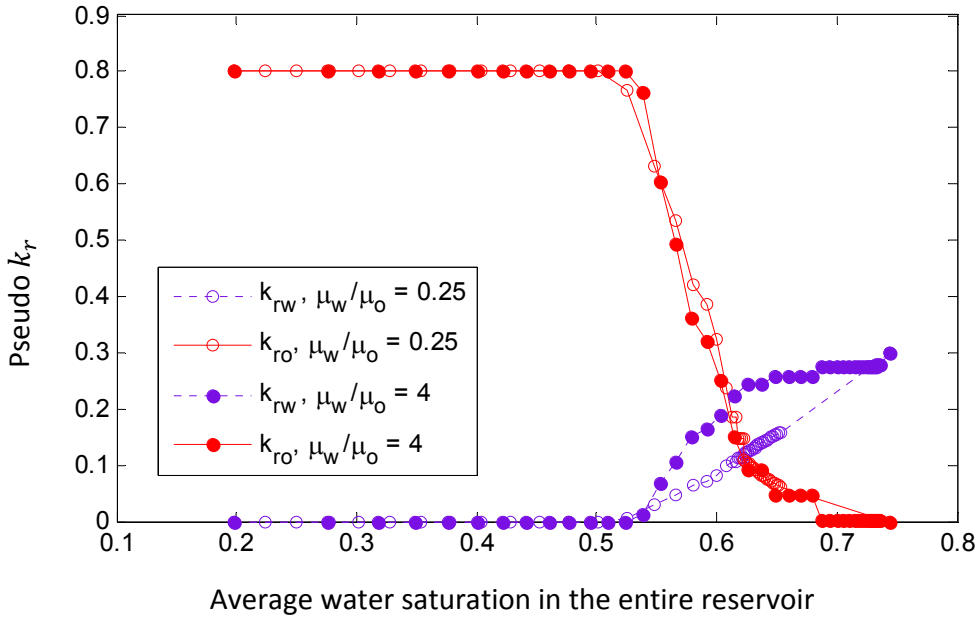

(a)

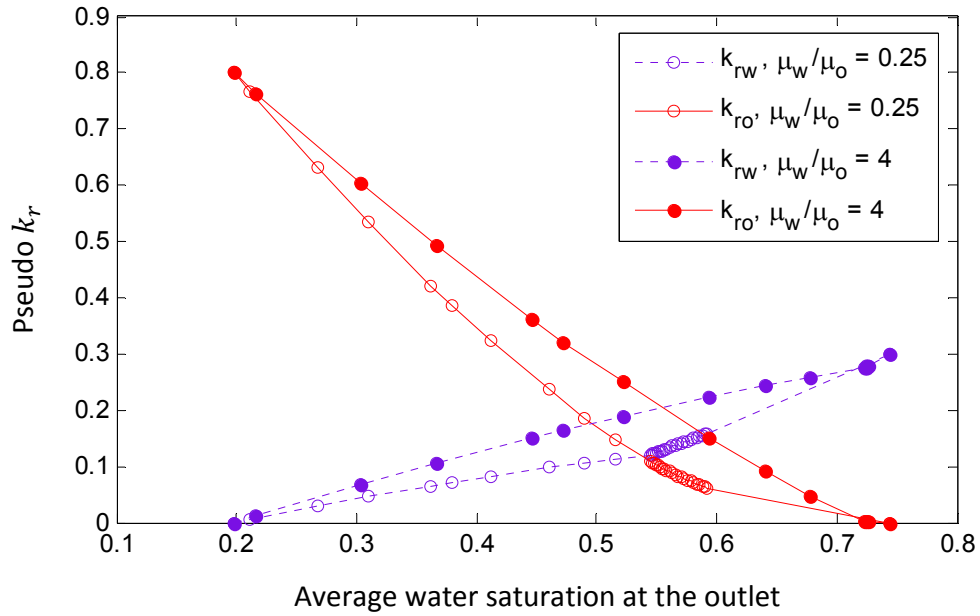

(b)

Figure 4.6: Effect of Viscosity Ratio on Up-Scaled Relative Permeability for Constant Pressure Boundary Case

Figure 4.6.a shows that, by increasing viscosity ratio of water to oil for the up-scaled relative permeability for the average water saturation in the entire reservoir for the **constant pressure boundary case**, the up-scaled relative permeability of oil increases almost for all saturation ranges. However, the up-scaled relative permeability of oil is not affected significantly.

Figure 4.6.b indicates that by increasing viscosity ratio of water to oil for the up-scaled relative permeability corresponding to average water saturation at the outlet reservoir for **the constant pressure boundary case**, both the up-scaled relative permeability of water and oil increases significantly.

Generally speaking, the effect of fluids viscosity ratio on up-scaled relative permeability corresponding to average water saturation at the outlet reservoir face is almost the same for constant flow rate case and constant pressure boundary case. In this case water saturation of displacing water-oil front (S^*) of layers in which water breakthrough occurs mainly control the shape of up-scaled relative permeability and this saturation is the same for both cases.

The effect of fluids viscosity ratio on up-scaled relative permeability corresponding to average water saturation in the entire reservoir is different for constant flow rate case and constant pressure boundary case. In this case, besides water saturation of displacing water-oil front (S^*) of layers in which water breakthrough occurs, the breakthrough time for that layer plays a role in the control of the shape of up-scaled relative permeability as well and

this causes the amount of change in up-scaled relative permeability to be different due to changes in viscosity ratio for constant flow rate and constant pressure boundary case.

4.1.6 The Comparison of Up-scaled Relative Permeability Curve

In this section the up-scaled relative permeability curves generated by different methods are compared.

In the constant pressure boundary case, unlike the case using the constant flow rate boundary condition, the total Darcy velocity ($u_T = q_T/A$) varies over time and consequently the calculation of breakthrough time and saturation positions is different. Since the outlet saturations and breakthrough time are different, the relative permeability of each layer and hence the up-scaled relative permeability curve is different.

I. New method constant pressure boundary vs. constant flow rate (using average water saturation in the entire reservoir)

Figure 4.7 shows the up-scaled relative permeability corresponding to average water saturation in the entire reservoir for the constant pressure boundary case versus the constant flow rate case.

By investigating this figure, it is shown that for the constant pressure boundary case the water breakthrough occurs at a higher average water saturation in the entire reservoir. Moreover, oil relative permeability for the constant pressure boundary is higher than the up-scaled oil relative permeability for the constant flow rate case for all saturation ranges. However, up-scaled water relative permeability for the constant pressure boundary is lower

than the up-scaled water relative permeability for the constant flow rate case for all saturation ranges by a significant amount.

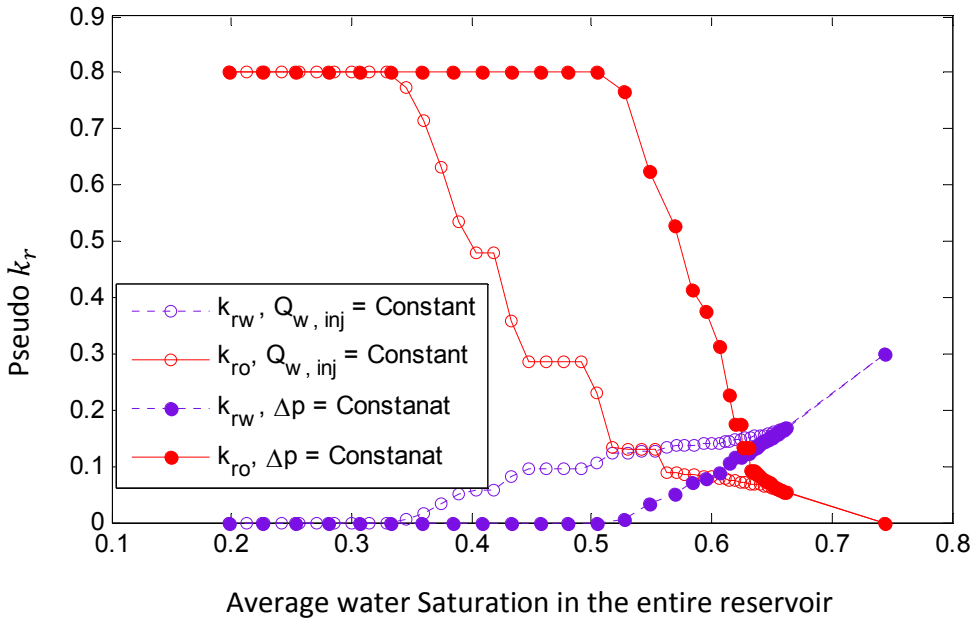

Figure 4.7: Up-scaled Relative Permeability Corresponding to Average Water Saturation in the Entire Reservoir **(Constant Pressure Boundary Case versus Constant Flow Rate Case)**

II. New method constant pressure boundary vs. constant flow rate (using average water at the outlet face)

Figure 4.8 compares the up-scaled relative permeability corresponding to the average water saturation at the outlet face by our new method for the constant pressure boundary case versus the constant flow rate case.

By investigating Figure 4.8, it is shown that the up-scaled oil relative permeability for constant pressure boundary is lower than the up-scaled oil relative permeability for the

constant flow rate case until water breakthrough occurs in all layers, after which up-scaled oil relative permeability becomes equal with the constant flow rate case. However, up-scaled water relative permeability for the constant pressure boundary is higher than up-scaled water relative permeability for the constant flow rate case until water breakthrough occurs in all layers and after that becomes equal with the constant flow rate case.

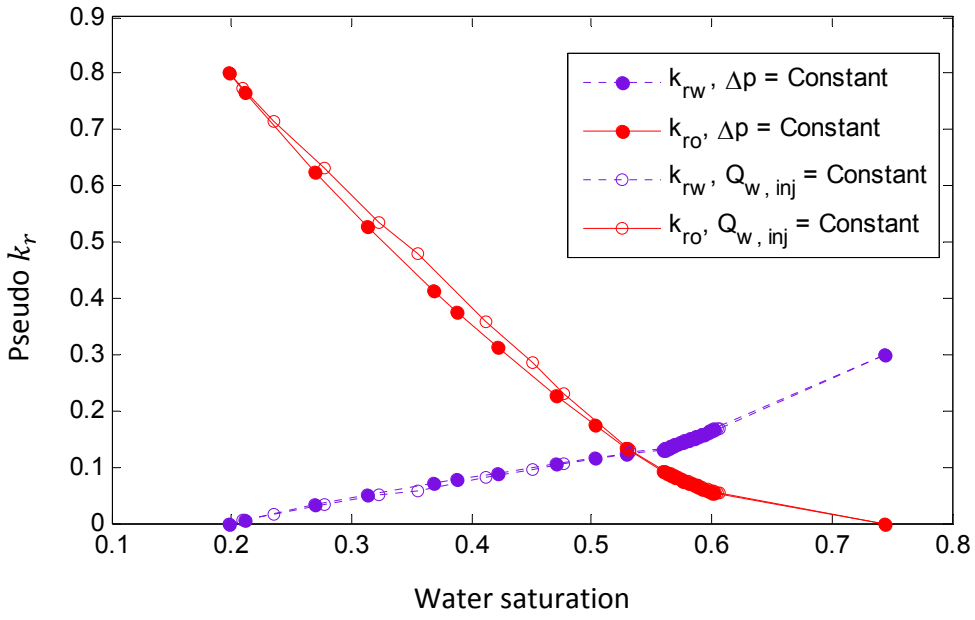

Figure 4.8: Up-scaled relative Permeability Corresponding to Average Water Saturation at the Outlet Reservoir Face **(Constant Pressure Boundary Case Versus Constant Flow Rate Case)**

These differences are unlike the behavior of intrinsic rock relative permeability curves, which are the same for constant pressure boundary and constant flow rate conditions. The pseudo relative permeability curves are the main controllers for flow in simulators and even a small change in these curves will cause a significant change in predicted recovery and water cut. Thus a generated pseudo relative permeability for constant pressure

boundary or constant flow rate operating condition cannot be used for the other operating condition. If a generated up-scaled relative permeability curve for constant pressure boundary condition is used for the constant flow rate case, the recovery factor will be underestimated. Vice versa if a generated up-scaled relative permeability curve for constant flow rate condition is used for the constant pressure case, the recovery factor will be overestimated.

III. Hearn's method (constant flow rate) vs. Dykstra-Parson's method (constant pressure boundary case)

Figure 4.9 compares the up-scaled relative permeability by Hearn's method (constant flow rate), and Dykstra-Parson's method (constant pressure boundary case).

By investigating Figure 4.9, it is shown that the up-scaled oil relative permeability generated using the Dykstra-Parson's method is lower than the up-scaled oil relative permeability shown by Hearn's method. However, the up-scaled water relative permeability generated by the Dykstra-Parson's method is higher than the up-scaled water relative permeability by Hearn's method. Similar to the last comparison, the difference between the two methods is larger for middle saturations and they overlap at their endpoints. Consequently, using Hearn's method instead of Dykstra-Parson will predict higher recovery factor; however, basically Hearn's method is for constant flow rate condition.

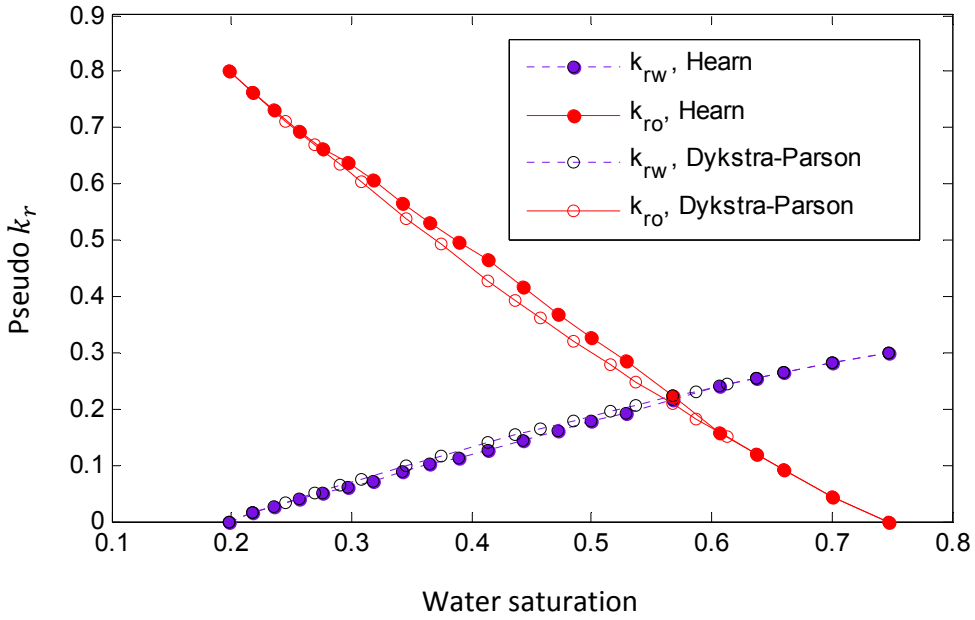

Figure 4.9: Up-scaled Relative Permeability **(Hearn Versus Dykstra-Parson's Method)**

4.2 ECLIPSE Set Up for The Constant Flow Rate Case:

In this section, two reservoir models are constructed using the ECLIPSE 100 BLACK OIL (Schlumberger, 2012) simulator for the constant flow rate case. One is a 3D fully layered model and each layer has its own properties as shown in Table 4.1. The other is a 2D areal model, which uses average porosity, average permeability and pseudo relative permeability generated both by the new method and alternative methods. The results of simulation including recovery factor, water cut, oil flow rate and total oil production over time are compared for these different scenarios. The 3D full layered model is considered realistic and used as the base case, however, with more computational expenses. Thus, any of the 2D scenarios resulted in good agreement with the results of the base case is considered as a successful scenario with less computational expenses.

4.2.1 How to overcome the non-monotonic error in ECLIPSE:

ECLIPSE simulator (Schlumberger, 2012) needs a monotonic relative permeability curve in which by increasing water saturation, oil relative permeability smoothly decreases and water relative permeability increases. If a crude up-scaled relative permeability curve generated by the MATLAB software is used in the ECLIPSE simulator, we will likely have a non-monotonic error in the ECLIPSE simulator because of the step jumping nature of the plot.

To solve this problem, a polynomial trend line that best fits to the curve is used; this makes the curve smooth enough to overcome the step jumping. An example of this process is shown in Figure 4.10.

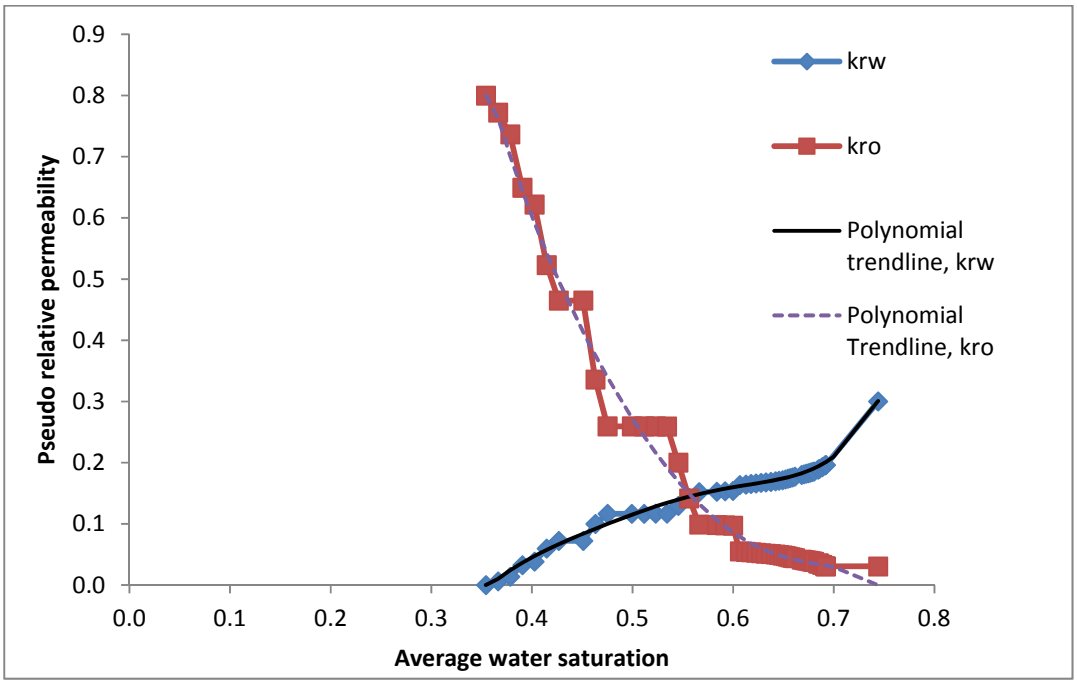

Figure 4.10: Procedure to Find a Polynomial Trend Line to the Up-scaled Relative Permeability

4.2.2 General Description of the model:

A horizontal reservoir with 100(5m)*1(50m)*20(2m) grid-blocks was constructed. The depth to the top layer is 2000m. In a block of only oil and water, the oil water contact is located at 2400m and initial formation pressure at 2000 m is 123 *bars*. For the one-layer model, the number of grid-blocks in the vertical direction changes to 1(40m) and the number of grid-blocks in the x and the y directions, the depth at top layer and the oil water contact remain the same as the multi-layer model.

The porosity and permeability of each layer is listed in Table 4.1. The permeability in the x and y directions is equal, and the permeability in the z direction is half the permeability of the x and y direction for all layers. Compressibility of rock is equal to $0.4 * 10^{-5}$ (1/ bars) at the initial pressure value of 150 *bars*. For the multi-layer model, each layer uses its own K, φ, h, S_{wc} and S_{or}, whereas for the one-layer model, the thickness-weighted average of the aforementioned parameters are used.

In a Cartesian block centered system, a vertical water injection well is located at (1, 1) penetrating through layers 1 to 20. Water injection has a control bottom hole reservoir flow rate at maximum or target of 10 res *bbl/day*.

The production well is vertical and is located at (100, 1) and penetrates through layers 1 to 20. The production well has a control bottom hole reservoir flow rate at a minimum or target of 10 res *bbl/day*.

Four scenarios were used to simulate a reservoir with a constant flow rate boundary condition. The first scenario used a full layered 3D model of the reservoir and using

different relative permeability curves (using equation 3.2 and 3.3) for each layer and used 20 grid-blocks in vertical direction, which is called base case model in this section. The second scenario used pseudo relative permeability generated by Hearn's method for reservoir modeling and used one grid-block in the vertical direction to generate a 2D model. The third scenario used the new method of up-scaling relative permeability corresponding to average water saturation at the outlet and used one grid-block in the vertical direction. The last scenario used the new up-scaling relative permeability corresponding to average water saturation in the entire reservoir and used one grid-block in the vertical direction.

The initial pressure distribution for the constant flow rate full layered case is shown in Figure 4.11.

After running all the scenarios the recovery factor, water cut, oil flow rate and total oil flow rate for all scenarios are compared in Figures 4.12-4.15.

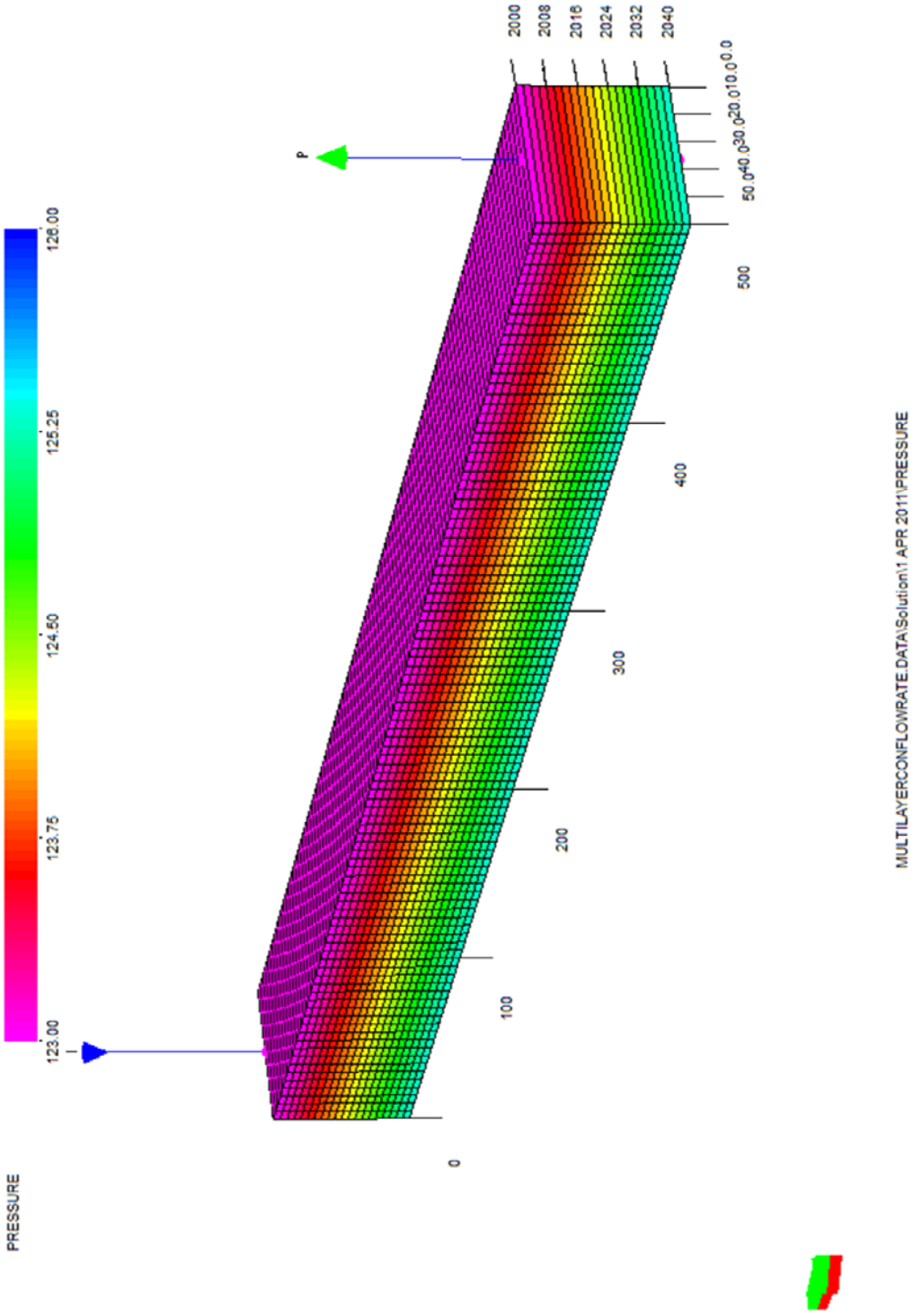

Figure 4.11: Initial Pressure Distribution for the Constant Flow Rate Case

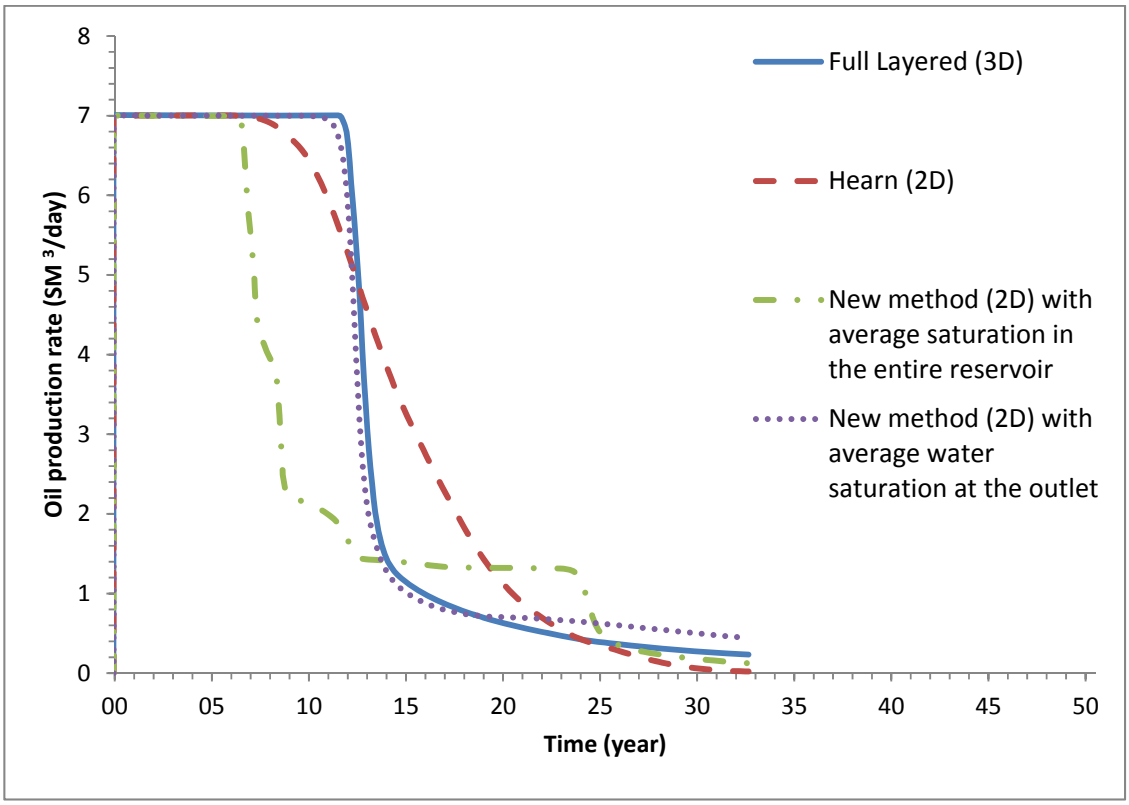

Figure 4.12: Oil Production Rate Comparison for the Constant Flow Rate Case

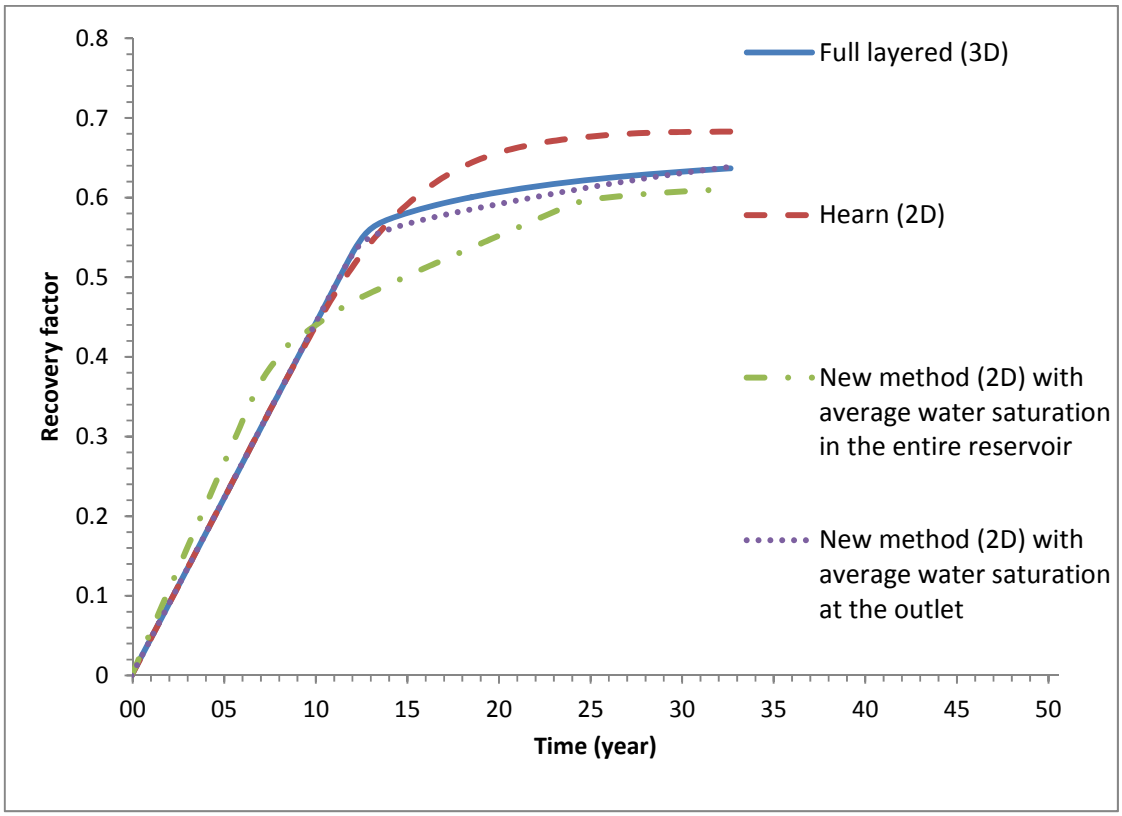

Figure 4.13: Oil Recovery Comparison for the Constant Flow Rate Case

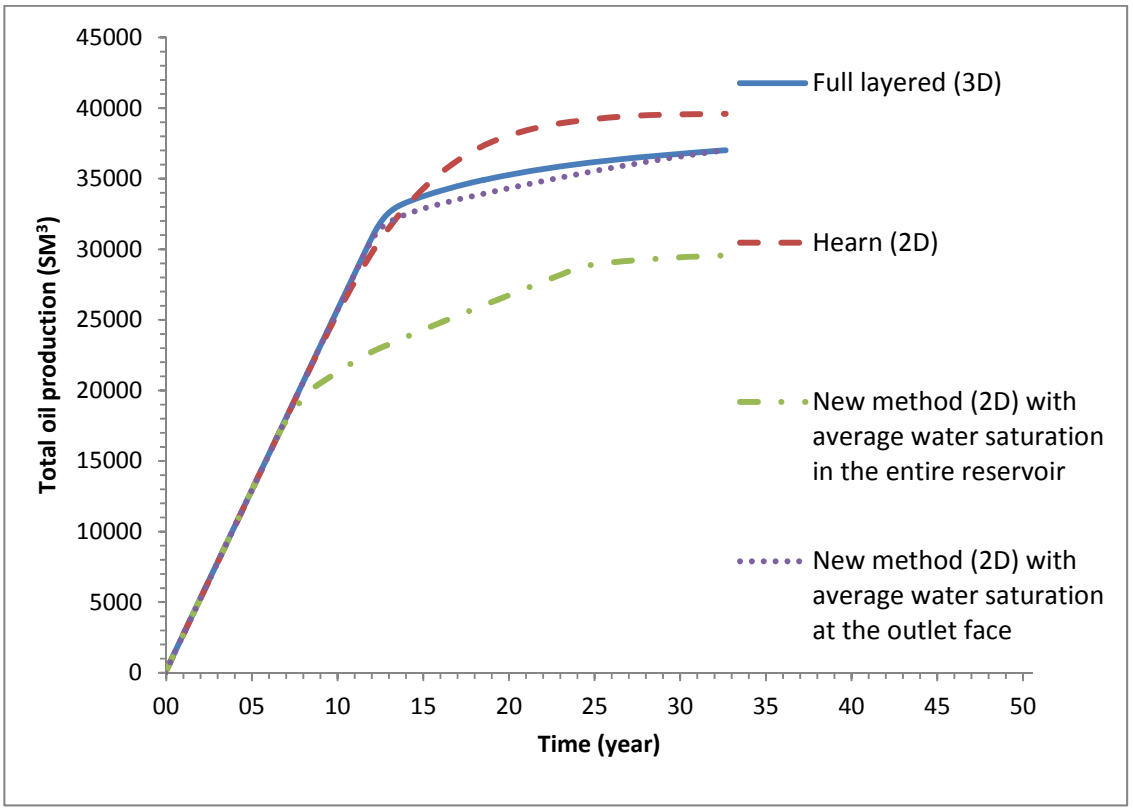

Figure 4.14: Total Oil Production Comparison for the Constant Flow Rate Case

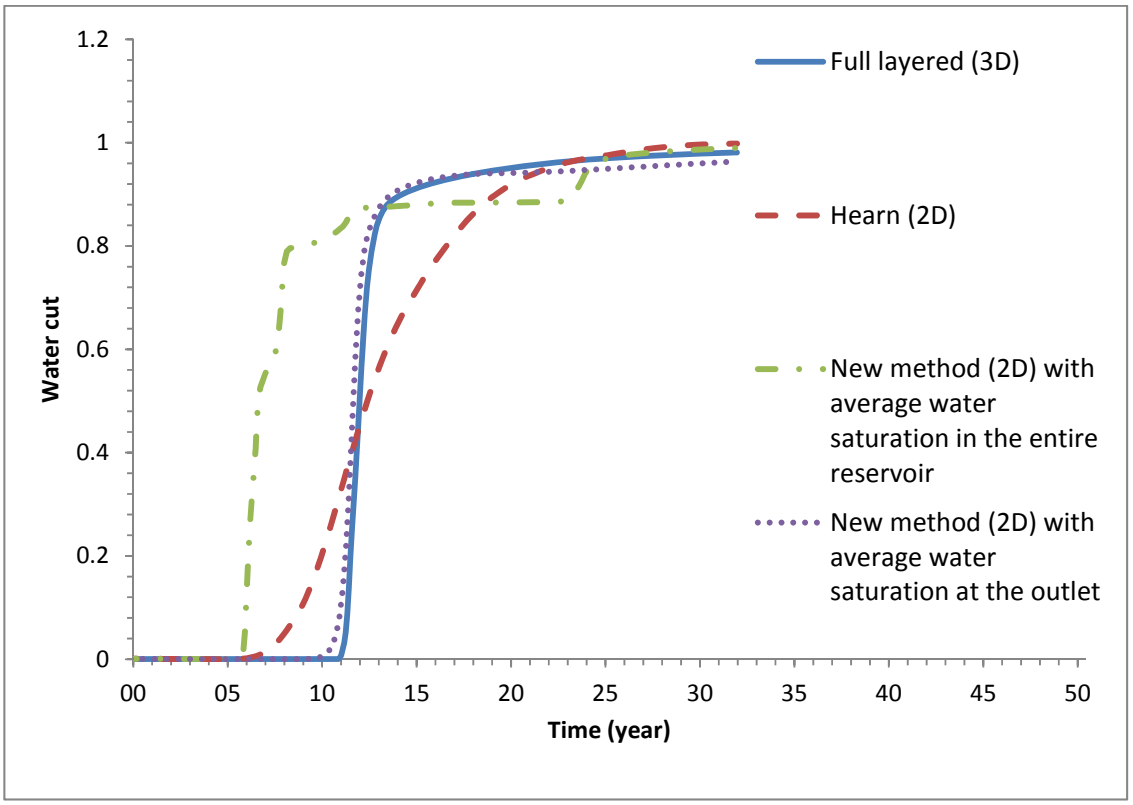

Figure 4.15: Water Cut Comparison for the Constant Flow Rate Case

Figure 4.12 shows that for the constant flow rate case, using Hearn's pseudo relative permeability curve results in a smooth decline in the oil production flow rate. This is equivalent to the smooth increase in water cut as it can be seen in Figure 4.15 and smooth bending in total oil production line in Figure 4.14. The base case model shows a sharp decline in the oil flow rate at year 13, which is equivalent to the sharp bending in total oil production line in Figure 4.14 at the time of water breakthrough. Using the new method with average water saturation at the outlet for generating pseudo curves captures this trend. The new method with average water saturation over the entire reservoir is unable to capture

the base case trend. This shows that new method with average water saturation in the entire reservoir is not an accurate method.

Figure 4.13 shows that using both Hearn's method and the new method with average water saturation at the outlet for generating pseudo relative permeability curves result in a good prediction of the recovery factor before breakthrough of water in the all layers. Before breakthrough of water, the reservoir models for these methods produce only oil with the same production rates. In other hand, the geo-model reserve for both cases are the same, therefore the recoveries are the same. After breakthrough, Hearn's method predicts the recovery factor to be 7.2 % more than the base case and the new method with average water saturation at the outlet predicts the recovery factor with less than 1 % difference compared to base case. The new method with average water saturation in the entire reservoir shows a higher oil recovery before breakthrough, and lower recovery after breakthrough in comparison to the base case. These differences are because of using different relative permeability curves, which cause differences in oil and water flow rates.

Figure 4.14 shows the total oil production over time for the constant flow rate case. This figure demonstrates that before breakthrough of water in all layers, all methods predict total oil production very well. However, the new method with average water saturation in the entire reservoir shows an early water breakthrough. After breakthrough, only the new method with average water saturation at the outlet catches the full layered (base case) trend for total oil production.

Figure 4.15 shows the water cut over time for the constant flow rate case; this figure illustrates that Hearn's method predicts the early water cut and smooth increase. This is equivalent to early and smooth flow rate drop in Figure 4.12 and the smooth bending in total oil production line in Figure 4.14. The base case shows a sharp increase in the water cut at year 11 and then becomes flat. Using the new method with average water saturation at the outlet successfully captures this trend. The new method with average water saturation in the entire reservoir shows an early water breakthrough followed by a sharp increase.

Overall, only using the new method with average water saturation at the outlet for generating up-scaled relative permeabilities provides reliable results. The results by this method are quite close to the full layered (3D) simulation results which are considered realistic and used as the base case. This method, through using fractional flow theory and considering the variation of water saturation after breakthrough of water-oil displacing front, predicts the behavior of the 3D reservoir model very well. Using the average water saturation in the entire reservoir with up-scaled relative permeability does not guarantee proper results in such a simulation.

4.3 ECLIPSE Set Up for the Constant Pressure Boundary Case:

In this section, as in section 4.2, two reservoir models are constructed in the ECLIPSE 100 BLACK OIL simulator (Schlumberger, 2012) for the constant pressure boundary case. One is a 3D fully layered model with 100(5m)*1(50m)*20(2m) grid-blocks where each layer has its own properties as shown in Table 4.1. The other is a 2D areal model with 100(5m)*1(50m)*1(40m) grid-blocks, which uses the average porosity, average

permeability and pseudo relative permeability generated both by the new method and alternative methods. The results of simulation are compared for these different scenarios. The 3D full layered model is considered realistic and used as the base case, however, with more computational expenses. Therefore, any of the 2D scenarios resulted in good agreement with the base case is considered as a successful scenario with less computational expenses.

4.3.1 General Description of the model:

The constant flow rate model in section 4.2.1 is modified for this section. The only changes are in the wells operating conditions of two wells. In the constant pressure boundary reservoir model, water injection has a controlled bottom-hole pressure at a maximum (or target) of 150 *bars* and the production well has a bottom-hole pressure at a minimum (or target) of 50 *bars*.

Four scenarios were developed to conduct the simulation of a reservoir in the constant pressure boundary condition. The first scenario used a full layered (3D) model of the reservoir and a different relative permeability curve for each layer which is called base case model. The second scenario used Dykstra-Parson's method for generating up-scaled relative permeability and a 2D model. The third one used the new method of up-scaling relative permeability with average water saturation in the entire reservoir and a 2D model. The last scenario used the new method of up-scaling relative permeability with average water saturation at the outlet.

The initial and final water saturation distributions for the full layered constant pressure boundary case are shown in Figures 4.16 and 4.17.

After running all the scenarios the oil flow rate, recovery factor, total oil production and water cut for all scenarios are compared in Figures 4.18 - 4.21.

It should be mentioned that there is no physical meaning to compare results of the constant pressure boundary to the results of constant flow rate case. Each case uses the generated pseudo relative permeability for that specific case and the results of each case are highly affected by the value of flow rate or pressure difference.

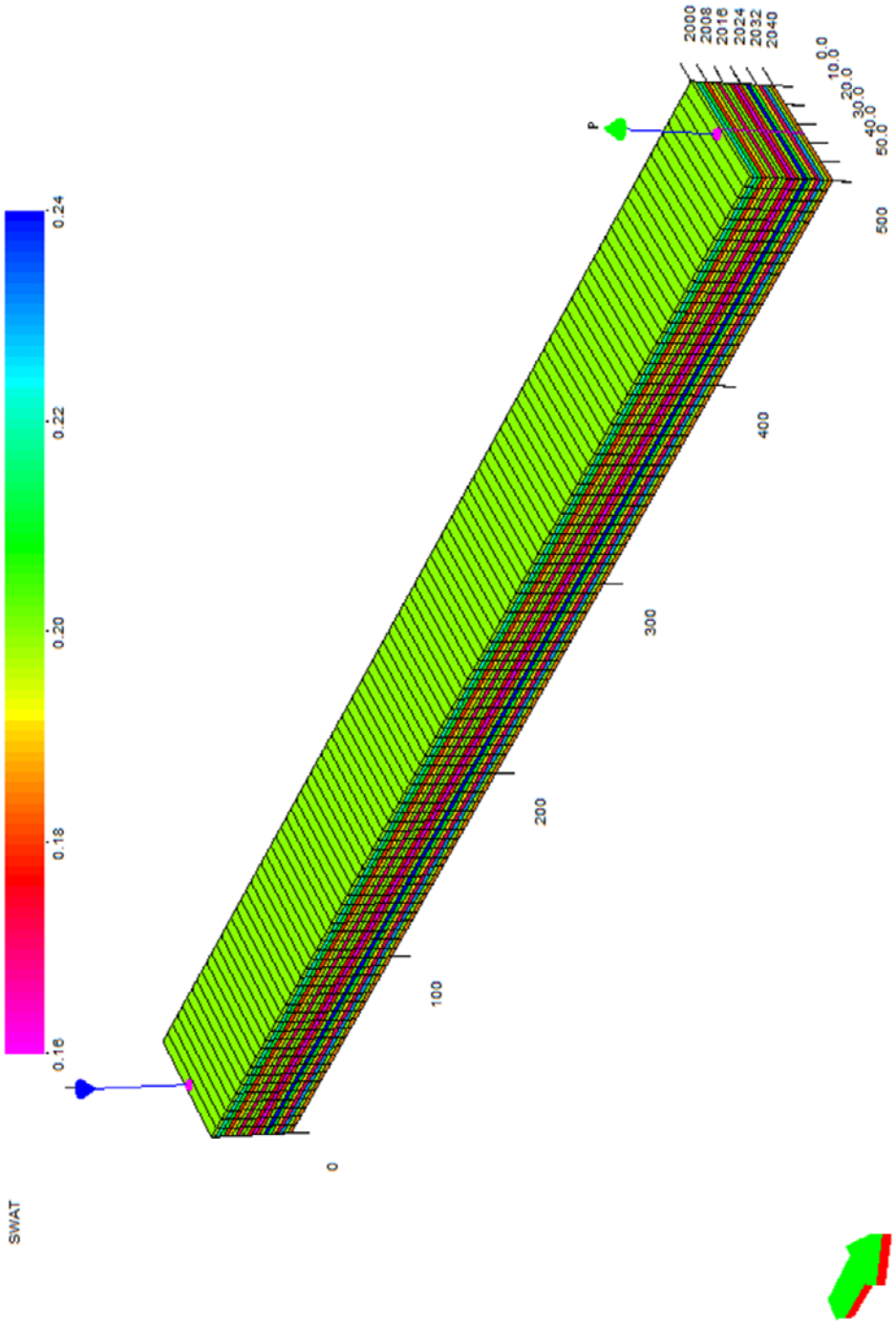

Figure 4.16: Initial Water Saturation Distribution for the Constant Pressure Boundary case

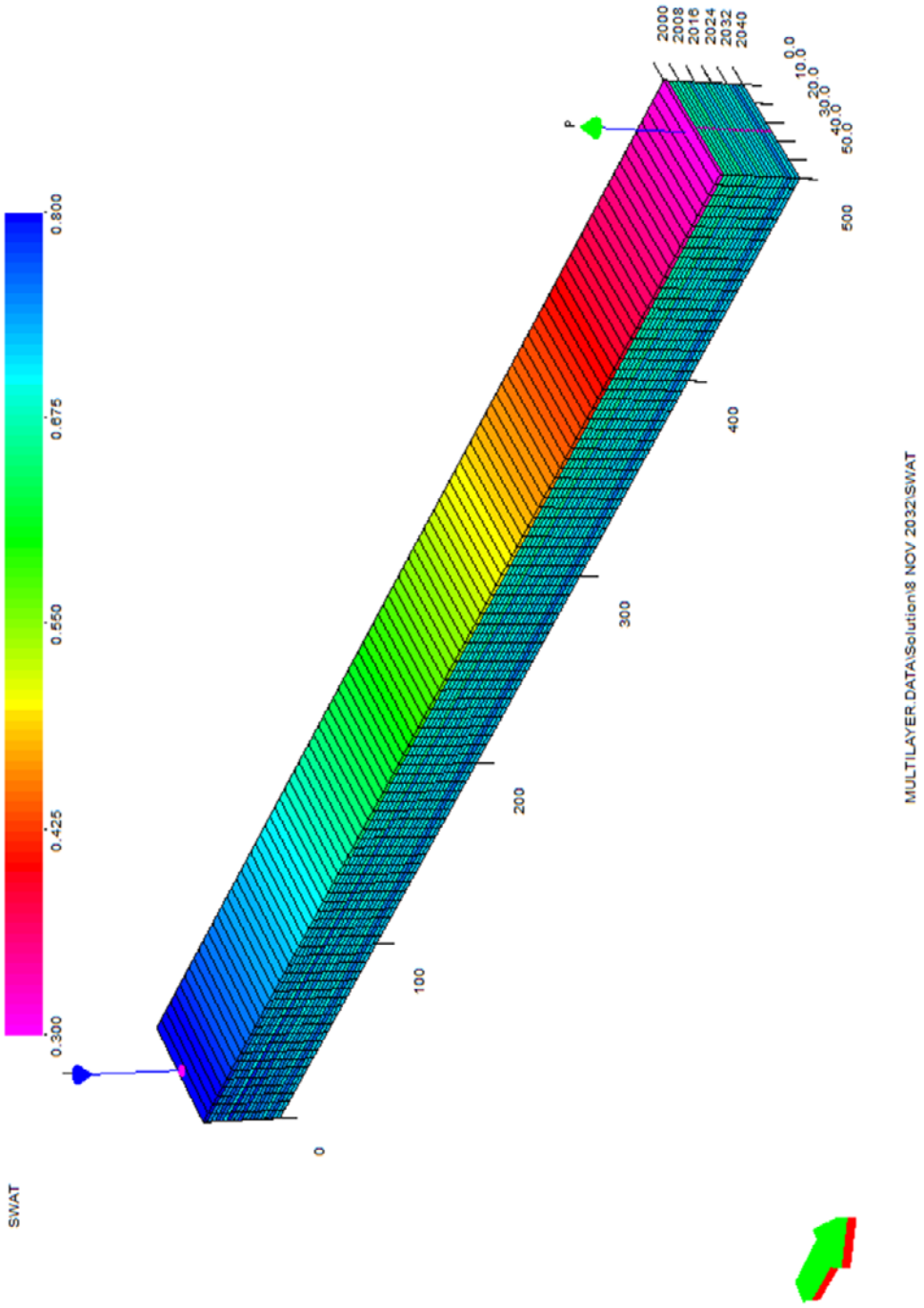

Figure 4.17: Final Water Saturation Distribution for the Constant Pressure Boundary Case

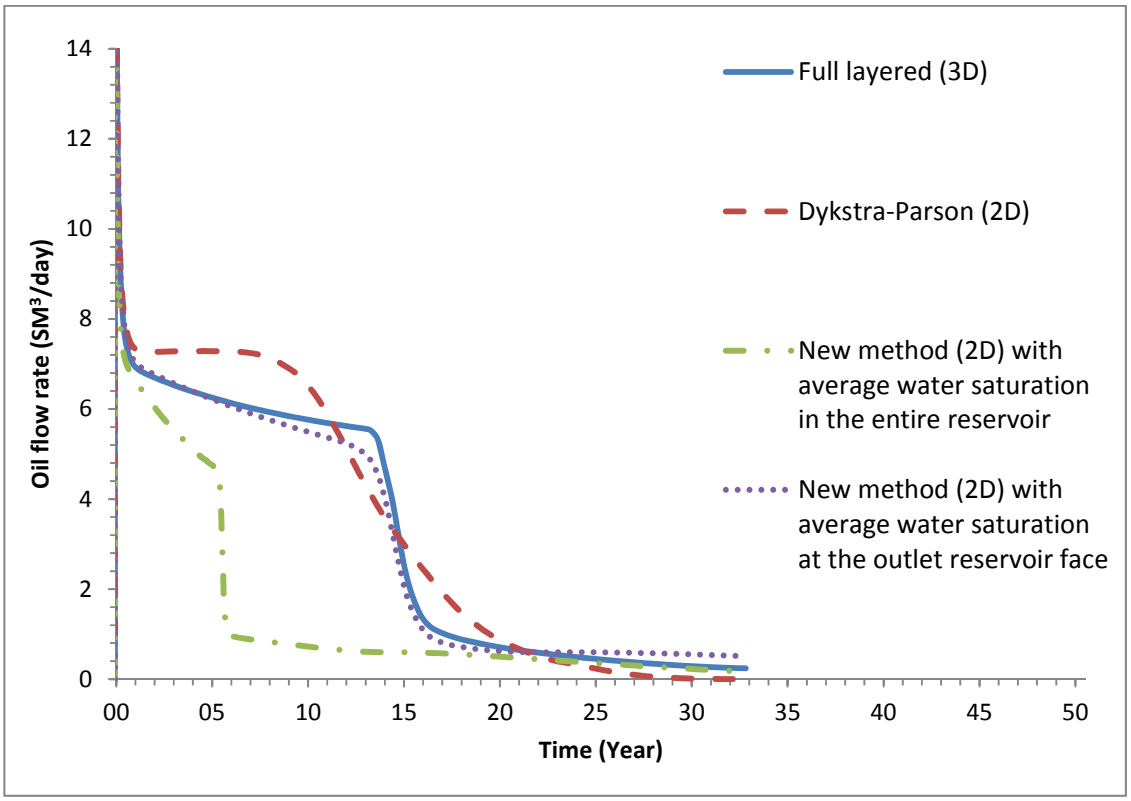

Figure 4.18: Oil Production Rate Comparison for the Constant Pressure Boundary Case

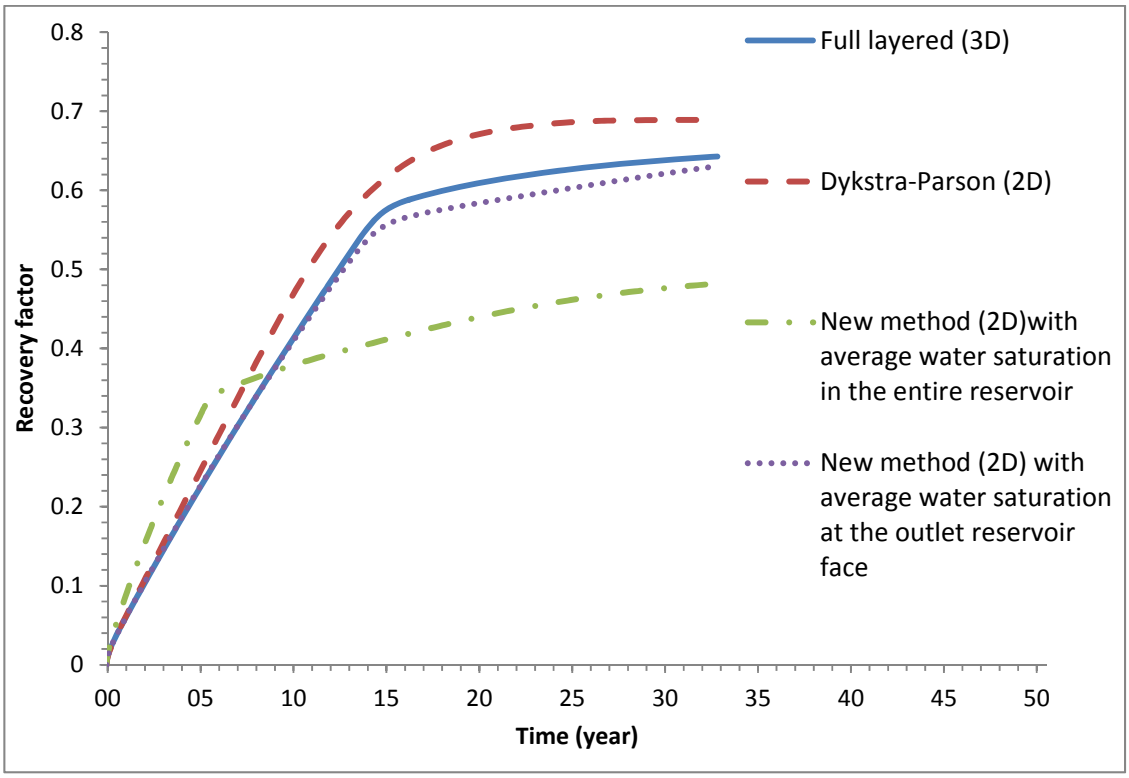

Figure 4.19: Oil Recovery Comparison for the Constant Pressure Boundary Case

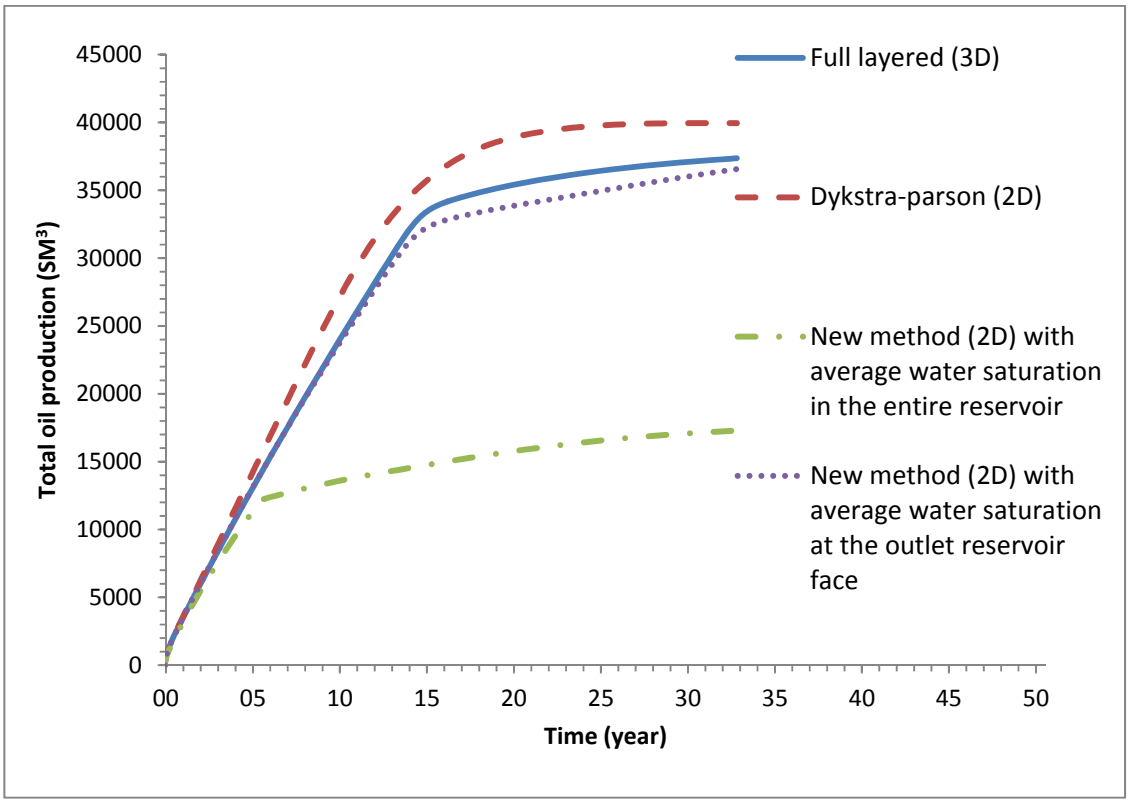

Figure 4.20: Total Oil Production Comparison for the Constant Pressure Boundary Case

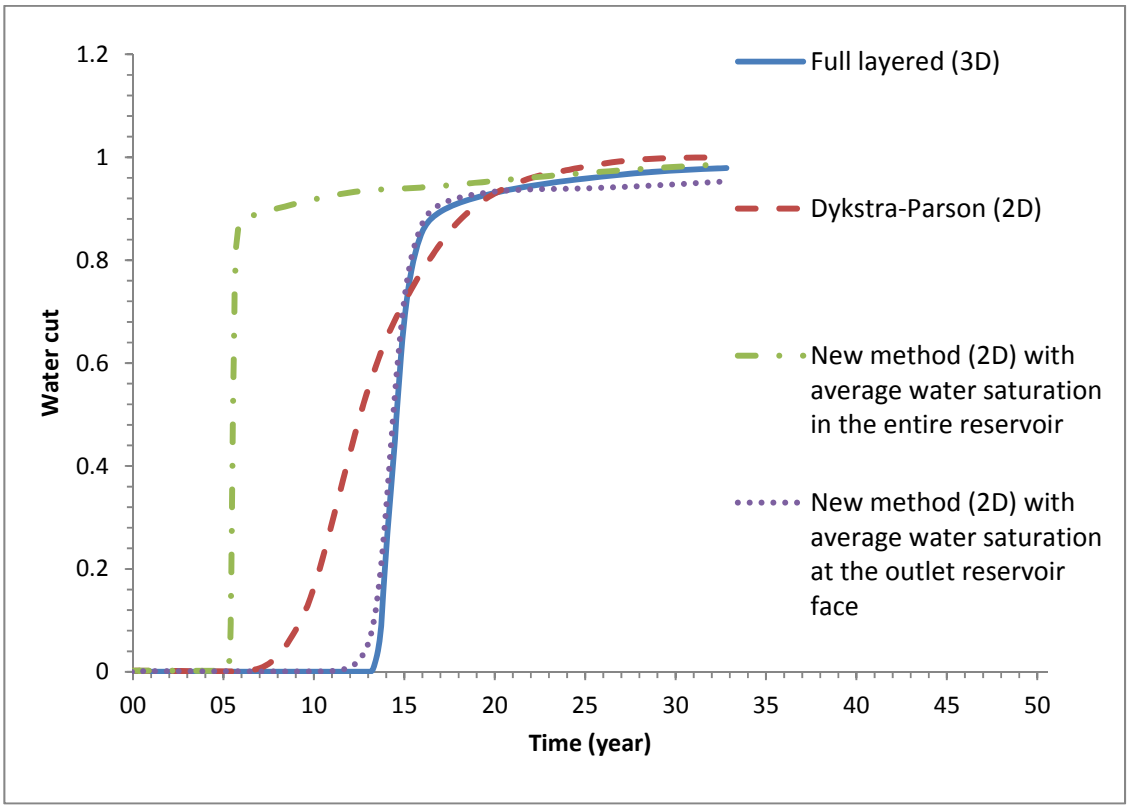

Figure 4.21: Water Cut Comparison for the Constant Pressure Boundary Case

Figure 4.18 shows the oil flow rate for the constant pressure boundary case. In this figure, the Dykstra-Parson's method predicts a fixed flow rate and then a smooth decline in flow rate. This is equivalent to the smooth bending in total oil production line in Figure 4.20 and smooth increase in water cut which is shown in Figure 4.21. The base case shows a smooth decline followed by a sharp decline and finally another smooth decline, which is equivalent to the sharp bending in total oil production line in Figure 4.20. Using the new method with average water saturation at the outlet captures the base case trend. The new method with average water saturation in the entire reservoir follows the base case trend, but it shows an

early drop in oil flow rate at year 6. This can be interpreted by unequal geo-model reserves, which is explained in the end of this section.

Figure 4.19 illustrates recovery factor versus time for the constant pressure boundary case. The Dykstra-Parson's method predicts a higher amount of recovery compared to the base case with an ultimate recovery of 7.2 % more than the base case. However, the new method with average water saturation at the outlet matches the base case before water breakthrough and underestimates oil recovery after water breakthrough. The ultimate recovery predicted by the new method for this case is 1.8 % lower than the base case. The new method with average water saturation in the entire reservoir predicts a higher oil recovery before water breakthrough and predicts lower oil recovery after breakthrough. The ultimate recovery predicted by this method for this case is 25 % lower than the base case. The recoveries are proportional to the total oil production, for example total oil production for the Dykstra-Parson's method would be higher than the base case.

Figure 4.20 shows the total oil production over time for constant pressure boundary case. This illustrates that before breakthrough of water only the new method with average water saturation at the outlet predicts total oil production properly. After breakthrough of water in the all layers, Dykstra-Parson over estimates the total oil production. Both the new method with average water saturation at the outlet and average water saturation in the entire reservoir underestimate total oil production, however, the difference between the new method with average water saturation in the entire reservoir is very different to the base case. The Dykstra-Parson's method predicts the ultimate total oil production to be 6.9 %

higher than the base case. The new method with average water saturation in the entire reservoir predicts the ultimate total oil production to be 53.7 % lower than the base case. The new method with average water saturation at the outlet predicts the ultimate total oil production to be 2.1 % lower than the base case.

Figure 4.21 shows the water cut versus time. The Dykstra-Parson shows an early water breakthrough at year 6 and then a smooth increase in water cut, which is equivalent to the smooth bending in total oil production line at the time of water breakthrough in figure 4.20. However, the base case has a sharp increase at year 13 and then stabilizes at a high value. The new method with average water saturation at the outlet successfully captures this trend. The new method with average water saturation in the entire reservoir is much different from the base case; however, it follows the shape of the base case trend with a time difference of 7 years. After year 17, all the methods have ±2% difference with the base case (fully layered) which indicates a good agreement.

Figures 4.18-4.21 demonstrate that the new method of up-scaling relative permeability corresponding to average water saturation at the outlet provide the closest results to the full layer simulation results, which are favorable. This method by considering the variation of water saturation after breakthrough of water-oil displacing front predicts the behavior of the 3D reservoir model very well.

The new method with average water saturation at the outlet reservoir face keeps the reserve the same as the multi-layered case (geo-model). This method merges the layers into one layer with average properties such as porosity, permeability, residual oil saturation and

connate water saturation. The new method with average water saturation in the entire reservoir does not keep the oil reserve the same as the multi-layered case because the generated up-scaled relative permeability shows that the connate water saturation is higher than the average connate water saturation of all the layers. This fact can be understood by investigating total oil production and recovery factor figures for both constant flow rate and constant pressure boundary cases (Figures 4.1, 4.14, 4.19 and 4.20).

If the reserve is the same as for the multi- layered case, the proportion of total oil production calculated by the different methods should be similar to the proportion of recovery factor calculated by them. However, the results do not show this fact. The total oil production calculated by the new method with average water saturation in the entire reservoir shows that the calculated total oil production is much smaller than the multi-layered case; however, the recovery factor calculated by the new method with average water saturation in the entire reservoir is close to the multi-layered case. Also, the water cut figures (Figure 4.15 and 4.21) show early water breakthrough by the new method with average water saturation in the entire reservoir compared to the multi-layered case. Therefore, using this evidence we can conclude that the new method with average water saturation at the outlet for both constant flow rate and constant pressure boundary cases best reduces the geo-model reserve.

4.4 Economic Analysis

In this section the net present value for both the constant injection rate and constant pressure boundary case is calculated for different methods. The following equation is used for the calculation of net present value:

$$NPV = \int_0^{t_f} Price \times oil\ flow\ rate \times (1+i)^{-t} dt \quad (4.1)$$

In this analysis the price of an oil barrel is assumed to be fixed at $100 and the discount rate also is assumed to be at 3% per year. The results are shown in Figures 4.22 - 4.25.

In these Figures, new method 1 and new method 2 represent for new method with average water saturation in the entire reservoir and at the outlet face, respectively.

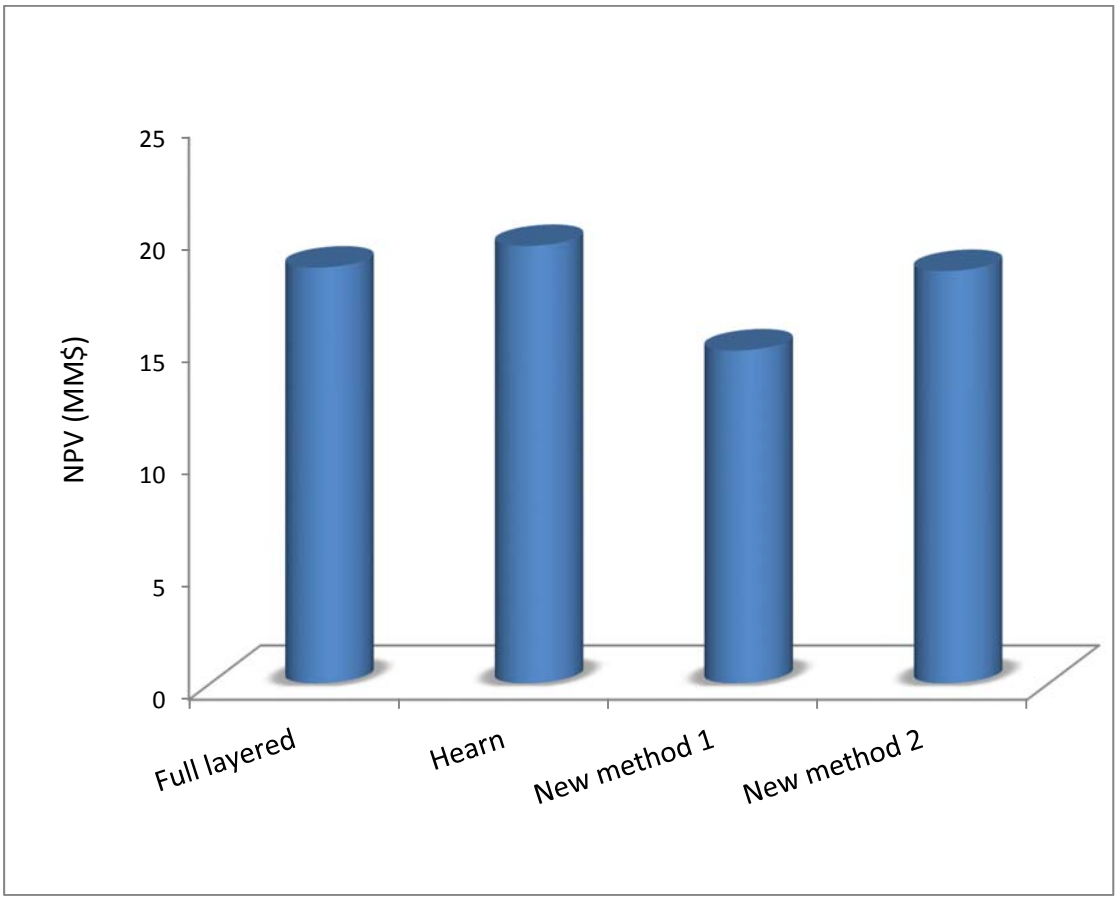

Figure 4.22: Net present value for the constant flow rate case

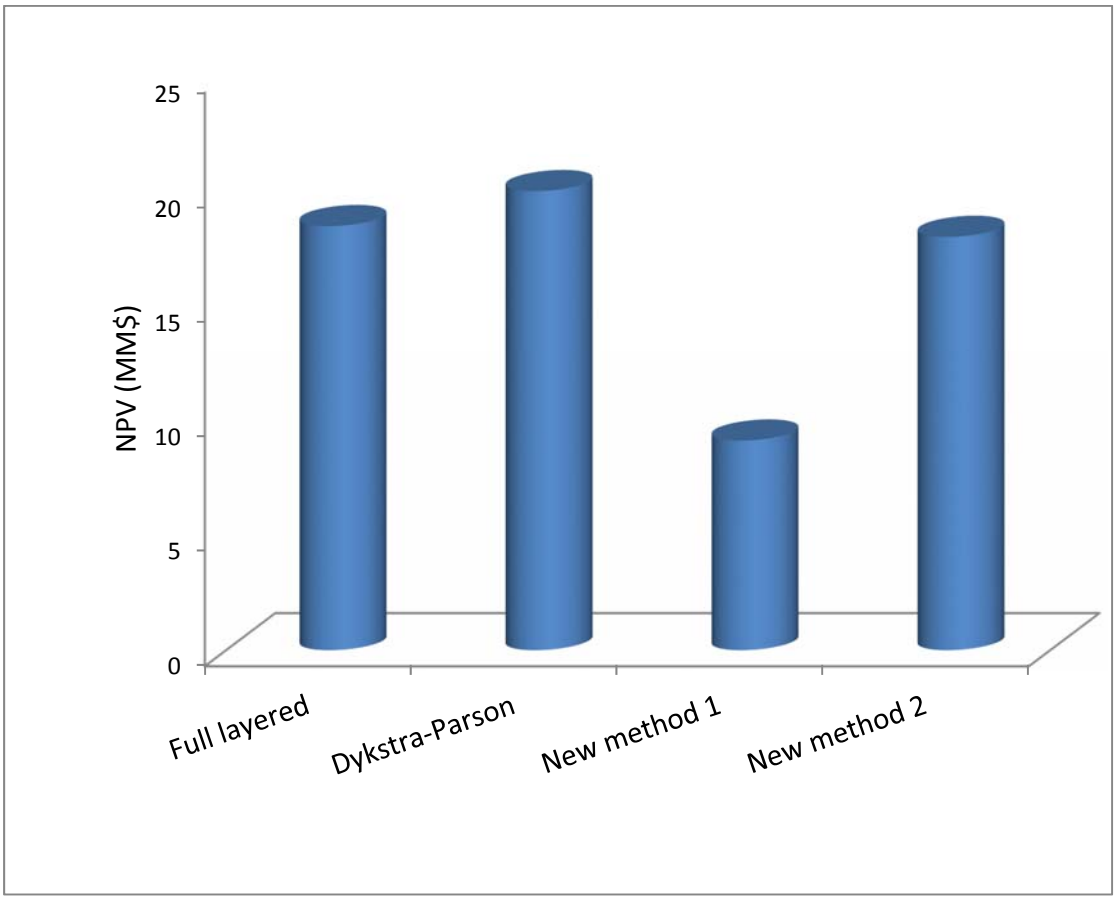

Figure 4.23: Net Present Value for the Constant Pressure Boundary Case

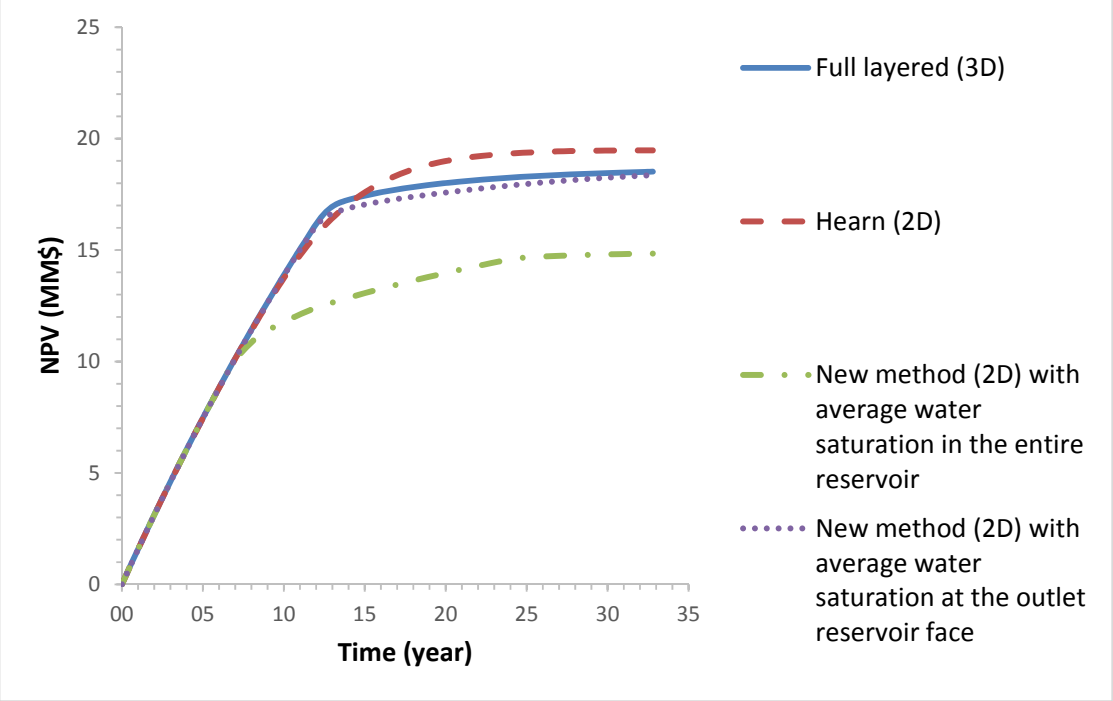

Figure 4.24: Net Present Value for the Constant Flow Rate Case over Production Time

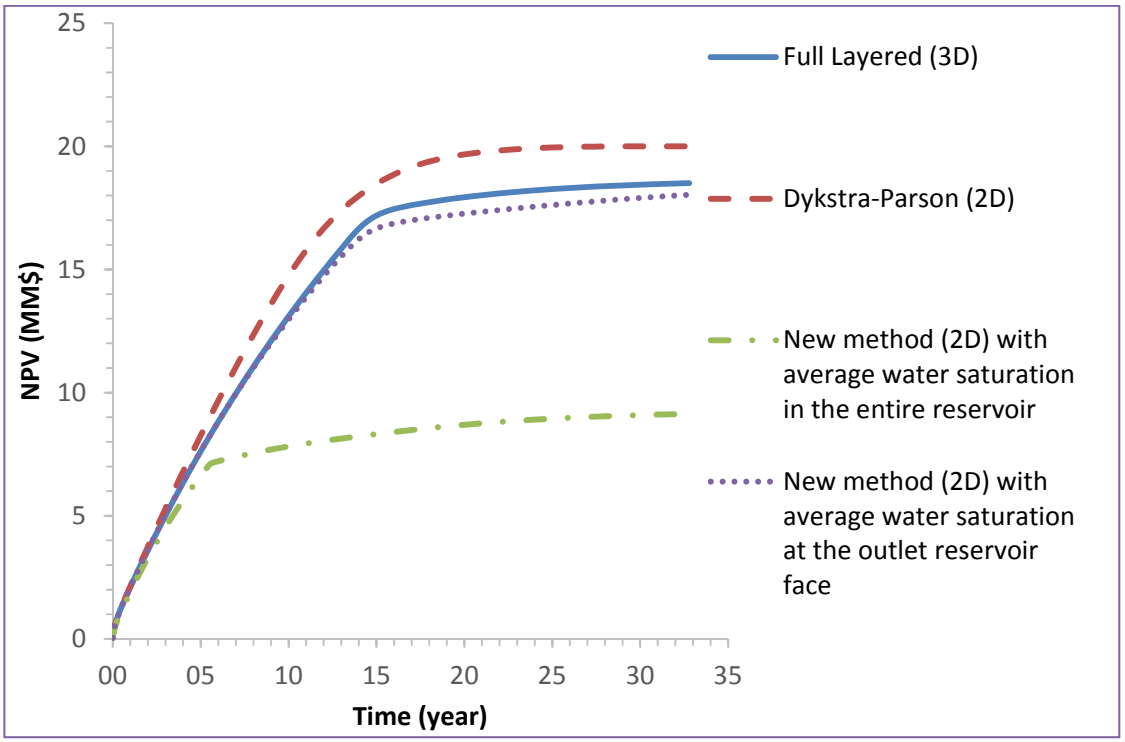

Figure 4.25: Net Present Value for the Constant Pressure Boundary Case over Production Time

Figure 4.22 shows NPV for total production time for constant flow rate case by different methods. In this Figure new method 1 represents new method of up-scaling corresponding to average water saturation in the entire reservoir, new method 2 represents for new method of up-scaling corresponding to average water saturation at the outlet reservoir face. This Figure shows that the new method with average water saturation at the outlet reservoir face predict the same NPV as full layered case. However, the Hearn's method and our new method with average water saturation in the entire reservoir predict the NPV with quite a large difference with the full layered case.

Figure 4.23 shows NPV for total production time for constant pressure boundary case by different methods. This Figure shows that the new method with average water saturation at the outlet reservoir face (new method 2) predict the same NPV as full layered case. However, the Dykstra-Parson's method and our new method with average water saturation in the entire reservoir predict the NPV with quite a large difference with full layered case.

Figures 4.24 and 4.25 show NPV over time for constant flow rate case and constant pressure boundary by different methods respectively. At first glance these figures, seem to mirror the corresponding total oil production curves in Figures 4.14 and 4.20, respectively. However, indeed this is an artifact of the relatively low discount rate of 3%.

These figures show that the new method with average water saturation at the outlet reservoir face predict almost the same NPV as full layered case for both constant flow rate and constant pressure boundary case. However, Hearn's method (Dykstra-Parson's method for constant pressure boundary) and our new method with average water saturation in the entire reservoir predict the NPV with quite a large difference with full layered case for both constant flow rate case and constant pressure boundary. This means that, using the new method of up-scaling of relative permeability both for constant flow rate and constant pressure boundary, promise an accurate forecasting for the future of the reservoir.

CHAPTER 5

CONCLUSIONS & RECOMMENDATIONS

5.1 Conclusions

1. A novel and improved procedure for calculating pseudo relative permeability by using basic reservoir data to generate a 2D areal reservoir simulation to approximate 3D reservoir behavior has been successfully completed.

2. The advantage of this new method over previously proposed methods is that it does not assume a piston-like displacement; instead it uses fractional flow theory which is more accurate.

3. This research presents two different methods of calculating pseudo relative permeability curves: i) for the constant pressure boundaries case by using the new fractional flow extension in Johansen and James (2015), and ii) for the constant flow rate case by using the Buckley-Leverett classical fractional theory.

4. Although the rock relative permeability curve is the same for the constant pressure boundaries condition and the constant flow rate boundaries condition, the pseudo

relative permeability curve for the constant pressure boundaries case and the constant flow rate case are significantly different.

5. Flow rate, pressure difference and reservoir length have no effect on the shape of up-scaled relative permeability generated by our new method for both constant flow rate and constant pressure boundary cases.

6. Viscosity ratio of water to oil has a significant effect on the shape of up-scaled relative permeability. By increasing viscosity ratio of water to oil, the up-scaled relative permeability of water and oil corresponding to average water saturation at the outlet reservoir face increases significantly for all saturation. This conclusion is valid for both constant flow rate and constant pressure boundaries cases.

7. The effect of viscosity ratio on up-scaled relative permeability corresponding to average water saturation in the entire reservoir is not uniform and depends on the specific average saturation.

8. Only the new methods of up-scaling relative permeability corresponding to average water saturation at the outlet for both constant flow rate and constant pressure boundaries provide results close to the full layer (3D) simulation results and is completely superior to all other methods considered in this work, which are favorable.

9. The new method using average water saturation at the outlet reservoir face offers a new opportunity for substantial CPU saving in simulation of layered reservoirs.

10. For the investigated examples, we see no dependence of quantity on parameter. However, a truly exhaustive search of various parameters may needed to see our method is independent of parameter.

5.2 Recommendations

1. In the present work up-scaled relative permeability is generated for two-phase system. Although straight forwarded to generate to three phase pseudo relative permeabilities. A study similar to this one should be conducted to three phase systems.

2. In the present work a hypothetical reservoir has been used. A real reservoir model can be used to generate pseudo relative permeability and compare the results of the simulation with production history, allowing for history matching.

REFERENCES

1. Beier, R.A. (1992), ‘‘*Pseudo relative Permeabilities from Fractal Distributions*’’, paper SPE 24371 presented at the SPE Rocky Mountain Regional Meeting, Casper, Wyoming, 18–21 May.

2. Buckley, S. E. and Leverett, M. C. (1941), “*Mechanism of Fluid Displacement in Sands*”, Tram. AIME 146, 107-116

3. Cao, H., & Aziz, K. (1999), “*Evaluation of Pseudo Functions*”, Society of Petroleum Engineers. 54589-MS

4. Christie, M.A. (1996), "*Upscaling for Reservoir Simulation*", JPT, pp. 1004-1010

5. Coats, K. H., Dempsey, J. R. and Henderson, J. H. (1971), “*The Use of Vertical Equilibrium in Two-Dimensional Simulation of Three-Dimensional Reservoir Performance*”, Soc. Pet. Eng. J. 63-71

6. Coats, K. H., Nielson, R. L., Terhune, M. H. and Weber, A. G. (1967), “*Simulation of Three-Dimensional, Two-Phase Flow in Oil and Gas Reservoirs*”, Soc. Pet. Eng. J. 377-388

7. Corey, A. T. (1954), “*The Interrelation Between Gas and Oil Relative Permeabilities*”, Prod. Mon., pp. 19, 38

8. Dykstra, H, and Parson, R. L. (1950), "*The Prediction of Oil Recovery by Waterflood*", Secondary recovery of Oil in the United States, API 160-174

9. Guzman, R.E., Giordano, D., Fayers, F.J., Godi, A. and Aziz, K. (1996), "*Evaluation of Dynamic Pseudo Functions for Reservoir Simulation*", SPE 35157, the SPE Annual Technical Conference and Exhibition, Denver, Colorado, U.S.A. Oct. 6

10. Hearn, C. L. (1971), "*Simulation of Stratified Water flooding by Pseudo Relative Permeability Curves*", JPT, 805-813

11. Hewett, T.A., and Behrens, R.A. (1991), ''*Scaling Laws in Reservoir Simulation and Their Use in a Hybrid Finite-Difference/Stream-tube Approach to Simulating the Effects of Permeability Heterogeneity*'', Reservoir Characterization II, Academic Presss Inc., New York City

12. Hewett, T.A., and Yamada, T. (1997), "*Theory for the Semi analytical Calculation of Oil Recovery and Effective Relative Permeabilities Using Stream tubes*", Advances in water resources, 20(5-6), pp. 279-292

13. Honarpour, M. M., Koederitz, L. F., and Harvey, A. H. (1982), "*Empirical Equations for Estimating Two-Phase Relative Permeability in Consolidated Rock* ", Trans. AIME

14. Honarpour, M. M., Koederitz, L. F., and Harvey, A. H. (1988), "*Relative Permeability of Petroleum Reservoirs*", CRC Press, Inc.

15. Intera Information Technologies LTD (1994), "*PSEDO Reference manual*", 94A Release

16. Jacks, H. H., Smith, O. J. E., and Mattax, C. C. (1973), "*The Modelling of a Three Dimensional Reservoir With a Two Dimensional Reservoir Simulator- The Use of Dynamic Pseudo Functions*", Soc. Pet. Eng. J. 175-185

17. Johansen, T.E. (2008), "*Principles of Reservoir Engineering*", Memorial University of Newfoundland

18. Johansen T.E., James L.A. (2015), *Solutions of Multi-Component, Two-Phase Riemann Problems with Constant Pressure Boundaries*, To Appear in Journal of Engineering Mathematics, Springer Verlag.

19. Kleppe, J. (2012), "*Dykstra-Parson´s Method. In Reservoir Recovery Techniques*". (Published Online www.ipt.ntnu.no/~kleppe/TPG4150/dp.pdf)

20. Kyte, J. R., and Berry, D. W. (1975), "*New Pseudo Functions to Control Numerical Dispersion",* Soc. Pet. Eng. J. 269-276

21. Li, D., Beckner, B., Kumar, A. (1999), "*A New Efficient Averaging Technique for Scaleup of Multimillion-Cell Geologic Models*", Paper SPE 56554 presented at the SPE Annual Technical Conference and Exhibition held in Houston, TX, October 3 - 6

22. Li, D., Beckner, B. (2000) "*Optimal Uplayering for Scaleup of Multimillion-Cell Geologic Models*", Paper SPE 62927 presented at the SPE Annual Technical Conference and Exhibition held in Dallas, October 1-4

23. Lomeland F., Ebeltoft E. and Hammervold Thomas W. "*A New Versatile Relative Permeability Correlation"* Reviewed Proceedings of the International Symposium of the SCA, Abu Dhabi, United Arab Emirates, Oct. 31- Nov. 2

24. Lomeland, F., Hasanov, B., Ebeltoft, E., & Berge, M. (2012), "*A Versatile Representation of Upscaled Relative Permeability for Field Applications. Society of Petroleum Engineers*", doi:10.2118/154487-MS

25. Pirson, S. J. (1958), "*Oil Reservoir Engineering"*. New York: McGraw-Hill

26. Rose, W. D. and Bruce, W. A. (1949), "*Evaluation of capillary character in petroleum reservoir rock*", Trans., AIME, pp. 127,186

27. Schlumberger Information Systems, (2012), "*ECLIPSE 100 User's Manual*", GEOQUEST

28. Stone, H.L. (1991), "*Rigorous Black Oil Pseudo Functions*" paper SPE 21207 presented at the 11th SPE Symposium on Reservoir Simulation held in Anaheim, CA, February 17-20

29. Tarek, A. (2000), "*Reservoir Engineering Handbook*", Second Edition, Gulf Publishing Company, Houston, Texas, pp. 280-320

30. Testerman, J.D. (1962), "*A Statistical Reservoir Zonation Technique*" JPT, pp. 889-893

31. Tompang, R., & Kelkar, B. G. (1988), "*Prediction of Waterflood Performance in Stratified Reservoirs*", Society of Petroleum Engineers. 17289-MS

32. Warren, J. E. and Cosgrove, J. J.: (1964), "*Prediction of Waterflood Behavior in a Stratified System*", Soc. Pet. Eng. J. 149-157

33. Welge, H. J. (1964), "*A Simplified Method for Computing Oil Recovery by Gas or Water Drive",* AIME Transactions, 195, pp. 99–108

34. Wyllie, M. R. J., and Gardner, G. H. F. (1958), "*The generalized Kozeny-Carmen equation-Its Application To problems of Multi-Phase Flow in Porous Media*" World Oil, pp. 121-146

APPENDIX A

A.1 Dimensionless group G developed by Coates *et al.* (1971)

Saturation profile development for gravity segregation from an initially uniform saturation distribution in a closed vertical column is shown in Figure A.1.

In Figure A.1, $\underline{S_i}$ is the initial uniform column saturation. Shocks form instantaneously at the top and bottom of the column and saturations of zero and unity remain fixed at the column ends. The upper shock saturation is $\underline{S_b}$ and lower shock saturation is $\underline{S_e}$.

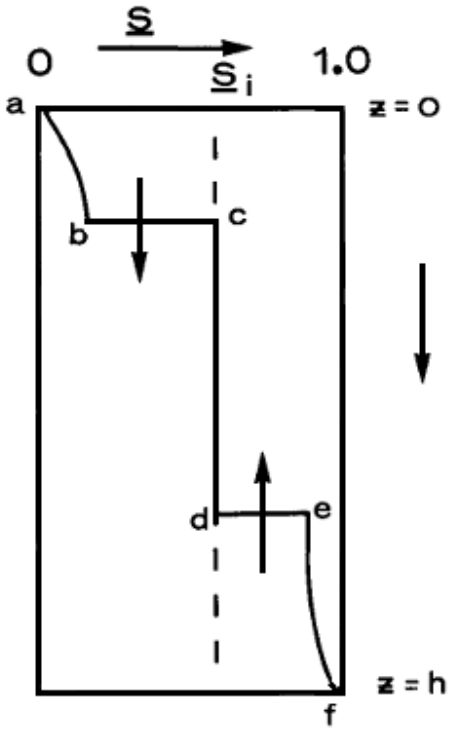

Figure A.1: Gravity Segregation in a Closed Vertical Column. (after Coats *et al.,* 1971)

Dimensionless group G is defined by

$$G = \frac{K\Delta\gamma({\psi_b}' - {\psi_e}')}{\bar{u}\Delta S}, \tag{A.1}$$

where

$$\psi(S) = \frac{1}{\frac{\mu_{nw}}{k_{rnwt}} + \frac{\mu_{wt}}{k_{rwt}}}, \tag{A.2}$$

$$\Delta S = 1 - S_{rnwt} - S_{rwt}, \tag{A.3}$$

$$\underline{S} = \frac{S_{wt} - S_{rwt}}{1 - S_{rnwt} - S_{rwt}}, \tag{A.4}$$

$$\psi' = \frac{d\psi}{d\underline{S}}, \tag{A.5}$$

$${\psi_b}' = \frac{\psi_i - \psi_b}{\underline{S_i} - \underline{S_b}}, \tag{A.6}$$

$${\psi_e}' = \frac{\psi_e - \psi_i}{\underline{S_e} - \underline{S_i}}, \tag{A.7}$$

$\gamma =$ fluid density, psi/ft

$\bar{u} =$ the mean superficial velocity of fluids in the reservoir

As the authors claimed, the value of dimensionless group G is then directly proportional to the degree of validity of the vertical equilibrium assumption. The above analysis is only

trivially altered by consideration of a column inclined at an angle θ from the vertical. The term $\Delta\gamma$ is simply replaced by $\Delta\gamma \cos\theta$.

APPENDIX B

B.1 MATLAB code for constant pressure boundary condition:

```
---------------------------------------------------------------------------------------------------

% UPSCALING RELATIVE PERMEBILITY FOR CONSTANT PREESURE BOUNDARY CASE
FOR %
%**************           MOHAMMAD SHADADEH        **************%
%************************   JULY 2013   ************************%
%-------------------------------------------------------------------------
-


clc
clear all

%%%%%%%%%%%%%%%%%%%%%%         DATA SECTION        %%%%%%%%%%%%%%%%%%%%%%%%
K=[8.3  10.1 8.6 7.3 8.2 11.1 11.7  13.2 11.4 7.9 10.6  11.2 8.4 8.9
12.3 17.5 17.4 13.9 12.6 10 ]*10^-15;     % absolut permeability (m^2)
h=2*ones (size (K));                      % thickness of each layer (m)
phi=[6  9   8   7   8   12  10  11  9   8   7   10.5    9   10  18  15
14  11  16  8];                           % porosity
swc=[.2 .22 .21 .18 .19 .20 .17 .23 .2 .175 .16 .18 .2 .24 .21 .19 .17
.23 .2 .185];                             % connate water saturation

sor=[.2 .25 .26 .23 .24 .28 .21 .23 .26 .22 .27 .265 .24 .25 .26 .29
.25 .24 .28 .275];            % residual oil saturation
miow=.8;                % viscosity of water
mioo=2.8;               % viscosity of oil
L=1000;                 % length of reservoir
dp=10^6;                % pressure difference in pa.
m=miow/mioo;            % viscosity ratio
n=1000;                 % number of saturation discretion
b=50;                   % number of time steps between the min BTH time
                        % and max BTH
aw=0.3;                 % indices for water in Corey correlation
ao=0.8;                 % indices for oil in Corey correlation


%%%%%%%%%%%%%%%%%%    FRACTIONAL FLOW CURVES  %%%%%%%%%%%%%%%%%%%%%%%%%

for i=1:length(swc)
    sw(i,1:(n+1))=swc(i):(1-sor(i)-swc(i))/n:(1-sor(i));
end
```

```
for i=1:length(swc)/2
    for j=1:(n+1)
        kro(i,j)=ao*((1-sw(i,j)-sor(i))./(1-swc(i)-sor(i))).^2;
        krw(i,j)=aw*((sw(i,j)-swc(i))./(1-swc(i)-sor(i))).^2;
    end
end

for i=length(swc)/2+1:length(swc)
    for j=1:(n+1)
        kro(i,j)=ao*((1-sw(i,j)-sor(i))./(1-swc(i)-sor(i))).^2;
        krw(i,j)=aw*((sw(i,j)-swc(i))./(1-swc(i)-sor(i))).^2;
    end
end

% fw=fractional flow   dfw=fractional flow derivative
% ddfw=secod derivative of fractional flow

for i=1:length(swc)
    for j=1:length(sw)
        fw(i,j)=1./(1+(ao/aw).*(miow./mioo).*((1-sw(i,j)-
sor(i))./(sw(i,j)-swc(i))).^2);
        dfr1(i,j)=(1+(ao/aw).*(miow./mioo).*((1-sw(i,j)-
sor(i))./(sw(i,j)-swc(i))).^2);
        dfw(i,j)=((ao/aw).*2*miow/mioo).*(1-swc(i)-sor(i)).*(1-sw(i,j)-
sor(i))./((dfr1(i,j).^2).*(sw(i,j)-swc(i)).^3);
        dfr2(i,j)=-((ao*2/aw)*miow/mioo).*(1-swc(i)-sor(i)).*(1-
sw(i,j)-sor(i))./((sw(i,j)-swc(i)).^3);
        dfr3(i,j)=((ao*2/aw)*miow/mioo).*(1-swc(i)-sor(i)).*((sw(i,j)-
swc(i)).^3+3*(sw(i,j)-swc(i)).^2.*(1-sw(i,j)-sor(i)))./((sw(i,j)-
swc(i)).^6);
        ddfw(i,j)=(-
dfr3(i,j).*dfr1(i,j).^2+2*dfr1(i,j).*dfr2(i,j).^2)./dfr1(i,j).^4;
    end
end

dfw(:,1)=0;
subplot(2,3,1)
hold on;

for i=1:length(swc)
    plot(sw(i,1:(n+1)),krw(i,1:(n+1)))
    plot(sw(i,1:(n+1)),kro(i,1:(n+1)))
    axis([0 1 0 1])
    title('Kr Vs. Sw')
```

```
    xlabel('Sw')
    ylabel('Kr')
end

subplot(2,3,2)
hold on;

for i=1:length(swc)
    plot(sw(i,1:(n+1)),fw(i,1:(n+1)))
    plot(sw(i,1:(n+1)),dfw(i,1:(n+1)))
    title('fw & dfw Vs. Sw')
    xlabel('Sw')
    ylabel('fw')
    axis([0 1 0 5])
end

subplot(2,3,3)
hold on;

for i=1:length(swc)
    plot(sw(i,1:(n+1)),ddfw(i,1:(n+1)))
    title('ddfw Vs. Sw')
    xlabel('Sw')
    ylabel('fw')
end

%%%%%%%%%%%%%    SLOPE OF FRACTIONAL FLOW CURVE    %%%%%%%%%%%%%%%%%%%%

for i=1:length(swc)
    for j=2:(n+1);
        slope(j,i)=(fw(i,j)-fw(i,1))/(sw(i,j)-sw(i,1));
    end
end

for j=1:length(swc)
    [maxVal maxInd] = max(slope);
end

%%%%%%%%%%%%%   AVERAGE WATER SATURATION BEHIND FRONT   %%%%%%%%%%%%%%%%

for i=1:length(swc)
    swavv(i)=sw(i,maxInd(i))-(fw(i,maxInd(i))-
fw(i,(n+1)))./dfw(i,maxInd(i));
end
```

```
%%%%%%%%%%%%       BREACKTHROUGH TIME CALCULATION          %%%%%%%%%

for i=1:length(swc)
    for j=1:length(sw)
        lambdat(i,j)=K(i).*((kro(i,j)./mioo)+(krw(i,j)./miow));
    end
end

v2=maxVal;
fdl=ddfw./lambdat;

for i=1:length(swc);
    ds(i)=(1-sor(i)-swc(i))/n;
    I1(i)=-
((fdl(i,maxInd(i)).*ds(i)./2)+sum(fdl(i,(maxInd(i)+1):n).*ds(i))+(fdl(i
,(n+1)).*ds(i)./2));
end

A=(I1./v2)-(1./transpose(lambdat(:,1)));
B=L./transpose(lambdat(:,1));
C=2*dp*v2./phi;
tbt=((A*L^2+2*B*L)./C);

%%%%% MONITORING SATURATION POSITION FOR EACH LAYE AT EACH TIME   %%%%%

t(1,1:(b+1))=0:(max(tbt))/b:max(tbt);
subplot(2,3,4);
hold on

for j=1:b;
    for i=1:length(swc);
        x(i,j)=(-B(i)+((B(i).^2+4.*A(i).*C(i).*t(j))).^.5)./(2*A(i));

xx(i,maxInd(i):(n+1))=dfw(i,maxInd(i):(n+1))./dfw(i,maxInd(i))*x(i,j);
        xtx(i,1:(n+1))=x(i,j):(L-x(i,j))/n:L;
        stss(i,1:(n+1))=sw(i,1);
        sww(i,:)=sw(i,:);
        sww(i,maxInd(i))=sw(i,1);
        plot([xtx(i, 1:(n+1)) xx(i,maxInd(i):(n+1))],[stss(i, 1:(n+1))
sww(i,maxInd(i):(n+1))])
        title('Sw Vs. x')
        xlabel('x (m)')
        ylabel('Sw')
        axis([0 L 0 1])
        hold on;
```

```
    end
    hold off;
    pause(.1)
end

%%%%   CALCULATING OUTLET WATER SATURATION FOR EACH TIME AND LAYER
%%%

for i=1:length(swc)
    for j=1:length(sw)
        fdll(i,j)=ddfw(i,j)./lambdat(i,j);
    end
end

for i=1:length(swc);
    ds(i)=(1-sor(i)-swc(i))/n;
    for j=maxInd(i):n+1
        11(i,j)=-
((fdll(i,j).*ds(i)./2)+sum((fdll(i,j+1:n).*ds(i))+(fdll(i,n+1).*ds(i)./
2)));
    end
end

for i=1:length(swc);
    xxxx(i,maxInd(i):(n+1))=dfw(i,maxInd(i):(n+1))./dfw(i,maxInd(i))*L;
end

for i=1:length(swc)
    for j=maxInd:length(sw)
        ts(i,j)=tbt(i)+(phi(i).*I11(i,j).*(L^2-
xxxx(i,j)^2)./(2.*dp.*dfw(i,j).^2));
    end
end

ttt=min(tbt):(max(tbt)-min(tbt))/b:max(tbt);
t(1,1:(b+1))=0:(max(tbt))/b:max(tbt);

for i=1:(b+1)
    for j=1:length(swc)
        xts(:,i,j)=abs(t(i)-ts(j,:));
    end
end

[minVal minInd] = min((xts));
```

```
for i=1:length(swc)
    for j=1:length(ttt)
        swout(i,j)=sw(i,minInd(1,j,i));
    end
end

for i=1:length(swc)
    for j=1:length(ttt)
        for k=1:length(sw)
            xswout(k,j,i)=abs(swout(i,j)-sw(i,k));
        end
    end
end

[Valsw Indsw] = min((xswout));

%%%% AVERAGE WATER SATURATION BEHIND FRONT AFTER BTH AND BEFOR BTH
%%%%%

for i=1:length(swc)
    for j=1:length(t)
        if swout(i,j)> swc(i)
            swavvv(i,j)=swout(i,j)-(fw(i,Indsw(1,j,i))-
fw(i,(n+1)))./dfw(i,Indsw(1,j,i));
        else
            swavvv(i,j)=swavv(i);
        end
    end
end

%%%%%%%    RELATIVE PERM CORESPOND TO OUTLET SATURATION    %%%%%%%%%%

for i=1:length(swc)
    for j=1:length(ttt)
        kroout(i,j)=ao*((1-swout(i,j)-sor(i))./(1-swc(i)-sor(i))).^2;
        krwout(i,j)=aw*((swout(i,j)-swc(i))./(1-swc(i)-sor(i))).^2;
    end
end

%%%%%%%%%      FRONT POSITION FOR ECH LAYER AT EACH TIME       %%%%%%%%

for i=1:length(swc)
    for j=1:length(ttt)
        xup(i,j)=(-B(i)+(B(i).^2+4.*A(i).*C(i).*t(j)).^.5)./(2*A(i));
        if xup(i,j)>=L
```

```
            xup(i,j)=L;
        end
    end
end

%%%%%%%%%%%%          UP-SCALED RELATIVE PERM
%%%%%%%%%%%%%%%

for i=1:length(t)
      upkrw(i)=sum(transpose(krwout(:,i)).*K.*h)./sum(h.*K);
      upkro(i)=sum(transpose(kroout(:,i)).*K.*h)./sum(h.*K);

      swav(i)=(sum(swavvv(:,i).*(xup(:,i)).*transpose(h).*transpose(phi
      ))+sum(swc.*(L-
      (transpose(xup(:,i)))).*(h).*phi))./sum(L.*h.*phi);
      swavout(i)=(sum(transpose(swout(:,i)).*(h).*phi )./sum(h.*phi));
      (swout(:,i)).*(h).*phi )./sum(h.*phi));
end

subplot(2,3,5)
swavout(b+2)=0.744;
upkrw(b+2)=aw;
upkro(b+2)=0;
hold on
plot(swavout(1:(b+2)),upkrw(1:(b+2)),'--k', 'LineWidth',2)
title('Up Kr Vs. Swavout')
xlabel('Sw')
ylabel('Up Kr')
hold on
plot(swavout(1:(b+2)),upkro(1:(b+2)),'-k','LineWidth',2)
hold on
subplot(2,3,6)
hold on
plot(swav(1:(b+1)),upkrw(1:(b+1)),'--ko', 'MarkerSize',4)
hold on
plot(swav(1:(b+1)),upkro(1:(b+1)),'-ko', 'MarkerSize',4)
title('Up kr Vs. Swav')
xlabel('Swav')
ylabel('Up Kr')
```

B.2 MATLAB code for constant flux boundary condition:

```
---------------------------------------------------------------------------------------------

% UPSCALING RELATIVE PERMEBILITY FOR CONSTANT FLOW RATE CASE FOR %
%**************           MOHAMMAD SHADADEH         **************%
%************************   JULY 2013   **********************%
%-------------------------------------------------------------------------

clc
clear all

%%%%%%%%%%%%%%%%%%%%%%         DATA SECTION         %%%%%%%%%%%%%%%%%%%%%%%%
K=[8.3  10.1 8.6 7.3 8.2 11.1 11.7  13.2 11.4 7.9 10.6  11.2 8.4 8.9
12.3 17.5 17.4 13.9 12.6 10 ]*10^-15;     % absolut permeability (m^2)
h=2*ones (size (K));                      % thickness of each layer (m)
phi=[6  9   8   7   8   12  10  11  9   8   7   10.5    9   10  18  15
14  11  16  8];                           % porosity
swc=[.2 .22 .21 .18 .19 .20 .17 .23 .2 .175 .16 .18 .2 .24 .21 .19 .17
.23 .2 .185];                             % connate water saturation

sor=[.2 .25 .26 .23 .24 .28 .21 .23 .26 .22 .27 .265 .24 .25 .26 .29
.25 .24 .28 .275];            % residual oil saturation
miow=.8;                % viscosity of water
mioo=2.8;               % viscosity of oil
L=1000;                 % length of reservoir
dp=10^6;                % pressure difference in pa.
m=miow/mioo;            % viscosity ratio
n=1000;                 % number of saturation discretion
b=50;                   % number of time steps between the min BTH time
                        % and max BTH
aw=0.3;                 % indices for water in Corey correlation
ao=0.8;                 % indices for oil in Corey correlation

%%%%%%%%%%%%%%%%%%    FRACTIONAL FLOW   %%%%%%%%%%%%%%%%%%%%%%%%%%%%

for i=1:length(swc)
    sw(i,1:(n+1))=swc(i):(1-sor(i)-swc(i))/n:(1-sor(i));
end

for i=1:length(swc)/2
    for j=1:(n+1)
        kro(i,j)=ao*((1-sw(i,j)-sor(i))./(1-swc(i)-sor(i))).^2;
        krw(i,j)=aw*((sw(i,j)-swc(i))./(1-swc(i)-sor(i))).^2;
    end
```

```
end

for i=length(swc)/2+1:length(swc)
    for j=1:(n+1)
        kro(i,j)=ao*((1-sw(i,j)-sor(i))./(1-swc(i)-sor(i))).^2;
        krw(i,j)=aw*((sw(i,j)-swc(i))./(1-swc(i)-sor(i))).^2;
    end
end

% fw=fractional flow   dfw=fractional flow derivative
% ddfw=secod derivative of fractional flow

for i=1:length(swc)
    for j=1:length(sw)
        fw(i,j)=1./(1+(ao/aw).*(miow./mioo).*((1-sw(i,j)-
sor(i))./(sw(i,j)-swc(i))).^2);
        dfr1(i,j)=(1+(ao/aw).*(miow./mioo).*((1-sw(i,j)-
sor(i))./(sw(i,j)-swc(i))).^2);
        dfw(i,j)=((ao/aw).*2*miow/mioo).*(1-swc(i)-sor(i)).*(1-sw(i,j)-
sor(i))./((dfr1(i,j).^2).*(sw(i,j)-swc(i)).^3);
        dfr2(i,j)=-((ao*2/aw)*miow/mioo).*(1-swc(i)-sor(i)).*(1-
sw(i,j)-sor(i))./((sw(i,j)-swc(i)).^3);
        dfr3(i,j)=((ao*2/aw)*miow/mioo).*(1-swc(i)-sor(i)).*((sw(i,j)-
swc(i)).^3+3*(sw(i,j)-swc(i)).^2.*(1-sw(i,j)-sor(i))./((sw(i,j)-
swc(i)).^6);
        ddfw(i,j)=(-
dfr3(i,j).*dfr1(i,j).^2+2*dfr1(i,j).*dfr2(i,j).^2)./dfr1(i,j).^4;
    end
end

dfw(:,1)=0;
subplot(2,3,1)
hold on;

for i=1:length(swc)
    plot(sw(i,1:(n+1)),krw(i,1:(n+1)))
    plot(sw(i,1:(n+1)),kro(i,1:(n+1)))
    axis([0 1 0 1])
    title('Kr Vs. Sw')
    xlabel('Sw')
    ylabel('Kr')
end

subplot(2,3,2)
hold on;
```

```
for i=1:length(swc)
    plot(sw(i,1:(n+1)),fw(i,1:(n+1)))
    plot(sw(i,1:(n+1)),dfw(i,1:(n+1)))
    title('fw & dfw Vs. Sw')
    xlabel('Sw')
    ylabel('fw')
    axis([0 1 0 5])
end

subplot(2,3,3)
hold on;

for i=1:length(swc)
    plot(sw(i,1:(n+1)),ddfw(i,1:(n+1)))
    title('ddfw Vs. Sw')
    xlabel('Sw')
    ylabel('fw')
end

%%%%%%%%%%%%%    SLOPE OF FRACTIONAL FLOW    %%%%%%%%%%%%%%%%%%%%%%%%%%

slope=zeros([(n+1) length(swc)]);
for i=1:length(swc)
    for j=2:(n+1);
        slope(j,i)=(fw(i,j)-fw(i,1))/(sw(i,j)-sw(i,1));
    end
end

for j=1:length(swc)
    [maxVal maxInd] = max(slope);
end

%%%%%%%%%%%%%%%%%   AVERAGE SATURATION BEHIND FRONT
%%%%%%%%%%%%%%%%%

swavv=zeros(length(swc));
for i=1:length(swc)
    swavv(i)=sw(i,maxInd(i))-(fw(i,maxInd(i))-
fw(i,(n+1)))./dfw(i,maxInd(i));
end

%%%%%%%%%%%%%%%       BREACKTHROUGH TIME CALCULATION
%%%%%%%%%%%%%
```

```
velocity=qt.*transpose(dfw(:,870))./(h.*w.*phi);
tbt=L./velocity;

%%%% MONITORING SATURATION POSITION FOR EACH LAYER AT EACH TIME    %%%%

t(1,1:(b+1))=0:(max(tbt))/b:max(tbt);
        subplot(2,3,4);
    hold on
for j=1:b;
    for i=1:length(swc);
        x(i,j)=velocity(i).*t(j);

xx(i,maxInd(i):(n+1))=dfw(i,maxInd(i):(n+1))./dfw(i,maxInd(i))*x(i,j);
        xtx(i, 1:(n+1))=x(i,j):(L-x(i,j))/n:L;
        stss(i,1:(n+1))=sw(i,1);
        sww(i,:)=sw(i,:);
        sww(i,maxInd(i))=sw(i,1);
        plot([xtx(i, 1:(n+1)) xx(i,maxInd(i):(n+1))],[stss(i, 1:(n+1))
sww(i,maxInd(i):(n+1))])
        axis([0 L 0 1])
        title('Sw Vs. x')
        xlabel('x (m)')
        ylabel('Sw')
        hold on;
    end
    hold off;
   pause(.1)
end

%%%%% CALCULATING OUTLET WATER SATURATION FOR EACH TIME AND LAYER
%%%%

for i=1:length(swc)
    for j=maxInd:length(sw)
        ts(i,j)=tbt(i).*dfw(i,maxInd(i))./dfw(i,j);
    end
end

ttt=min(tbt):(max(tbt)-min(tbt))/b:max(tbt);

for i=1:(b+1)
    for j=1:length(swc)
        xts(:,i,j)=abs(t(i)-ts(j,:));
    end
end
```

```
[minVal minInd] = min((xts));

for i=1:length(swc)
    for j=1:length(ttt)
        swout(i,j)=sw(i,minInd(1,j,i));
    end
end

for i=1:length(swc)
    for j=1:length(ttt)
        for k=1:length(sw)
            xswout(k,j,i)=abs(swout(i,j)-sw(i,k));
        end
    end
end
[Valsw Indsw] = min((xswout));

%%%% AVERAGE WATER SATURATION BEHIND FRONT AFTER BTH AND BEFOR BTH
%%%%%

for i=1:length(swc)
    for j=1:length(ttt)
        if swout(i,j)> swc(i)
            swavvv(i,j)=swout(i,j)-(fw(i,Indsw(1,j,i))-
fw(i,(n+1)))./dfw(i,Indsw(1,j,i));
        else
            swavvv(i,j)=swavv(i);
        end
    end
end

for i=1:length(swc)
    for j=1:length(ttt)
        kroout(i,j)=ao*((1-swout(i,j)-sor(i))./(1-swc(i)-sor(i))).^2;
        krwout(i,j)=aw*((swout(i,j)-swc(i))./(1-swc(i)-sor(i))).^2;
    end
end
 %%%%%%%     FRONT POSITION FOR ECH LAYER AT EACH TIME       %%%%%%%%%%

for i=1:length(swc)
    for j=1:length(ttt)
        xup(i,j)=velocity(i).*t(j);
        if xup(i,j)>=L
            xup(i,j)=L;
        end
```

```
    end
end

%%%%%%%%%%%%%%%%%%    UP-SCALED RELATIVE PERM          %%%%%%%%%%%%%%%%%%

for i=1:length(t)
      upkrw(i)=sum(transpose(krwout(:,i)).*K.*h)./sum(h.*K);
      upkro(i)=sum(transpose(kroout(:,i)).*K.*h)./sum(h.*K);

      swav(i)=(sum(swavvv(:,i).*(xup(:,i)).*transpose(h).*transpose(phi
      ))+sum(swc.*(L-
      (transpose(xup(:,i)))).*(h).*phi))./sum(L.*h.*phi);
      swavout(i)=(sum(transpose(swout(:,i)).*(h).*phi )./sum(h.*phi));
      (swout(:,i)).*(h).*phi )./sum(h.*phi));
end

subplot(2,3,5)
hold on
swavout(b+2)=0.744;
upkrw(b+2)=aw;
upkro(b+2)=0;
hold on
plot(swavout(1:(b+2)),upkrw(1:(b+2)),'--k', 'LineWidth',2)
title('Up Kr Vs. Swavout')
xlabel('Sw')
ylabel('Up Kr')
hold on
plot(swavout(1:(b+2)),upkro(1:(b+2)),'-k','LineWidth',2)
plot(swavout(1:(b+1)),upkrw(1:(b+1)),'--ksq','MarkerEdgeColor','k',
'MarkerFaceColor','k','MarkerSize',3)
hold on
plot(swavout(1:(b+1)),upkro(1:(b+1)),'-ksq','MarkerEdgeColor','k',
'MarkerFaceColor','k','MarkerSize',3)
title('Up kr Vs. Swavout')
xlabel('Sw')
ylabel('Up kr')
subplot(2,3,6)
hold on
plot(swav(1:(b+1)),upkrw(1:(b+1)),'--ksq',
'MarkerSize',3,'MarkerFaceColor','k')
hold on
plot(swav(1:(b+1)),upkro(1:(b+1)),'-ko',
'MarkerSize',4,'MarkerFaceColor','k')
title('Up kr Vs. Swav')
xlabel('Swav')
ylabel('Up kr')
```

B.3 MATLAB code for Hearn's method:

```
---------------------------------------------------------------------------------------------------

%%%% UPSCALING RELATIVE PERMEBILITY USING HEARN'S METHOD   %%%%
%**************           MOHAMMAD SHADADEH        ************%
%************************   JULY 2013   ************************%
%-------------------------------------------------------------------
clc
clear all

%%%%%%%%%%%%%%%%%%   DATA SECTION     %%%%%%%%%%%%%%%%%%%%%%%%%

KK=[8.3  10.1 8.6 7.3 8.2 11.1 11.7  13.2 11.4 7.9 10.6  11.2 8.4 8.9
12.3 17.5 17.4 13.9 12.6 10 ]*10^-15;           % Absolute permeability
hh=2*ones(size(K));                          % Thickness
phii=[6  9   8   7   8   12  10  11  9   8   7   10.5    9   10  18  15
14  11  16  8];                              % Porosity
swcc=[.2 .22 .21 .18 .19 .20 .17 .23 .2 .175 .16 .18 .2 .24 .21 .19 .17
.23 .2 .185];
sorr=[.2 .25 .26 .23 .24 .28 .21 .23 .26 .22 .27 .265 .24 .25 .26 .29
.25 .24 .28 .275];
miow=.8;                % Viscosity of water
mioo=2.8;               % Viscosity of oil
L=1000;                 % Length of reservoir
m=miow/mioo;            % Viscosity ratio
qt=1000*.15889/86400./h;% FLOW RATE m^3/s
w=400;                  % Wedth
n=20;

%%%%%%%%%%%%%%%%%%%%%%%%%%%%%%%%%%%%%%%%%%%%%%%%%%%%%%%%%%%%%%%%%%%%%%%

koc=0.8;
krw=0.3;
A=KK./(phii.*(1-swcc-sorr));
[B, IX]=sort(A, 'descend');
eee=1;
error=1;

while error > 10^(-30)
    for i=1:n
        K(i)=KK(IX(i));
        h(i)=hh(IX(i));
        phi(i)=phii(IX(i));
        swc(i)=swcc(IX(i));
```

```
    sor(i)=sorr(IX(i));
end
ds=1-swc-sor;

for i=1:length(K)
    xx=0
    for j=1:i
        xx(j)=K(j).*h(j);
    end
    mr(i)=sum(xx);
    fw1(i)=krw.*mr(i)./miow;
end

fw2(1)=0
for i=2:length(K)
    xx=0
    for j=1:(i-1)
        xx2(j)=K(j).*h(j);
    end
    mr(i)=sum(xx2);
    fw2(i)=krw.*mr(i)./miow;
end

for i=i:length(K)
    xxx=0
    for j=(i+1):n
        xxx(j)=K(j).*h(j);
    end
    mh(i)=sum(xxx)
    fo1(i)=koc.*mh(i)./mioo;
end

for i=1:length(K)
    xxx2=0
    for j=i:n;
        xxx2(j)=K(j).*h(j);
    end
    mh(i)=sum(xxx2)
    fo2(i)=koc.*mh(i)./mioo;
end

df=fw1./(fw1+fo1)-fw2./(fw2+fo2);
v=(qt.*df)./(w.*h.*phi.*ds)

eee=eee+1;
```

```
    vvv(:,:,eee)=v;
    error=sum(abs((vvv(:,:,eee))-(vvv(:,:,(eee-1)))));
    B=sort(v, 'descend');

    for i=1:length(v)
        for j=1:length(v)
            if v(j)-B(i)==0
                IX(i)=j;
            end
        end
    end
    KK=K;
    hh=h;
    phii=phi;
    swcc=swc;
    sorr=sor;
end

krrw(1)=0;
krro(1)=koc;
sw(1)=sum(h.*phi.*swc)/sum(h.*phi);
kk=sum(h.*phi);

%%%%%%%%%%%%%    CALCULATING AVERAGE WATER SATURATION     %%%%%%%%%%%%%

for i=2:length(K)
    for j=1:(i-1)
        gg(j)=h(j).*phi(j).*(1-sor(j))
    end
    g(i)=sum(gg)
    mm=0;
    for j=i:n
        mm(j)=h(j).*phi(j).*swc(j)
    end
    m(i)=sum(mm);
    sw(i)=((g(i)+m(i))./kk)
end

%%%%%    CALCULATING UP-SCALED REALTIVE PERMEABILITY OF WATER
%%%%%%%%

for i=2:length(K)
    mm=0
    for j=1:(i-1)
        mm(j)=K(j).*h(j);
```

```
    end
    mr(i)=sum(mm);
    krrw(i)=krw.*mr(i)./sum(K.*h);
end

%%%%%%   CALCULATING UP-SCALED REALTIVE PERMEABILITY OF OIL
%%%%%%%%%

for i=2:length(K)
    mmm=0
    for j=i:n
        mmm(j)=K(j).*h(j)
    end
    mh(i)=sum(mmm)
    krro(i)=koc.*mh(i)./sum(K.*h)
end

sw(n+1)=sum(h.*phi.*(1-sor))./sum(h.*phi);
krrw(n+1)=krw;
krro(n+1)=0;
sw;
krrw;
krro;
plot(sw, krrw ,'--ksq','MarkerEdgeColor','k',
'MarkerFaceColor','k','MarkerSize',5)
hold on
plot(sw, krro,'-ksq','MarkerSize',5)
title('Up kr Vs. Swav')
xlabel('Sw')
ylabel('Up kr')
```

B.4 MATLAB code for Dykstra-Parson's method:

```
-----------------------------------------------------------------------------------------

% UPSCALING RELATIVE PERMEBILITY USING DYKSTRA-PARSON'S METHOD   %%
%**************           MOHAMMAD SHADADEH        ************%
%************************   JULY 2013   ************************%
%-------------------------------------------------------------------

clc
clear all

%%%%%%%%%%%%%%%%%%%   DATA SECTION   %%%%%%%%%%%%%%%%%%%%%%%%%%%%%%%

KK=[8.3 10.1 8.6 7.3 8.2 11.1 11.7  13.2 11.4 7.9 10.6  11.2 8.4 8.9
12.3 17.5 17.4 13.9 12.6 10 ]*10^-15;
hh=2*ones(size(KK));
phii=[6 9   8   7   8   12  10  11  9   8   7   10.5    9   10  18  15
14  11  16  8];
swcc=[.2 .22 .21 .18 .19 .20 .17 .23 .2 .175 .16 .18 .2 .24 .21 .19 .17
.23 .2 .185];
sorr=[.2 .25 .26 .23 .24 .28 .21 .23 .26 .22 .27 .265 .24 .25 .26 .29
.25 .24 .28 .275];
miow=.8;
mioo=2.8;
L=1000;
dp=10^9;
m=miow/mioo;
qt=1000*.15889/86400./hh;
w=400;
m=miow/mioo;
n=20

%%%%%%%%%%%%%%%%%%%%%%%%%%%%%%%%%%%%%%%%%%%%%%%%%%%%%%%%%%%%%%%%%%%%%
koc=0.8;
krw=0.3;
M=krw*mioo./(miow.*koc)

%%%%%%%%%%%%%%%%%%%%    HETEROGINITY FACTOR    %%%%%%%%%%%%%%%%%%5

A=KK.*krw./(phii.*miow.*(1-sorr-swcc).*(1+(M)));
[B, IX]=sort(A, 'descend')

for i=1:n
```

```
    K(i)=KK(IX(i));
    h(i)=hh(IX(i));
    phi(i)=phii(IX(i));
    swc(i)=swcc(IX(i));
    sor(i)=sorr(IX(i));
end

krrw(1)=0;
krro(1)=koc;
sw(1)=sum(h.*phi.*swc)/sum(h.*phi);
kk=sum(h.*phi);

for i=2:length(K)
    for j=1:(i-1)
        gg(j)=h(j).*phi(j).*(1-sor(j))
    end
    g(i)=sum(gg)
    mm=0;
    for j=i:n
        mm(j)=h(j).*phi(j).*swc(j)
    end
    m(i)=sum(mm);
    sw(i)=((g(i)+m(i))./kk)
end

%%%%%%%%%%%%%%%%%%%%%%%%%%%%%%%%%%%%%%%%%%%%%%%%%%%%%%%%%%%%%%%%%%%%%%%%%
%

for i=2:length(K)
    mm=0
    for j=1:(i-1)
        mm(j)=K(j).*h(j);
    end
    mr(i)=sum(mm);
    krrw(i)=krw.*mr(i)./sum(K.*h);
end

for i=2:length(K)
    mmm=0
    for j=i:n
        mmm(j)=K(j).*h(j)
    end
    mh(i)=sum(mmm)
    krro(i)=koc.*mh(i)./sum(K.*h)
end
```

```
sw(n+1)=sum(h.*phi.*(1-sor))./sum(h.*phi);
krrw(n+1)=krw;
krro(n+1)=0;
plot(sw, krrw ,'--ksq','MarkerEdgeColor','k',
'MarkerFaceColor','k','MarkerSize',4)
hold on
plot(sw, krro,'-ksq','MarkerSize',4)
title('Up kr Vs. Swav')
title('Up kr Vs. Swavout')
xlabel('Sw')
ylabel('Up kr')
```

B.5 ECLIPSE code for multi-layer constant pressure boundary reservoir model:

```
--------------------------------------------------------------------
RUNSPEC
TITLE
MULTI-LAYER REERVOIR MODEL

DIMENS
  100    1    20 /

ENDSCALE
/
OIL
WATER
METRIC
EQLDIMS
    1 2000/

TABDIMS
    20    1   40   40    1   20 /

REGDIMS

 1 1 1 1 2 /

WELLDIMS
    2   100   1    3 /

START
   1 'Jan' 2000/

GRID
ECHO

GRIDFILE
  1    /

BOX
1 100 1 1 1 20 /

DXV
   100*5
/

DYV
   1*50
```

```
/

-- Depth to top layer must be specified

BOX
 1 100 1 1 1 1 /

TOPS
100*2000 /

DZ
100*2
/

EQUALS

PORO 0.06 1 100 1 1 1 1/
PORO 0.09 1 100 1 1 2 2/
PORO 0.08 1 100 1 1 3 3/
PORO 0.07 1 100 1 1 4 4/
PORO 0.08 1 100 1 1 5 5/
PORO 0.12 1 100 1 1 6 6/
PORO 0.10 1 100 1 1 7 7/
PORO 0.11 1 100 1 1 8 8/
PORO 0.09 1 100 1 1 9 9/
PORO 0.08 1 100 1 1 10 10/
PORO 0.07 1 100 1 1 11 11/
PORO 0.105 1 100 1 1 12 12/
PORO 0.09 1 100 1 1 13 13/
PORO 0.10 1 100 1 1 14 14/
PORO 0.18 1 100 1 1 15 15/
PORO 0.15 1 100 1 1 16 16/
PORO 0.14 1 100 1 1 17 17/
PORO 0.11 1 100 1 1 18 18/
PORO 0.16 1 100 1 1 19 19/
PORO 0.08 1 100 1 1 20 20/


PERMX 8.3 1 100 1 1 1 1/
PERMY 8.3 /
PERMZ 4.15 /
PERMX 10.1 1 100 1 1 2 2/
PERMY 10.1 /
PERMZ 5.05 /
PERMX 8.6 1 100 1 1 3 3/
PERMY 8.6 /
PERMZ 4.3 /
```

```
PERMX 7.3 1 100 1 1 4 4/
PERMY 7.3 /
PERMZ 3.65 /
PERMX 8.2 1 100 1 1 5 5/
PERMY 8.2 /
PERMZ 4.1 /
PERMX 11.1 1 100 1 1 6 6/
PERMY 11.1 /
PERMZ 5.6 /
PERMX 11.7 1 100 1 1 7 7/
PERMY 11.7 /
PERMZ 5.85 /
PERMX 13.2 1 100 1 1 8 8/
PERMY 13.2 /
PERMZ 6.6 /
PERMX 11.4 1 100 1 1 9 9/
PERMY 11.4 /
PERMZ 5.7 /
PERMX 7.9 1 100 1 1 10 10/
PERMY 7.9 /
PERMZ 3.95 /
PERMX 10.6 1 100 1 1 11 11/
PERMY 10.6 /
PERMZ 5.3 /
PERMX 11.2 1 100 1 1 12 12/
PERMY 11.2 /
PERMZ 5.6 /
PERMX 8.4 1 100 1 1 13 13/
PERMY 8.4 /
PERMZ 4.2 /
PERMX 8.9 1 100 1 1 14 14/
PERMY 8.9 /
PERMZ 4.45 /
PERMX 12.3 1 100 1 1 15 15/
PERMY 12.3 /
PERMZ 6.15 /
PERMX 17.5 1 100 1 1 16 16/
PERMY 17.5 /
PERMZ 8.75 /
PERMX 17.4 1 100 1 1 17 17/
PERMY 17.4 /
PERMZ 8.7 /
PERMX 13.9 1 100 1 1 18 18/
PERMY 13.9 /
PERMZ 6.95 /
PERMX 12.6 1 100 1 1 19 19/
PERMY 12.6 /
```

```
PERMZ 6.3/
PERMX 10 1 100 1 1 20 20/
PERMY 10 /
PERMZ 5 /
/

INIT

RPTGRID
  -- Report Levels for Grid Section Data
  --
  'DX' 'DY' 'DZ'
 /

PROPS

PVDO
  150 1.4 2.8
  200 1.35 2.9
 /

PVTW
 150   .8    4.0E-05   1.0    0.00E+00 /

DENSITY
 850 1000 /

ROCK
 150       0.40E-05 /

SWOF
--swav krw  kro   pc
0.200 0.000 0.800 0.000
0.230 0.001 0.722 0.000
0.260 0.003 0.648 0.000
0.290 0.007 0.578 0.000
0.320 0.012 0.512 0.000
0.350 0.019 0.450 0.000
0.380 0.027 0.392 0.000
0.410 0.037 0.338 0.000
0.440 0.048 0.288 0.000
0.470 0.061 0.242 0.000
0.500 0.075 0.200 0.000
0.530 0.091 0.162 0.000
0.560 0.108 0.128 0.000
0.590 0.127 0.098 0.000
0.620 0.147 0.072 0.000
```

```
0.650 0.169 0.050 0.000
0.680 0.192 0.032 0.000
0.710 0.217 0.018 0.000
0.740 0.243 0.008 0.000
0.770 0.271 0.002 0.000
0.800 0.300 0.000 0.000/table 1
0.220 0.000 0.800 0.000
0.247 0.001 0.722 0.000
0.273 0.003 0.648 0.000
0.300 0.007 0.578 0.000
0.326 0.012 0.512 0.000
0.353 0.019 0.450 0.000
0.379 0.027 0.392 0.000
0.406 0.037 0.338 0.000
0.432 0.048 0.288 0.000
0.459 0.061 0.242 0.000
0.485 0.075 0.200 0.000
0.512 0.091 0.162 0.000
0.538 0.108 0.128 0.000
0.565 0.127 0.098 0.000
0.591 0.147 0.072 0.000
0.618 0.169 0.050 0.000
0.644 0.192 0.032 0.000
0.671 0.217 0.018 0.000
0.697 0.243 0.008 0.000
0.724 0.271 0.002 0.000
0.750 0.300 0.000 0.000/ table 2
0.210 0.000 0.800 0.000
0.237 0.001 0.722 0.000
0.263 0.003 0.648 0.000
0.290 0.007 0.578 0.000
0.316 0.012 0.512 0.000
0.343 0.019 0.450 0.000
0.369 0.027 0.392 0.000
0.396 0.037 0.338 0.000
0.422 0.048 0.288 0.000
0.449 0.061 0.242 0.000
0.475 0.075 0.200 0.000
0.502 0.091 0.162 0.000
0.528 0.108 0.128 0.000
0.555 0.127 0.098 0.000
0.581 0.147 0.072 0.000
0.608 0.169 0.050 0.000
0.634 0.192 0.032 0.000
0.661 0.217 0.018 0.000
0.687 0.243 0.008 0.000
0.714 0.271 0.002 0.000
```

```
0.740 0.300 0.000 0.000/table 3
0.180 0.000 0.800 0.000
0.210 0.001 0.722 0.000
0.239 0.003 0.648 0.000
0.269 0.007 0.578 0.000
0.298 0.012 0.512 0.000
0.328 0.019 0.450 0.000
0.357 0.027 0.392 0.000
0.387 0.037 0.338 0.000
0.416 0.048 0.288 0.000
0.446 0.061 0.242 0.000
0.475 0.075 0.200 0.000
0.505 0.091 0.162 0.000
0.534 0.108 0.128 0.000
0.564 0.127 0.098 0.000
0.593 0.147 0.072 0.000
0.623 0.169 0.050 0.000
0.652 0.192 0.032 0.000
0.682 0.217 0.018 0.000
0.711 0.243 0.008 0.000
0.741 0.271 0.002 0.000
0.770 0.300 0.000 0.000/ table 4
0.190 0.000 0.800 0.000
0.219 0.001 0.722 0.000
0.247 0.003 0.648 0.000
0.276 0.007 0.578 0.000
0.304 0.012 0.512 0.000
0.333 0.019 0.450 0.000
0.361 0.027 0.392 0.000
0.390 0.037 0.338 0.000
0.418 0.048 0.288 0.000
0.447 0.061 0.242 0.000
0.475 0.075 0.200 0.000
0.504 0.091 0.162 0.000
0.532 0.108 0.128 0.000
0.561 0.127 0.098 0.000
0.589 0.147 0.072 0.000
0.618 0.169 0.050 0.000
0.646 0.192 0.032 0.000
0.675 0.217 0.018 0.000
0.703 0.243 0.008 0.000
0.732 0.271 0.002 0.000
0.760 0.300 0.000 0.000/ table 5
0.200 0.000 0.800 0.000
0.226 0.001 0.722 0.000
0.252 0.003 0.648 0.000
0.278 0.007 0.578 0.000
```

```
0.304 0.012 0.512 0.000
0.330 0.019 0.450 0.000
0.356 0.027 0.392 0.000
0.382 0.037 0.338 0.000
0.408 0.048 0.288 0.000
0.434 0.061 0.242 0.000
0.460 0.075 0.200 0.000
0.486 0.091 0.162 0.000
0.512 0.108 0.128 0.000
0.538 0.127 0.098 0.000
0.564 0.147 0.072 0.000
0.590 0.169 0.050 0.000
0.616 0.192 0.032 0.000
0.642 0.217 0.018 0.000
0.668 0.243 0.008 0.000
0.694 0.271 0.002 0.000
0.720 0.300 0.000 0.000/ table 6
0.170 0.000 0.800 0.000
0.201 0.001 0.722 0.000
0.232 0.003 0.648 0.000
0.263 0.007 0.578 0.000
0.294 0.012 0.512 0.000
0.325 0.019 0.450 0.000
0.356 0.027 0.392 0.000
0.387 0.037 0.338 0.000
0.418 0.048 0.288 0.000
0.449 0.061 0.242 0.000
0.480 0.075 0.200 0.000
0.511 0.091 0.162 0.000
0.542 0.108 0.128 0.000
0.573 0.127 0.098 0.000
0.604 0.147 0.072 0.000
0.635 0.169 0.050 0.000
0.666 0.192 0.032 0.000
0.697 0.217 0.018 0.000
0.728 0.243 0.008 0.000
0.759 0.271 0.002 0.000
0.790 0.300 0.000 0.000/ table 7
0.200 0.000 0.800 0.000
0.227 0.001 0.722 0.000
0.254 0.003 0.648 0.000
0.281 0.007 0.578 0.000
0.308 0.012 0.512 0.000
0.335 0.019 0.450 0.000
0.362 0.027 0.392 0.000
0.389 0.037 0.338 0.000
0.416 0.048 0.288 0.000
```

```
0.443 0.061 0.242 0.000
0.470 0.075 0.200 0.000
0.497 0.091 0.162 0.000
0.524 0.108 0.128 0.000
0.551 0.127 0.098 0.000
0.578 0.147 0.072 0.000
0.605 0.169 0.050 0.000
0.632 0.192 0.032 0.000
0.659 0.217 0.018 0.000
0.686 0.243 0.008 0.000
0.713 0.271 0.002 0.000
0.740 0.300 0.000 0.000/ table 8
0.20000     0.00000     0.80000     0.00000
0.22700     0.00075     0.72200     0.00000
0.25400     0.00300     0.64800     0.00000
0.28100     0.00675     0.57800     0.00000
0.30800     0.01200     0.51200     0.00000
0.33500     0.01875     0.45000     0.00000
0.36200     0.02700     0.39200     0.00000
0.38900     0.03675     0.33800     0.00000
0.41600     0.04800     0.28800     0.00000
0.44300     0.06075     0.24200     0.00000
0.47000     0.07500     0.20000     0.00000
0.49700     0.09075     0.16200     0.00000
0.52400     0.10800     0.12800     0.00000
0.55100     0.12675     0.09800     0.00000
0.57800     0.14700     0.07200     0.00000
0.60500     0.16875     0.05000     0.00000
0.63200     0.19200     0.03200     0.00000
0.65900     0.21675     0.01800     0.00000
0.68600     0.24300     0.00800     0.00000
0.71300     0.27075     0.00200     0.00000
0.74000     0.30000     0.00000     0.000/ table 9
0.17500     0.00000     0.80000     0.00000
0.20525     0.00075     0.72200     0.00000
0.23550     0.00300     0.64800     0.00000
0.26575     0.00675     0.57800     0.00000
0.29600     0.01200     0.51200     0.00000
0.32625     0.01875     0.45000     0.00000
0.35650     0.02700     0.39200     0.00000
0.38675     0.03675     0.33800     0.00000
0.41700     0.04800     0.28800     0.00000
0.44725     0.06075     0.24200     0.00000
0.47750     0.07500     0.20000     0.00000
0.50775     0.09075     0.16200     0.00000
0.53800     0.10800     0.12800     0.00000
0.56825     0.12675     0.09800     0.00000
```

```
0.59850     0.14700     0.07200     0.00000
0.62875     0.16875     0.05000     0.00000
0.65900     0.19200     0.03200     0.00000
0.68925     0.21675     0.01800     0.00000
0.71950     0.24300     0.00800     0.00000
0.74975     0.27075     0.00200     0.00000
0.78000     0.30000     0.00000     0.000/ table 10
0.16000     0.00000     0.80000     0.00000
0.18850     0.00075     0.72200     0.00000
0.21700     0.00300     0.64800     0.00000
0.24550     0.00675     0.57800     0.00000
0.27400     0.01200     0.51200     0.00000
0.30250     0.01875     0.45000     0.00000
0.33100     0.02700     0.39200     0.00000
0.35950     0.03675     0.33800     0.00000
0.38800     0.04800     0.28800     0.00000
0.41650     0.06075     0.24200     0.00000
0.44500     0.07500     0.20000     0.00000
0.47350     0.09075     0.16200     0.00000
0.50200     0.10800     0.12800     0.00000
0.53050     0.12675     0.09800     0.00000
0.55900     0.14700     0.07200     0.00000
0.58750     0.16875     0.05000     0.00000
0.61600     0.19200     0.03200     0.00000
0.64450     0.21675     0.01800     0.00000
0.67300     0.24300     0.00800     0.00000
0.70150     0.27075     0.00200     0.00000
0.73000     0.30000     0.00000     0.000/table 11
0.18000     0.00000     0.80000     0.00000
0.20775     0.00075     0.72200     0.00000
0.23550     0.00300     0.64800     0.00000
0.26325     0.00675     0.57800     0.00000
0.29100     0.01200     0.51200     0.00000
0.31875     0.01875     0.45000     0.00000
0.34650     0.02700     0.39200     0.00000
0.37425     0.03675     0.33800     0.00000
0.40200     0.04800     0.28800     0.00000
0.42975     0.06075     0.24200     0.00000
0.45750     0.07500     0.20000     0.00000
0.48525     0.09075     0.16200     0.00000
0.51300     0.10800     0.12800     0.00000
0.54075     0.12675     0.09800     0.00000
0.56850     0.14700     0.07200     0.00000
0.59625     0.16875     0.05000     0.00000
0.62400     0.19200     0.03200     0.00000
0.65175     0.21675     0.01800     0.00000
0.67950     0.24300     0.00800     0.00000
```

```
0.70725     0.27075     0.00200     0.00000
0.73500     0.30000     0.00000     0.000/table 12
0.20000     0.00000     0.80000     0.00000
0.22800     0.00075     0.72200     0.00000
0.25600     0.00300     0.64800     0.00000
0.28400     0.00675     0.57800     0.00000
0.31200     0.01200     0.51200     0.00000
0.34000     0.01875     0.45000     0.00000
0.36800     0.02700     0.39200     0.00000
0.39600     0.03675     0.33800     0.00000
0.42400     0.04800     0.28800     0.00000
0.45200     0.06075     0.24200     0.00000
0.48000     0.07500     0.20000     0.00000
0.50800     0.09075     0.16200     0.00000
0.53600     0.10800     0.12800     0.00000
0.56400     0.12675     0.09800     0.00000
0.59200     0.14700     0.07200     0.00000
0.62000     0.16875     0.05000     0.00000
0.64800     0.19200     0.03200     0.00000
0.67600     0.21675     0.01800     0.00000
0.70400     0.24300     0.00800     0.00000
0.73200     0.27075     0.00200     0.00000
0.76000     0.30000     0.00000     0.000/ table 13
0.24000     0.00000     0.80000     0.00000
0.26550     0.00075     0.72200     0.00000
0.29100     0.00300     0.64800     0.00000
0.31650     0.00675     0.57800     0.00000
0.34200     0.01200     0.51200     0.00000
0.36750     0.01875     0.45000     0.00000
0.39300     0.02700     0.39200     0.00000
0.41850     0.03675     0.33800     0.00000
0.44400     0.04800     0.28800     0.00000
0.46950     0.06075     0.24200     0.00000
0.49500     0.07500     0.20000     0.00000
0.52050     0.09075     0.16200     0.00000
0.54600     0.10800     0.12800     0.00000
0.57150     0.12675     0.09800     0.00000
0.59700     0.14700     0.07200     0.00000
0.62250     0.16875     0.05000     0.00000
0.64800     0.19200     0.03200     0.00000
0.67350     0.21675     0.01800     0.00000
0.69900     0.24300     0.00800     0.00000
0.72450     0.27075     0.00200     0.00000
0.75000     0.30000     0.00000     0.000/ table 14
0.210 0.000 0.800 0.000
0.237 0.001 0.722 0.000
0.263 0.003 0.648 0.000
```

```
0.290 0.007 0.578 0.000
0.316 0.012 0.512 0.000
0.343 0.019 0.450 0.000
0.369 0.027 0.392 0.000
0.396 0.037 0.338 0.000
0.422 0.048 0.288 0.000
0.449 0.061 0.242 0.000
0.475 0.075 0.200 0.000
0.502 0.091 0.162 0.000
0.528 0.108 0.128 0.000
0.555 0.127 0.098 0.000
0.581 0.147 0.072 0.000
0.608 0.169 0.050 0.000
0.634 0.192 0.032 0.000
0.661 0.217 0.018 0.000
0.687 0.243 0.008 0.000
0.714 0.271 0.002 0.000
0.740 0.300 0.000 0.000/ table 15
0.190 0.000 0.800 0.000
0.216 0.001 0.722 0.000
0.242 0.003 0.648 0.000
0.268 0.007 0.578 0.000
0.294 0.012 0.512 0.000
0.320 0.019 0.450 0.000
0.346 0.027 0.392 0.000
0.372 0.037 0.338 0.000
0.398 0.048 0.288 0.000
0.424 0.061 0.242 0.000
0.450 0.075 0.200 0.000
0.476 0.091 0.162 0.000
0.502 0.108 0.128 0.000
0.528 0.127 0.098 0.000
0.554 0.147 0.072 0.000
0.580 0.169 0.050 0.000
0.606 0.192 0.032 0.000
0.632 0.217 0.018 0.000
0.658 0.243 0.008 0.000
0.684 0.271 0.002 0.000
0.710 0.300 0.000 0.000/ table 16
0.170 0.000 0.800 0.000
0.199 0.001 0.722 0.000
0.228 0.003 0.648 0.000
0.257 0.007 0.578 0.000
0.286 0.012 0.512 0.000
0.315 0.019 0.450 0.000
0.344 0.027 0.392 0.000
0.373 0.037 0.338 0.000
```

```
0.402 0.048 0.288 0.000
0.431 0.061 0.242 0.000
0.460 0.075 0.200 0.000
0.489 0.091 0.162 0.000
0.518 0.108 0.128 0.000
0.547 0.127 0.098 0.000
0.576 0.147 0.072 0.000
0.605 0.169 0.050 0.000
0.634 0.192 0.032 0.000
0.663 0.217 0.018 0.000
0.692 0.243 0.008 0.000
0.721 0.271 0.002 0.000
0.750 0.300 0.000 0.000/ table 17
0.230 0.000 0.800 0.000
0.257 0.001 0.722 0.000
0.283 0.003 0.648 0.000
0.310 0.007 0.578 0.000
0.336 0.012 0.512 0.000
0.363 0.019 0.450 0.000
0.389 0.027 0.392 0.000
0.416 0.037 0.338 0.000
0.442 0.048 0.288 0.000
0.469 0.061 0.242 0.000
0.495 0.075 0.200 0.000
0.522 0.091 0.162 0.000
0.548 0.108 0.128 0.000
0.575 0.127 0.098 0.000
0.601 0.147 0.072 0.000
0.628 0.169 0.050 0.000
0.654 0.192 0.032 0.000
0.681 0.217 0.018 0.000
0.707 0.243 0.008 0.000
0.734 0.271 0.002 0.000
0.760 0.300 0.000 0.000/table 18
0.200 0.000 0.800 0.000
0.226 0.001 0.722 0.000
0.252 0.003 0.648 0.000
0.278 0.007 0.578 0.000
0.304 0.012 0.512 0.000
0.330 0.019 0.450 0.000
0.356 0.027 0.392 0.000
0.382 0.037 0.338 0.000
0.408 0.048 0.288 0.000
0.434 0.061 0.242 0.000
0.460 0.075 0.200 0.000
0.486 0.091 0.162 0.000
0.512 0.108 0.128 0.000
```

```
0.538 0.127 0.098 0.000
0.564 0.147 0.072 0.000
0.590 0.169 0.050 0.000
0.616 0.192 0.032 0.000
0.642 0.217 0.018 0.000
0.668 0.243 0.008 0.000
0.694 0.271 0.002 0.000
0.720 0.300 0.000 0.000/table 19
0.185 0.000 0.800 0.000
0.212 0.001 0.722 0.000
0.239 0.003 0.648 0.000
0.266 0.007 0.578 0.000
0.293 0.012 0.512 0.000
0.320 0.019 0.450 0.000
0.347 0.027 0.392 0.000
0.374 0.037 0.338 0.000
0.401 0.048 0.288 0.000
0.428 0.061 0.242 0.000
0.455 0.075 0.200 0.000
0.482 0.091 0.162 0.000
0.509 0.108 0.128 0.000
0.536 0.127 0.098 0.000
0.563 0.147 0.072 0.000
0.590 0.169 0.050 0.000
0.617 0.192 0.032 0.000
0.644 0.217 0.018 0.000
0.671 0.243 0.008 0.000
0.698 0.271 0.002 0.000
0.725 0.300 0.000 0.000/ table 20

RPTPROPS
   -- PROPS Reporting Options
   'PVDO' 'PVTW'
/

REGIONS

SATNUM
100*1 100*2 100*3 100*4 100*5 100*6 100*7 100*8 100*9 100*10 100*11
100*12 100*13 100*14 100*15 100*16 100*17 100*18 100*19 100*20/
/

SOLUTION

EQUIL
 2000 123 2400 /
```

```
DATUM
  2000.0 /

RPTSOL
  -- Initialization Print Output
  --
'SWAT' 'RESTART=2' 'FIP=1' /

SUMMARY

FOPR
FWCT
FOPT
FOE

SCHEDULE

-- WELSPECS and COMPDAT define well information in both
-- Standard and LGC models.

WELSPECS
I GROUP 1 1 2000 WAT /
P GROUP 100 1 2000 OIL /
/

COMPDAT
I 1 1 1 20 open 1* 1* 1 /
P 100 1 1 20 open 1* 1* 1 /
/

WCONPROD
P OPEN BHP 1* 4* 50 /
/

WCONINJE
I WAT OPEN BHP 1* 1* 150 /
/

RPTSCHED
'RESTART=2' 'FIP=1' 'WELLS=1' 'SUMMARY=1' 'CPU=2' 'WELSPECS' 'NEWTON=1'
/

TSTEP
    200*60
/

END
```

B.6 ECLIPSE code for multi-layer constant flux reservoir model:

In this section the Eclipse cod for multi-layer constant pressure reservoir model has been modified in order to have a constant flow rate reservoir model. The only changes are in the section related to operation condition. The changes are as below:

```
-------------------------------------------------------------------------
-
SCHEDULE

WCONPROD
P OPEN RESV 1* 3* 10 /
/

WCONINJE
I WAT OPEN RESV 1* 10/
/
```

B.7 ECLIPSE code for 2D constant pressure boundaries reservoir model:

```
-------------------------------------------------------------------------
-
RUNSPEC
TITLE
2D CONSTANT PRESSURE BOUNDARIES RESERVOIR MODEL

DIMENS
   100    1    1 /

OIL
WATER
METRIC

EQLDIMS
    1 2000 /

TABDIMS
    1    1   40   40    1   40 /

WELLDIMS
    2   100   1    3 /

START
   1 'Jan' 2000 /

GRID
ECHO

GRIDFILE
    1    /

BOX
1 100 1 1 1 1 /

DXV
   100*5
/

DYV
   1*50
/

-- Depth to top layer must be specified
```

```
BOX
 1 100 1 1 1 1 /

TOPS
100*2000 /

DZ
100*40
/

EQUALS
   PORO
0.1032 /

PERMX 11.03 /
PERMY 11.03 /
PERMZ 5.5 /
/

INIT

RPTGRID
  -- Report Levels for Grid Section Data
  'DX' 'DY' 'DZ'
 /

PROPS

PVDO
  150 1.4 2.8
  200 1.35 2.9
 /

PVTW
 150   .8   4.0E-05   1.0    0.00E+00 /

DENSITY
 850 1000 /

ROCK
 150       0.40E-05 /

SWOF
--swav      krw         kro         pc
  0.198063  0.000000  0.800000  0.000000
  0.210777  0.006241  0.766056  0.000000
```

```
  0.270077  0.031913  0.626435  0.000000
  0.313858  0.049989  0.528124  0.000000
  0.368442  0.071245  0.412521  0.000000
  0.387011  0.077839  0.376655  0.000000
  0.421297  0.089556  0.312929  0.000000
  0.470591  0.105631  0.225506  0.000000
  0.502073  0.115228  0.173309  0.000000
  0.528700  0.122761  0.132803  0.000000
  0.559370  0.130274  0.093061  0.000000
  0.559766  0.130641  0.092575  0.000000
  0.560607  0.131394  0.091578  0.000000
  0.561711  0.132369  0.090306  0.000000
  0.563115  0.133591  0.088732  0.000000
  0.564583  0.134867  0.087122  0.000000
  0.566097  0.136185  0.085496  0.000000
  0.567727  0.137607  0.083784  0.000000
  0.569509  0.139135  0.081961  0.000000
  0.571347  0.140709  0.080122  0.000000
  0.573349  0.142391  0.078172  0.000000
  0.575581  0.144237  0.076053  0.000000
  0.577786  0.146060  0.074001  0.000000
  0.580023  0.147901  0.071963  0.000000
  0.582304  0.149776  0.069924  0.000000
  0.586840  0.153516  0.065982  0.000000
  0.589117  0.155394  0.064060  0.000000
  0.593658  0.159113  0.060333  0.000000
  0.595955  0.161022  0.058492  0.000000
  0.600148  0.164526  0.055217  0.000000
  0.602233  0.166272  0.053628  0.000000
  0.744000  0.300000  0.000000  0.000000
/

RPTPROPS
   -- PROPS Reporting Options
   'PVDO' 'PVTW'
/

SOLUTION

EQUIL
 2000 123 2400 /
```

```
DATUM
  2000.0 /

RPTSOL
  -- Initialization Print Output
'SWAT' 'RESTART=2' 'FIP=1' /

SUMMARY

FOPR
FWCT
FOPT
FOE
SCHEDULE

-- WELSPECS and COMPDAT define well information in both
-- Standard and LGC models.

WELSPECS
I GROUP 1 1 2000 WAT /
P GROUP 100 1 2000 OIL /
/

COMPDAT
I 1 1 1 1 open 1* 1* 1/
P 100 1 1 1 open 1* 1* 1/
/

WCONPROD
P OPEN BHP 1* 4* 50 /
/

WCONINJE
I WAT OPEN BHP 1* 1* 150/
/

RPTSCHED
'RESTART=2' 'FIP=1' 'WELLS=1' 'SUMMARY=1' 'CPU=2' 'WELSPECS' 'NEWTON=1'
/

TSTEP
    200*60
/

END
```

B.8 ECLIPSE code for 2D constant flow rate reservoir model:

```
----------------------------------------------------------------------------------------------

RUNSPEC
TITLE
2D CONSTANT PRESSURE BOUNDARIES RESERVOIR MODEL
DIMENS
   100    1    1 /

OIL
WATER
METRIC

EQLDIMS
    1 2000 /

TABDIMS
    1    1   40   40    1   40 /

WELLDIMS
    2   100   1    3 /

START
   1 'Jan' 2000 /

GRID
ECHO
GRIDFILE
    1    /

BOX
1 100 1 1 1 1 /

DXV
   100*5
/

DYV
   1*50
/

-- Depth to top layer must be specified

BOX
 1 100 1 1 1 1 /
```

```
TOPS
100*2000 /

DZ
100*40
/

EQUALS
   PORO
0.1032 /

PERMX 11.03 /
PERMY 11.03 /
PERMZ 5.5 /
/

INIT

RPTGRID
  -- Report Levels for Grid Section Data
   'DX' 'DY' 'DZ'
 /

PROPS

PVDO
  150 1.4 2.8
  200 1.35 2.9
 /

PVTW
 150   .8   4.0E-05   1.0    0.00E+00 /

DENSITY
 850 1000 /

ROCK
 150       0.40E-05 /

SWOF
--swav      krw         kro         pc
  0.198063  0.000000  0.800000  0.000000
  0.210777  0.006241  0.766056  0.000000
  0.270077  0.031913  0.626435  0.000000
  0.313858  0.049989  0.528124  0.000000
```

```
  0.368442  0.071245  0.412521  0.000000
  0.387011  0.077839  0.376655  0.000000
  0.421297  0.089556  0.312929  0.000000
  0.470591  0.105631  0.225506  0.000000
  0.502073  0.115228  0.173309  0.000000
  0.528700  0.122761  0.132803  0.000000
  0.559370  0.130274  0.093061  0.000000
  0.559766  0.130641  0.092575  0.000000
  0.560607  0.131394  0.091578  0.000000
  0.561711  0.132369  0.090306  0.000000
  0.563115  0.133591  0.088732  0.000000
  0.564583  0.134867  0.087122  0.000000
  0.566097  0.136185  0.085496  0.000000
  0.567727  0.137607  0.083784  0.000000
  0.569509  0.139135  0.081961  0.000000
  0.571347  0.140709  0.080122  0.000000
  0.573349  0.142391  0.078172  0.000000
  0.575581  0.144237  0.076053  0.000000
  0.577786  0.146060  0.074001  0.000000
  0.580023  0.147901  0.071963  0.000000
  0.582304  0.149776  0.069924  0.000000
  0.586840  0.153516  0.065982  0.000000
  0.589117  0.155394  0.064060  0.000000
  0.593658  0.159113  0.060333  0.000000
  0.595955  0.161022  0.058492  0.000000
  0.600148  0.164526  0.055217  0.000000
  0.602233  0.166272  0.053628  0.000000
  0.744000  0.300000  0.000000  0.000000

/

RPTPROPS
   -- PROPS Reporting Options
     'PVDO' 'PVTW'
/

SOLUTION

EQUIL
 2000 123 2400 /

DATUM
```

```
  2000.0 /

RPTSOL
  -- Initialization Print Output
  --
'SWAT' 'RESTART=2' 'FIP=1' /

SUMMARY

FOPR
FWCT
FOPT
FOE

SCHEDULE

-- WELSPECS and COMPDAT define well information in both
-- Standard and LGC models.

WELSPECS
I GROUP 1 1 2000 WAT /
P GROUP 100 1 2000 OIL /
/

COMPDAT
I 1 1 1 1 open 1* 1* 1/
P 100 1 1 1 open 1* 1* 1/
/

WCONPROD
P OPEN RESV 1* 3* 10 /
/

WCONINJE
I WAT OPEN RESV 1* 10/
/

RPTSCHED
'RESTART=2' 'FIP=1' 'WELLS=1' 'SUMMARY=1' 'CPU=2' 'WELSPECS' 'NEWTON=1'
/

TSTEP
    200*60
/

END
```